

Stereoselective Activity of 1-Propargyl-4-styrylpiperidine-like Analogues That Can Discriminate between Monoamine Oxidase Isoforms A and B

Damijan Knez,[#] Natalia Colettis,[#] Luca G. Iacovino,[#] Matej Sova, Anja Pjšlar, Janez Konc, Samo Lešnik, Josefina Higgs, Fabiola Kamecki, Irene Mangialavori, Ana Dolšak, Simon Žakelj, Jurij Trontelj, Janko Kos, Claudia Binda,* Mariel Marder,* and Stanislav Gobec*



Cite This: *J. Med. Chem.* 2020, 63, 1361–1387



Read Online

ACCESS |



Metrics & More

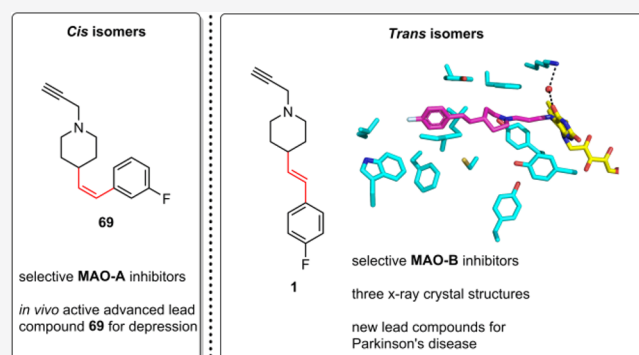


Article Recommendations



Supporting Information

ABSTRACT: The resurgence of interest in monoamine oxidases (MAOs) has been fueled by recent correlations of this enzymatic activity with cardiovascular, neurological, and oncological disorders. This has promoted increased research into selective MAO-A and MAO-B inhibitors. Here, we shed light on how selective inhibition of MAO-A and MAO-B can be achieved by geometric isomers of *cis*- and *trans*-1-propargyl-4-styrylpiperidines. While the *cis* isomers are potent human MAO-A inhibitors, the *trans* analogues selectively target only the MAO-B isoform. The inhibition was studied by kinetic analysis, UV–vis spectrum measurements, and X-ray crystallography. The selective inhibition of the MAO-A and MAO-B isoforms was confirmed *ex vivo* in mouse brain homogenates, and additional *in vivo* studies in mice show the therapeutic potential of 1-propargyl-4-styrylpiperidines for central nervous system disorders. This study represents a unique case of stereoselective activity of *cis/trans* isomers that can discriminate between structurally related enzyme isoforms.



INTRODUCTION

Specific interaction patterns and molecular geometry are critical factors that influence ligand binding affinity and ligand selectivity toward a target.¹ Numerous examples of “chiral switching” in drug development have highlighted the effects of spatial geometry on not only pharmacodynamics but also pharmacokinetics and toxicology of drugs.^{2,3} In addition to optical isomers, *cis* and *trans* isomers can have different pharmacological activities, as demonstrated by the well-known cases of cisplatin,⁴ tamoxifen,⁵ and combretastatin A4 (CA-4).⁶ This last includes a stilbene motif in the *cis* conformation (Figure 1A), which efficiently binds to the colchicine binding site of tubulin and acts as a microtubule-destabilizing agent.⁶ The binding of *trans*-combretastatin A4 (*trans*-CA-4, Figure 1A) to this site is thermodynamically less stable than that of *cis*-combretastatin A4 (*cis*-CA-4), and consequently the *trans* conformation does not prevent microtubule assembly.⁶ However, examples of stereoselective activities of *cis/trans* isomers are rare in comparison with optical isomers.

Human monoamine oxidase A (hMAO-A) and human monoamine oxidase B (hMAO-B) are flavoenzymes that are encoded by separate genes on the X chromosome, and they share 70% sequence identity.⁷ They are differentiated by their substrate specificities and inhibitor sensitivities. This arises

from the differences in the active site size and shape, and the altered amino acid residues between these isoforms. The hMAO-A and hMAO-B active sites are hydrophobic cavities with volumes of about 550 Å³ and 700 Å³, respectively.⁸ The active site of hMAO-B is flat and elongated, with a bipartite configuration, where Ile199 and Tyr326 are the gating residues that determine the shape of the cavity and the specificity of substrate/inhibitor binding.⁹ hMAO-A has a monopartite and more spherical active site, with Ile335 and Phe208 as the gating residues. MAOs catalyze the oxidative deamination of primary and some secondary amines, and they are responsible for neurotransmitter metabolism in peripheral tissues and in the central nervous system.¹⁰ This reaction produces an imino intermediate, which is spontaneously hydrolyzed to the corresponding aldehyde, with ammonia and hydrogen peroxide as side-products.¹¹ Reduced levels of neurotransmitters, increased activity and levels of MAOs, and the production of

Received: November 14, 2019

Published: January 9, 2020

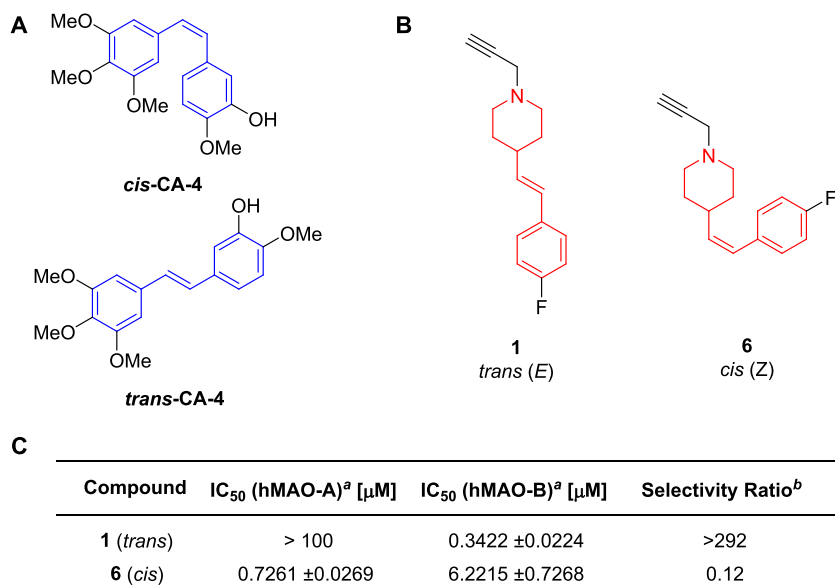
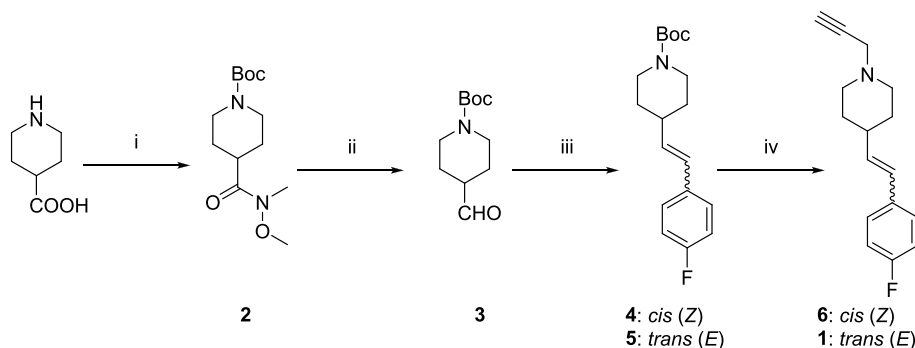


Figure 1. Stilbene derivatives and MAO inhibitory potencies. Chemical structures of *cis/trans*-combretastatin A4 (CA-4) (A) and hit inhibitor **1** (B) and *cis* isomer **6** (B). The stilbene core is blue, and the stilbene-like moiety of inhibitor **1** is red. (C) ^aIC₅₀ values are mean ± SEM values (*n* = 2, 3). ^bSelectivity ratio is defined as IC₅₀(hMAO-A)/IC₅₀(hMAO-B).

Scheme 1. Resynthesis of Hit Inhibitor **1**^a



^aReagents and conditions: (i) 1) Boc₂O, 1.0 M NaOH, 1,4-dioxane, 0 °C, rt, 1 h (91%); 2) *N,O*-dimethylhydroxylamine hydrochloride, Et₃N, TBTU, CH₂Cl₂, 0 °C to rt, overnight (76%); (ii) LiAlH₄, anh THF, 0 °C, 1 h (crude product, 83%); (iii) (4-fluorobenzyl)triphenylphosphonium bromide, sodium bis(trimethylsilyl)amide (NaHMDS, 2 N in THF), anh THF, Ar(g), rt, overnight (52%); (iv) (1) 4.0 M HCl in 1,4-dioxane, 80 °C, 2 h (100%); (2) propargyl bromide (80% solution in toluene), Cs₂CO₃, DMF, Ar(g), 0 °C, rt, overnight (yield, **1**, 26%; **6**, 72%).

toxic metabolites are linked with various neurological,^{12,13} psychological,¹⁴ and cardiovascular disorders¹⁵ and cancers.¹⁶

MAO-A inhibitors have been widely used for several decades in the therapy of depression and affective disorders.¹⁷ On the other hand, selective MAO-B inhibitors are used as monotherapies in the early stages of Parkinson's disease and as add-on therapy to levodopa in advanced forms of Parkinson's disease.¹⁸ MAO-A and MAO-B are recognized as validated targets. In terms of their contribution to increased cellular oxidative stress,¹⁹ novel inhibitors are emerging as important disease-modifying therapeutic agents in such devastating neurodegenerative diseases as Alzheimer's disease and a number of others.²⁰

To the best of our knowledge, *cis/trans* isomerisms of double bonds have never been used to achieve stereoselective inhibition of MAO isoforms. Here, we demonstrate a unique case study whereby configuration of the double bond in stilbene-like derivatives can define the selectivity for either MAO-A or MAO-B. We identify 1-propargyl-4-((*E*)-styryl)-piperidines as potent, selective, and irreversible hMAO-B

inhibitors. *Cis* analogues with small substituents on the phenyl ring selectively inhibit hMAO-A. These inhibitors were evaluated for their MAO inhibitory activities and pharmacological properties.

RESULTS

Identification, Design, Synthesis, and Selectivity Profile of Potent and Selective hMAO-A and hMAO-B Inhibitors. Compound **1** (Figure 1B) contains a stilbene-like motif, and it was identified as a hit inhibitor in an in-house library screening campaign. Indeed, compound **1** is a potent selective hMAO-B inhibitor, with no significant inhibition of hMAO-A at 100 μM (Figure 1C).

This hit inhibitor was resynthesized using an efficient and straightforward synthesis (Scheme 1) that started from readily available isonipecotic acid, which was transformed into Weinreb's amide **2** and subsequently reduced to obtain aldehyde **3**. The aldehyde then underwent the Wittig reaction with phosphonium ylide to yield a mixture of *cis* (**4**) and *trans* (**5**) Boc-protected piperidines, which were separated using

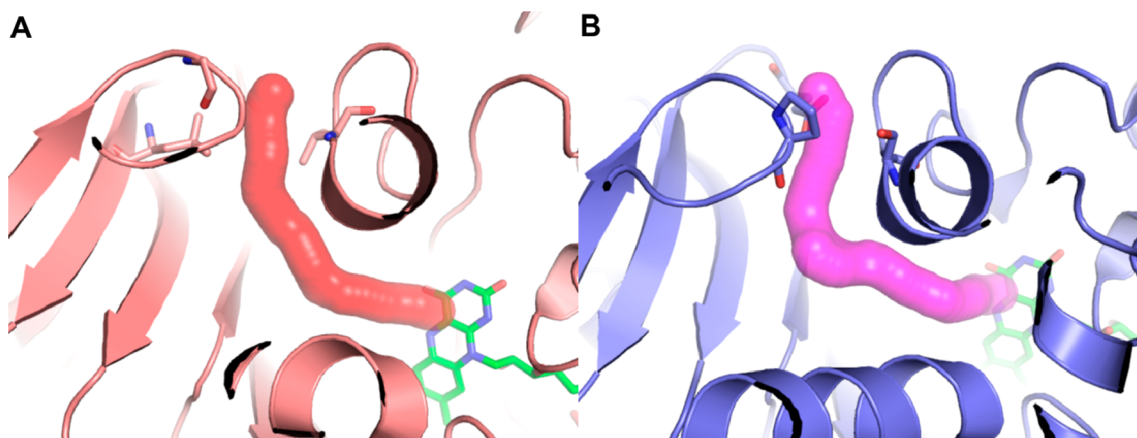


Figure 2. Active sites of hMAO-A (PDB code 2Z5X) and hMAO-B (PDB code 6FVZ). (A) MAO-A; FAD cofactor (green sticks); active site (red surface) spans from FAD to the entrance; bottleneck residues Leu97, Gly110, and Val210 at the entrance (salmon sticks). (B) MAO-B; FAD cofactor (green sticks); active site (violet surface) spans from FAD to the entrance; bottleneck residues Glu84, Pro102, and Ser200 at the entrance (purple sticks).

column chromatography. Following acidolysis, the corresponding secondary amine was reacted with propargyl bromide to obtain hit compound **1** and the *cis* isomer **6**. Compound **6** showed preferential inhibition of hMAO-A over hMAO-B (Figure 1C).

The selectivity profile was explained through analysis of the binding cavity using the Caver tool.²¹ Human (h)MAO-A (Figure 2A) has a wide cavity at the active site near the FAD cofactor ($r = 2.1$ Å), which is lined with Tyr407, Phe352, and Gly215. In the direction toward the entrance, the cavity widens ($r \approx 2.5$ Å) and remains wide to Val210, Gln215, and Ile335, and then it narrows to Val210, Cys323, and Ile335 ($r = 1.9$ Å) and remains narrow to the entrance, which is also the narrowest part of the active site ($r = 1.9$ Å) and is composed of Leu97, Gly110, and Val210. In hMAO-B (Figure 2B), the entrance is even wider in the active site near the FAD cofactor ($r = 2.3$ Å), with Gln206, Tyr398, and Tyr435, but then narrows in the direction of the entrance ($r = 1.9$ Å) at Leu171 and Ile199 and then widens again ($r = 2.5$ Å) to Ile199, Ile316, and Tyr326. The narrowest part is at the entrance ($r = 1.6$ Å), and it is composed of Glu84, Pro102, and Ser200. The hMAO-A active site entrance is thus significantly wider ($r = 1.9$ Å) than the hMAO-B active site entrance ($r = 1.6$ Å). Both entrances are also the bottlenecks, which indicates that the active site of hMAO-B might be more difficult to reach by wider ligands.

The active site of hMAO-B is also significantly more curved than the active site of hMAO-A, with a bend of 90° , while in hMAO-A, the cavity bends at an angle of $\sim 60^\circ$ (compare Figure 2A,B). The narrow entrance of hMAO-B and the higher curvature might prevent the relatively wider *cis* isomer **6** from entering the hMAO-B binding site. Indeed, **6** has a maximum width of 4.1 Å when measured as the height of the triangle composed of the fluorine atom, one of the sp^2 carbons, and the carbon bonded to the nitrogen, while the maximum width of the *trans* isomer **1** is only 2.5 Å when measured as the distance between two opposing carbon atoms in the piperidine ring. The *cis* isomer thus appears to inhibit hMAO-A but not hMAO-B because it is too wide to enter the narrower hMAO-B entrance. Its maximum width is only slightly greater than the 3.8 Å diameter of the hMAO-A entrance, while it is significantly greater than the 3.2 Å diameter of the hMAO-B entrance, which suggests that the hMAO-B entrance would

need to undergo more substantial conformational changes to accommodate the *cis* isomer **6**. The active site loop in hMAO-A contains Gly (i.e., Gly110), which is replaced by Pro102 in hMAO-B. This produces much higher rigidity in comparison to hMAO-A, where the active site loop is more flexible. This lack of flexibility of hMAO-B adds to the restricted access of the *cis* isomer to the hMAO-B active site. The *cis* isomer **6** inactivity against hMAO-B thus appears to be caused by steric hindrance in the active site, compound **6** being unable to fit into the elongated and rigid cavity (Figure 2).

However, the selectivity of the *trans* isomer **1** is not explained only by the analysis of its access to the active site, as *trans* isomer **1** can bind to both hMAO-A and hMAO-B. To simulate the transport process of the inhibitor from the active site to the surface of the protein, these two isomers were undocked from hMAO-A and hMAO-B using the CaverDock software.²² Starting from the docked conformations of both ligands at the active sites, the energetically most favorable trajectories of the ligands to the protein surfaces were investigated (Figure 3). In hMAO-A, *cis* isomer **6** is oriented with the propargyl group facing the FAD cofactor, with a binding energy of -8.3 kcal/mol (Figure 3A, movie file [j9b01886_si_002.mp4](https://doi.org/10.1021/acs.jmedchem.9b01886) in Supporting Information). As *cis* isomer **6** moves toward the entrance, its energy peaks at 0.4 kcal/mol and then falls to -3.8 kcal/mol at the entrance (Figure 3B). *Trans* isomer **1** in the correct orientation has a binding energy of -6.2 kcal/mol (Figure 3C), which is higher than for **6**. As the *trans* isomer is undocked, its binding energy peaks at -3.4 kcal/mol and then falls to -4.1 kcal/mol at the entrance (Figure 3D). Further, the *trans* ligand in the “wrong” orientation in the active site (i.e., with the fluorophenyl group facing the FAD cofactor) has a much lower energy of -10.1 kcal/mol (Figure 3D; lower-bounds energy curve). However, in this orientation, the *trans* ligand cannot form the covalent bond with FAD. Thus, in agreement with the experimental findings, the computational undocking simulation of hMAO-A showed that *cis* isomer **6** has lower binding energy at the active site than *trans* isomer **1**, which indicates that the *cis* isomer is more likely to bind to hMAO-A than the *trans* isomer. In addition, the *trans* isomer might preferentially access the active site in an orientation that does not allow formation of the covalent bond, as can be seen by the lower binding energy of the “wrong” conformation compared to the energy of the

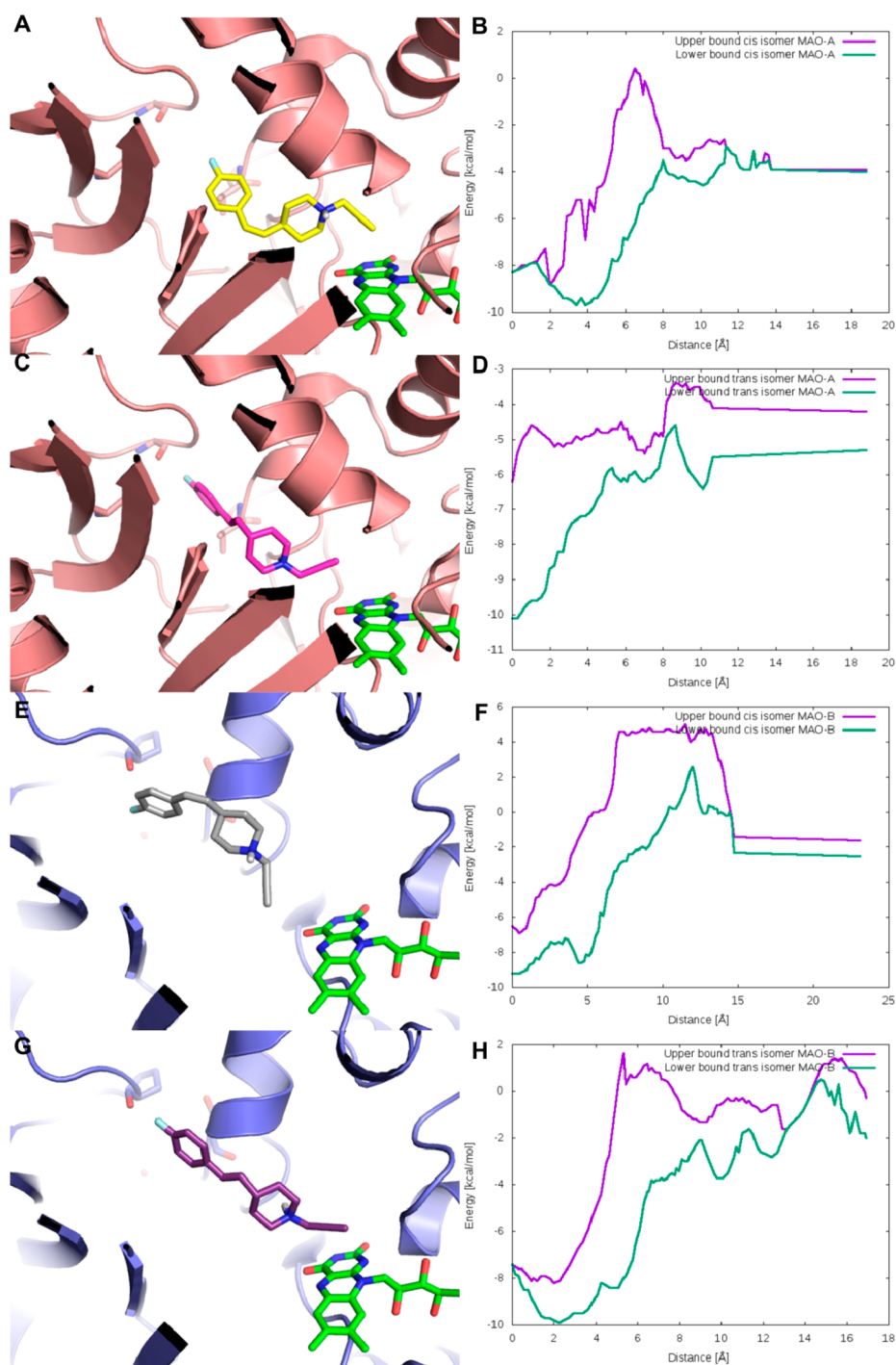
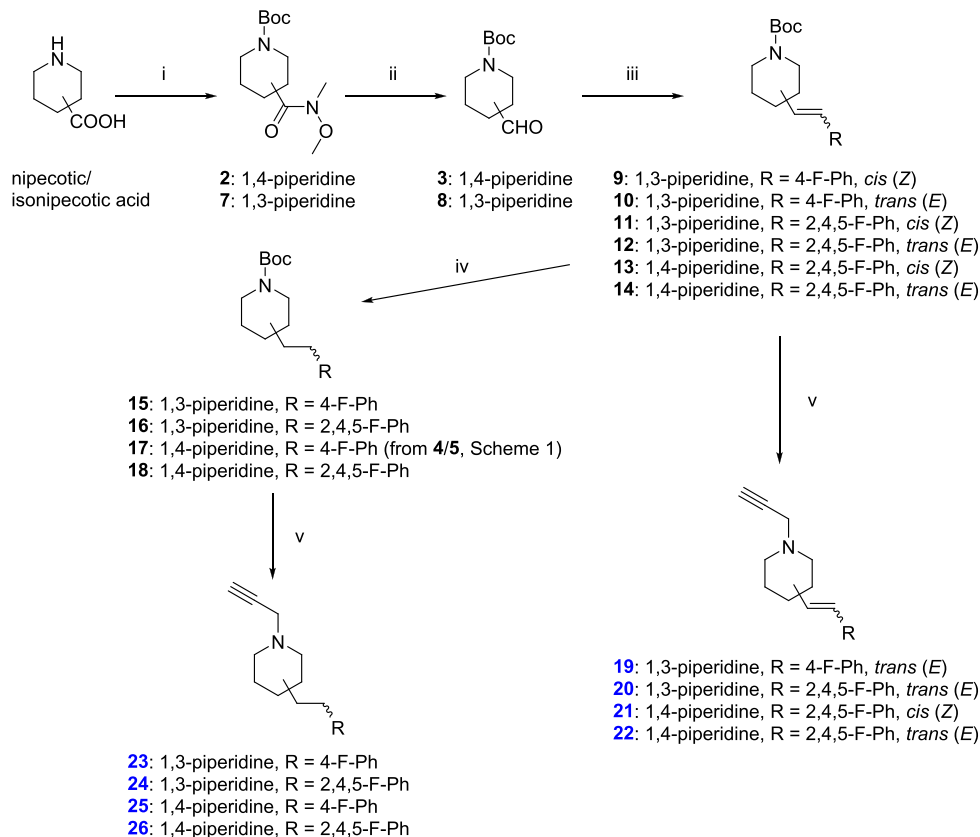


Figure 3. Undocking of *trans* (1) and *cis* (6) isomers in hMAO-A and hMAO-B. (A) Docked 6 in hMAO-A: *cis* isomer (yellow sticks) with propargyl group facing the FAD cofactor (green sticks), with binding energy of -8.3 kcal/mol; bottleneck residues at the active site entrance at the back (salmon sticks). (B) Energy profile for undocking of 6 from active site of hMAO-A in the correct conformation (propargyl facing FAD). (C) Docked 1 in hMAO-A: *trans* isomer (violet sticks) with propargyl group facing the FAD cofactor (green sticks), with binding energy of -6.2 kcal/mol; bottleneck residues at active site entrance at the back (salmon sticks). (D) Energy profile for undocking of 1 from active site of hMAO-A. (E) Docked 6 in hMAO-B: *cis* isomer (gray sticks) with propargyl group facing FAD cofactor (green sticks), with binding energy of -6.5 kcal/mol; bottleneck residues at entrance at the back (violet sticks). (F) Energy profile for undocking of 6 from active site of hMAO-B. (G) Docked 1 in hMAO-B: *trans* isomer (purple sticks) with propargyl group facing FAD cofactor (green sticks), with binding energy of -7.4 kcal/mol; bottleneck residues at entrance at the back (violet sticks). (H) Energy profile for undocking of 1 from active site of hMAO-B.

correctly oriented *trans* isomer. This noncovalent only binding of the *trans* isomer might lead to the worse performance observed experimentally of this inhibitor with hMAO-A.

In hMAO-B, the docked *cis* ligand 6 in the correct orientation in the active site has energy of -6.5 kcal/mol

(Figure 3E; movie file [jm9b01886_si_003.mp4](#) in Supporting Information). No energy peaks were observed along the active site for this isomer, whereby the energy reaches a plateau of 4.6 kcal/mol near the active site entrance (Figure 3F). *Trans* isomer 1 in the correct orientation has the energy of -7.4 kcal/

Scheme 2. Synthesis of Inhibitors 19–26^a

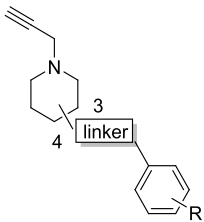
^aReagents and conditions: (i) 1) Boc_2O , 1.0 M NaOH, 1,4-dioxane, 0 °C, rt, 1–3 h (86–91%); (2) N,O -dimethylhydroxylamine hydrochloride, Et_3N , TBTU, CH_2Cl_2 , 0 °C to rt, overnight (76–82%); (ii) LiAlH_4 , anh THF, 0 °C, 1–2 h (crude products, 79–83%); (iii) corresponding Wittig salts ((4-fluorobenzyl)triphenylphosphonium bromide or (2,4,5-trifluorobenzyl)triphenylphosphonium bromide), NaHMDS (2 N in THF), anh THF, Ar(g), rt, overnight (overall yield for both isomers combined, 47–56%); (iv) corresponding mixture of *cis* and *trans* isomer (9–14), H_2 (g), Pd/C, EtOH, rt, overnight (97–100%); (v) (1) 4.0 M HCl in 1,4-dioxane, 80 °C, 2 h (100%); (2) propargyl bromide (80% solution in toluene), Cs_2CO_3 , DMF, Ar(g), 0 °C, rt, overnight (26–85%).

mol (Figure 3G; movie file [jm9b01886_si_003.mp4](#) in Supporting Information), which is lower than the energy of the *cis* isomer, and then this falls further to -8.2 kcal/mol at the lowest point on the way out of the entrance (Figure 3H). The energy barrier to reach the active site is lower for the *trans* isomer than it is for the *cis* isomer, with the highest peak of 1.5 kcal/mol near the entrance, which is lower than the 4.6 kcal/mol energy barrier for the *cis* isomer. This lower energy barrier of the *trans* isomer at the entrance might be explained by the smaller maximum width of the *trans* isomer compared to the *cis* isomer, as discussed above. We also note that the docked *trans* inhibitor position in the active site has a root-mean-square deviation of 2.1 Å, compared to the cocrystal structure of inhibitor 1 in hMAO-B reported in the present study (PDB code 6RKB). This indicates that the docking successfully predicted the positioning of this inhibitor in the active site. In agreement with the experimental findings, the lower binding energies at the active site for the *trans* isomer and the lower energy barrier to reach the active site for the *trans* isomer indicate that the binding of *trans* isomer 1 to hMAO-B is favored compared to the binding of *cis* isomer 6.

The distinct activity of this geometric isomer pair prompted us to study the structure–activity relationships (SARs) through the construction of a focused library of substituted piperidines (19–26; Scheme 2, Table 1) to probe the effect of piperidine disubstitution pattern on the inhibitory potency.

1,4-Disubstituted piperidines were the most tolerated and showed the highest selectivity for both hMAO-A and hMAO-B, and thus several analogues with various substituents on the phenyl ring were synthesized (Scheme 3, compounds 67–107).

Structure–Activity Relationships and Stability of Compounds. Hit inhibitor 1 and the synthesized analogues 6, 19–26, and 67–107 were evaluated for their inhibition of both hMAO-A and hMAO-B using a horseradish peroxidase (HRP)–Amplex Red coupled assay (Table 1). The most important findings regarding the SARs are summarized in Figure 4. Scanning the 1,3- and 1,4-disubstitution patterns of piperidine derivatives with the *trans* configuration of the double bond revealed at least 5-fold superior inhibition of hMAO-B for the 1,4-disubstitution (e.g., 19 IC_{50} = 1470 nM vs 1 IC_{50} = 342 nM). Interestingly, reduction of the double bond retained this selective hMAO-B inhibition (IC_{50} of 243 nM and 370 nM for hit compound 1 and analogue 25, respectively). Broadening the series of 1,4-disubstituted piperidines showcased selective inhibition of hMAO-A by *cis* analogues with small substituents on the phenyl ring (e.g., fluorine). The most potent was 69, a 3-fluorophenyl derivative, with an IC_{50} of 68.4 nM and almost a 3-log unit selectivity over hMAO-B. On the other hand, the *trans* derivatives preferentially inhibited hMAO-B, with a general trend of improved inhibitory potencies with increasing hydrophobicity/size of the sub-

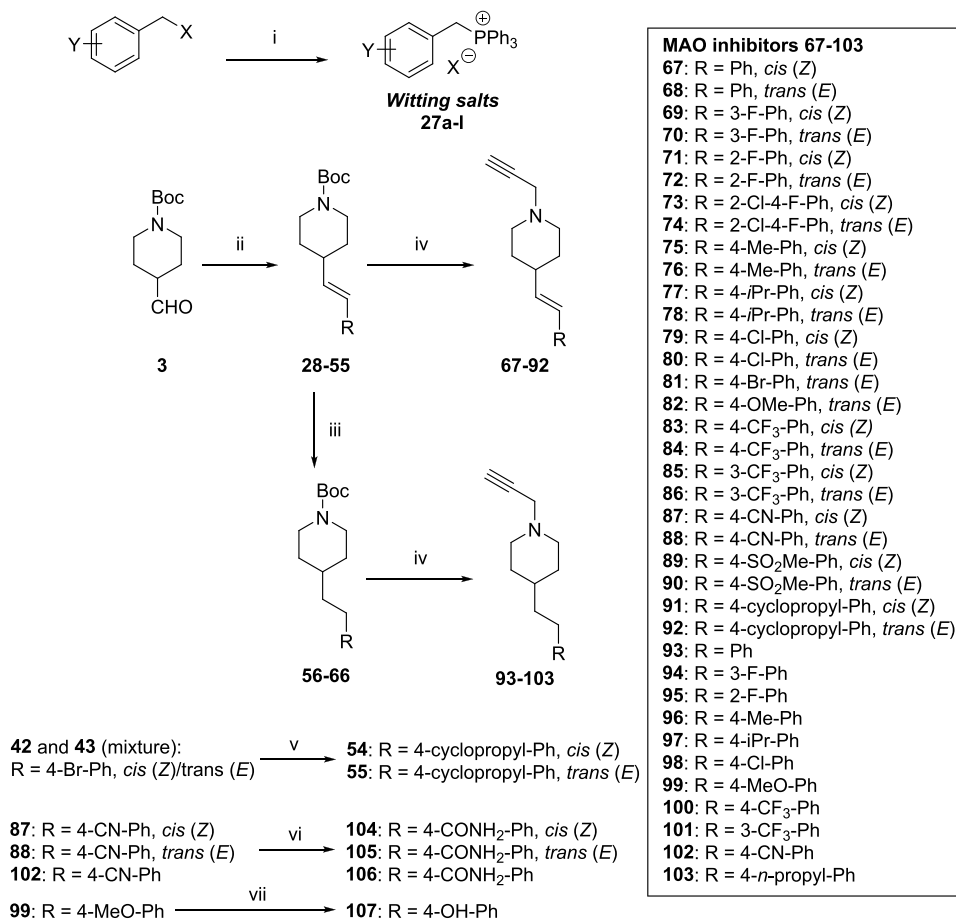
Table 1. Inhibitory Potencies and Structures of Hit Compound 1 and All of the Synthesized Inhibitors and Positive Controls^a


compd	structure			IC ₅₀ ± SEM [nM] or % RA ± SD at 100 μM		selectivity ratio ^c
	Pdp ^b	linker	R	hMAO-A	hMAO-B	
1	1,4	trans-vinyl	4-F	60.2 ± 1.6%	342.2 ± 22.4	>292
6	1,4	cis-vinyl	4-F	726.1 ± 26.9	6221.5 ± 726.8	0.12
25	1,4	ethyl	4-F	76.9 ± 2.2%	370.1 ± 37.3	>270
21	1,4	cis-vinyl	2,4,5-F	5243.7 ± 323.4	66.5 ± 3.9%	<0.05
22	1,4	trans-vinyl	2,4,5-F	81.2 ± 3.1%	436.2 ± 11.7	>229
26	1,4	ethyl	2,4,5-F	65.6 ± 4.4%	216.4 ± 14.2	>462
19	1,3	trans-vinyl	4-F	91.0 ± 3.1%	1469.5 ± 233.2	>68
23	1,3	ethyl	4-F	93.1 ± 3.2%	7411.6 ± 1190.0	>13
20	1,3	trans-vinyl	2,4,5-F	102.5 ± 5.2%	2195.6 ± 228.3	>46
24	1,3	ethyl	2,4,5-F	86.0 ± 5.2%	11229.4 ± 974.7	>9
67	1,4	cis-vinyl	H	168.8 ± 8.5	79.1 ± 4.0%	<0.002
68	1,4	trans-vinyl	H	32960.7 ± 3476.5	3540.2 ± 611.8	9
93	1,4	ethyl	H	75779.6 ± 7566.0 ^d	4603.4 ± 371.1	16
69	1,4	cis-vinyl	3-F	68.4 ± 4.3	48912.0 ± 2525.4	0.001
70	1,4	trans-vinyl	3-F	6906.8 ± 860.2	5048.7 ± 1224.6	1.4
94	1,4	ethyl	3-F	19927.3 ± 1608.5	3363.5 ± 310.5	6
71	1,4	cis-vinyl	2-F	3013.7 ± 207.3	65.5 ± 0.3%	<0.03
72	1,4	trans-vinyl	2-F	27293.2 ± 1758.4	11830.4 ± 766.5	2
95	1,4	ethyl	2-F	5927.3 ± 223.8	14159.5 ± 708.9	0.4
73	1,4	cis-vinyl	2-Cl-4-F	46121.5 ± 10141.6	53000.5 ± 2662.5	0.9
74	1,4	trans-vinyl	2-Cl-4-F	66028.4 ± 8419.0	417.6 ± 46.9	158
75	1,4	cis-vinyl	4-Me	62.2 ± 4.4%	19162.8 ± 5139.7	>5
76	1,4	trans-vinyl	4-Me	57.3 ± 2.9%	147.0 ± 13.8	>680
96	1,4	ethyl	4-Me	68.1 ± 1.6%	159.0 ± 13.3	>630
77	1,4	cis-vinyl	4-iPr	83.2 ± 0.5%	1883.9 ± 278.6	>53
78	1,4	trans-vinyl	4-iPr	73638.2 ± 11010.1 ^d	44.4 ± 8.2	1658
97	1,4	ethyl	4-iPr	162399.3 ± 9715.9 ^d	7.0 ± 2.2	23200
79	1,4	cis-vinyl	4-Cl	118844.3 ± 26412.7 ^d	11745.1 ± 555.9	10
80	1,4	trans-vinyl	4-Cl	71.7 ± 0.2%	50.4 ± 4.7	>1984
98	1,4	ethyl	4-Cl	67.7 ± 0.0%	38.1 ± 6.8	>2625
81	1,4	trans-vinyl	4-Br	54.5 ± 1.2%	21.2 ± 4.2	>4717
82	1,4	trans-vinyl	4-OMe	56.1 ± 1.6%	68.1 ± 11.1	>1468
99	1,4	ethyl	4-OMe	62.2 ± 1.9%	67.0 ± 11.4	>1493
83	1,4	cis-vinyl	4-CF ₃	80.1 ± 4.5%	1506.6 ± 216.3	>66
84	1,4	trans-vinyl	4-CF ₃	64.9 ± 0.5%	18.6 ± 3.3	>5376
100	1,4	ethyl	4-CF ₃	62.3 ± 0.7%	10.9 ± 3.0	>9174
85	1,4	cis-vinyl	3-CF ₃	858.0 ± 29.2	9352.5 ± 1512.9	0.09
86	1,4	trans-vinyl	3-CF ₃	64.8 ± 4.0%	549.7 ± 127.5	>182
101	1,4	ethyl	3-CF ₃	71.6 ± 2.2%	501.8 ± 107.1	>199
87	1,4	cis-vinyl	4-CN	68.1 ± 2.7%	1745.3 ± 315.4	>57
88	1,4	trans-vinyl	4-CN	129064.0 ± 8079.7 ^d	57.0 ± 7.1	2264
102	1,4	ethyl	4-CN	21478.3 ± 6280.3	56.6 ± 8.7	379
89	1,4	cis-vinyl	4-SO ₂ Me	70.6 ± 5.8%	8444.7 ± 627.1	>12
90	1,4	trans-vinyl	4-SO ₂ Me	68.7 ± 0.2%	32.7 ± 2.5	>3058
91	1,4	cis-vinyl	4-cyclopropyl	7398.7 ± 661.8	2640.1 ± 342.8	3
92	1,4	trans-vinyl	4-cyclopropyl	20564.5 ± 2315.8	43.7 ± 6.4	471
103	1,4	ethyl	4-propyl	80305.3 ± 9033.0	36.1 ± 4.1	2225
104	1,4	cis-vinyl	4-CONH ₂	89.5 ± 0.6%	51019.0 ± 6046.5	2
105	1,4	trans-vinyl	4-CONH ₂	64.8 ± 1.1%	1737.0 ± 691.0	58
106	1,4	ethyl	4-CONH ₂	75.1 ± 2.2%	5554.5 ± 1778.9	>18
107	1,4	ethyl	4-OH	67.7 ± 0.5%	7440.7 ± 1291.3	>13

Table 1. continued

compd	structure			IC ₅₀ ± SEM [nM] or % RA ± SD at 100 μM		selectivity ratio ^c
	Pdp ^b	linker	R	hMAO-A	hMAO-B	
pargyline				3967.9 ± 275.1	195.5 ± 19.1	20
L-deprenyl				62663.8 ± 4113.6	12.1 ± 4.2	5179
rasagiline				29520 ± 8597	36.0 ± 4.1	820
clorgiline				3.4 ± 0.3	13568.4 ± 1157.3	0.0003

^aData are mean values ± SEM: IC₅₀ (in boldface), *n* = 2, 3; residual activity (RA), *n* = 2. ^bPdpn: piperidine disubstitution pattern. ^cSelectivity ratio is defined as IC₅₀(hMAO-A)/IC₅₀(hMAO-B). ^dEstimated IC₅₀ values from the RAs below 100 μM. Compounds showed precipitation in the assay buffer at concentrations above 100 μM.

Scheme 3. Synthesis of Inhibitors 67–107^a

^aReagents and conditions: (i) benzyl halide, PPh₃, MeCN, 85 °C, overnight (80–97%); (ii) corresponding Wittig salts (27a–l), NaHMDS (2 N in THF)/KHMDs (0.5 M in toluene), anhyd THF, Ar(g), rt, overnight (overall yield, 30–66%); (iii) mixture of *cis* and *trans* isomers (28–55), H₂(g), Pd/C, EtOH, rt, overnight (83–100%); (iv) (1) 4.0 M HCl in 1,4-dioxane (or HCl in EtOH), 80 °C, 2 h (100%); (2) propargyl bromide (80% in toluene), K₂CO₃, MeCN, Ar(g), 0 °C, rt, overnight (6–89%); (v) cyclopropylboronic acid, K₃PO₄, tricyclohexylphosphine (20% in toluene), Pd(OAc)₂, toluene, water, Ar(g), 100 °C, 3 h (78%); (vi) KOH, *t*BuOH, 90 °C, 12–24 h (42–63%); (vii) BBr₃ (1 M in CH₂Cl₂), toluene, Ar(g), –20 °C, 1 h, rt, 1 h (57%).

stituents on phenyl ring position 4 (–H < –F < –Cl < –Br and –H < –Me < –*i*Pr ~ –cyclopropyl). Double-digit nanomolar inhibition of hMAO-B was also obtained for 82, 84, 88, and 90 with –OMe, –CF₃, –CN, –SO₂Me substituents, respectively, on position 4 of the phenyl ring. Compounds with an ethyl moiety that connected the rings showed comparable selective inhibition of hMAO-B as their *trans* congeners. All the *N*-propargylpiperidine derivatives inhibited corresponding isoenzyme in an irreversible manner as demonstrated by the 100-fold dilution assay.

For additional experiments, compounds 1, 6, 67, 69, 84, 97, and 100 were used in the form of hydrochloride salts to avoid possible solubility issues. The thermodynamic solubility of the compounds in PBS (pH 7.4) was at least 17.6 g/250 mL, 10.5 g/250 mL, 8.6 g/250 mL, 12.5 g/250 mL, 14.5 g/250 mL, and 16.3 g/250 mL for 6, 67, 69, 84, 97, and 100, respectively, which is good solubility according to biopharmaceutical classification for any realistically expected dose of investigated compounds.

Possible chemical instability and photoisomerization of *E/Z* isomers were also addressed as these are known liabilities of

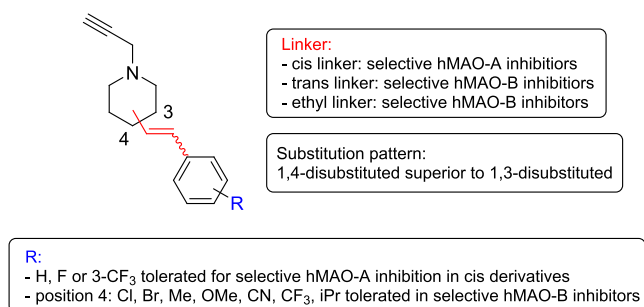


Figure 4. Crucial observations regarding SARs of the stilbene-like MAO inhibitors.

stilbene derivatives.²³ Proton NMRs of **69** (*cis* derivative), **84** (*trans* derivative), and **100** (ethyl analogue) in the form of hydrochloride salts were recorded in D₂O (Figures S1–S3). Inspection of the spectra confirmed that these compounds are relatively stable after more than 1 year of storage at room temperature (protected from sunlight) as only smaller amounts of impurities were detected for **84** (in the aromatic area), whereas compounds **69** and **100** showed no signs of chemical instability. The samples dissolved in the NMR tubes were then left on the benchtop exposed to natural daylight for 7 days, which could induce photoisomerization. No spectral changes were observed in comparison to spectra of freshly prepared samples. Altogether, these studies imply reasonable stability of the compounds.

Kinetic Evaluation. The exploration of SARs allowed the identification of a few compounds for more in-depth kinetic analysis with the purified enzyme samples, which allowed their inhibition mechanism to be better defined. On the basis of

their inhibitory potencies and molecular features, compounds **1**, **84**, and **97** were selected for hMAO-B, whereas for hMAO-A the analysis was restricted to **69**. The inhibitors were tested using UV–vis spectrum measurements (Figure 5) and steady-state enzymatic assays (Table 2). The propargyl unit is known to react covalently with the N5 atom of the flavin cofactor by rapidly forming a stable covalent adduct that produces a typical modification of the spectrum; this is seen as bleaching of the peak at 450 nm and appearance of a stronger peak at 415 nm.²⁴ All of these selected compounds were tested by adding them in 10-fold excess to the protein solution in the spectrophotometer cuvette and measuring the spectra over time until no further modification was detected. All of the irreversible inhibitors produced a clear change in the enzyme spectra (Figure 5), similar to other classic acetylenic inhibitors, like L-deprenyl and clorgyline.²⁴ However, there were differences in the times required to complete the reactions for the adduct formation, i.e., to reach the final spectrum with no further modification. While **69** fully inactivated hMAO-A almost instantaneously (Figure 5A), similar to clorgyline, the hMAO-B selective compounds were slower. In particular, **84** initiated the reaction with the flavin within 1 min, showing an intermediate spectrum profile that evolved into the final 415 nm peak in 30 min (Figure 5B). Instead, **1** and **97** did not show any spectral modifications in the first few minutes and required half an hour to obtain an intermediate profile and more than 2 h to complete the reaction (Figure 5C and Figure 5D, respectively).

Full kinetic analysis was then undertaken for hMAO-A and hMAO-B inhibition by the selected compounds, using purified enzyme samples and the spectrophotometric version of the assay coupled to HRP that was used for IC₅₀ determination, as described above. As enzyme inhibition by propargyl-based

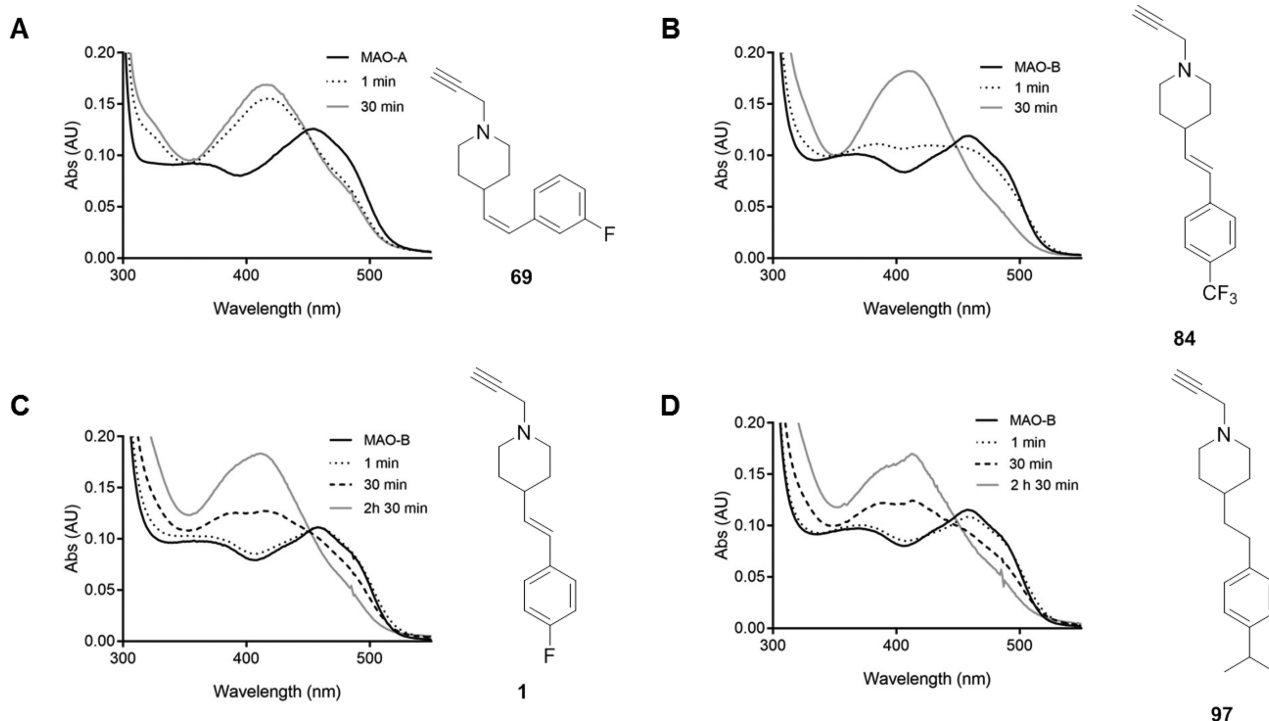


Figure 5. UV–vis absorption spectra of the hMAO enzymes after FAD cofactor modification by irreversible covalent inhibitors. The oxidized enzyme (10 μ M) before inhibitor addition (100 μ M) is shown as the continuous black line, whereas the gray profile indicates the final spectrum (i.e., no further changes were observed), which was reached at different times depending on the inhibitor. The intermediate spectra are shown as either dotted or dashed lines. (A) hMAO-A and **69**; (B) hMAO-B and **84**; (C) hMAO-B and **1**; (D) hMAO-B and **97**.

Table 2. Kinetic Parameters for the Reversible and Irreversible Inhibition of the hMAOs by the Selected 4-Styrylpyridine Inhibitors

MAO	inhibitor	reversible inhibition		irreversible inhibition	
		K_i (μM)	K_i (μM)	k_{inact} (min^{-1})	k_{inact}/K_i ($\text{min}^{-1} \mu\text{M}^{-1}$)
hMAO-A	69	0.23 ± 0.02	1.01 ± 0.76	1.25 ± 0.25	1.24
	clorgyline ^a	0.040 ± 0.004^b	0.22 ± 0.08^b	0.12 ± 0.05^b	0.55^b
hMAO-B	1	1.92 ± 0.32	1.38 ± 0.29	0.66 ± 0.04	0.48
	84	1.25 ± 0.23	17.25 ± 4.38	2.03 ± 0.38	0.12
	97	1.36 ± 0.31	6.55 ± 1.62	1.04 ± 0.12	0.16
	L-deprenyl ^a	0.97 ± 0.11	5.68 ± 0.78	2.56 ± 0.24	0.45

^aKinetic parameters were compared to clorgyline and L-deprenyl in the cases of hMAO-A and hMAO-B selective inhibitors, respectively. ^bData from Esteban et al. (2014).²⁵

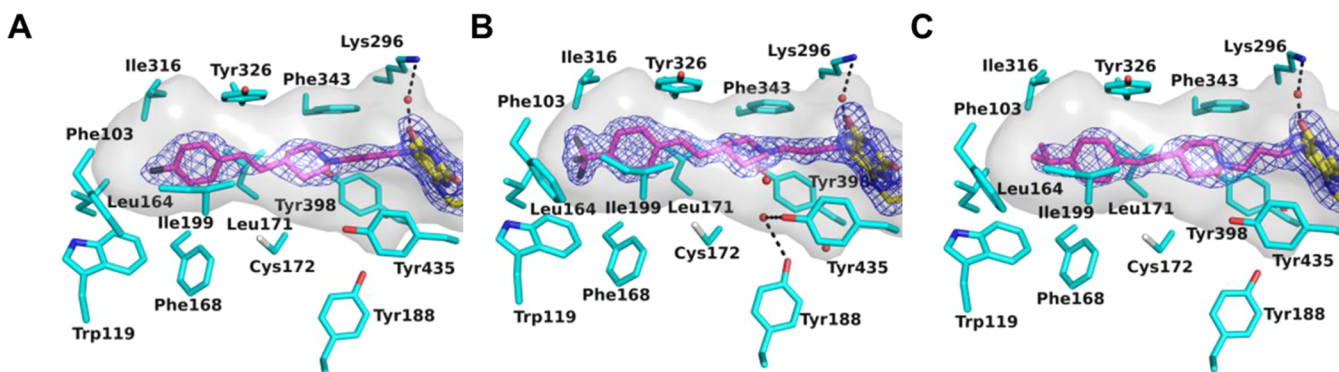


Figure 6. Crystal structures of the active site of hMAO-B-inhibitor complexes. The hMAO-B active site cavity is shown as a gray semitransparent surface, which is lined by the protein residues (represented in cyan). Water molecules are red spheres, and hydrogen bonds are dashed lines. The FAD cofactor is in yellow stick representation. The inhibitor molecule bound in the hMAO-B active site cavity is shown as sticks, with carbon, nitrogen, and fluorine in magenta, blue, and black, respectively. The refined $2F_o - F_c$ electron density map contoured at 1.2σ is shown in blue for the inhibitor and the FAD molecules. (A) Active site of hMAO-B in complex with **1** (2.3 Å resolution; PDB code 6RKB). (B) Active site of hMAO-B in complex with **84** (1.7 Å resolution; PDB code 6RKP). (C) Active site of hMAO-B in complex with **97** (2.3 Å resolution; PDB code 6RLE).

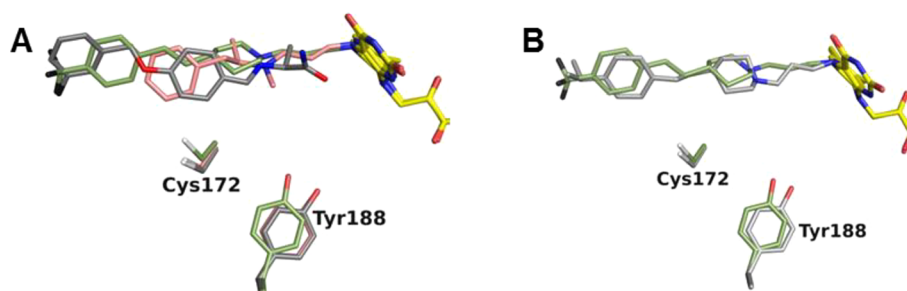


Figure 7. Structural superposition to highlight differences and common features in the binding modes of the hMAO-B inhibitors. The protein, inhibitor, and cofactor atoms are represented as sticks (color code as in Figure 6 except for the carbon atoms of protein and inhibitor molecules, which are depicted accordingly to distinguish the different structures). For clarity, only Cys172 and Tyr188 of the protein active site residues are shown, which undergo some conformational changes. (A) Superposition of structures in complex with **84** (green), safinamide (gray) and L-deprenyl (pink). (B) Superposition of structures in complex with **84** (green) and **97** (light gray).

inhibitors involves a first step in which the ligand is accommodated into the protein active site to be correctly oriented for flavin adduct formation, competitive inhibition can be measured under steady-state conditions using kynuramine and benzylamine as substrates for hMAO-A and hMAO-B, respectively. Thus, both the reversible and irreversible inhibition parameters were determined (Table 2). Compound **69** is a potent hMAO-A inhibitor with a reversible K_i of 0.23 μM , which is 5-fold higher than that reported for clorgyline. This difference is in line with the irreversible constant K_i , and it is balanced by the irreversible inactivation velocity that is 10-fold higher than that for clorgyline. Overall, **69** is a very potent

hMAO-A inhibitor with comparable activity to clorgyline. Similar to L-deprenyl, in the case of hMAO-B selective ligands, the reversible K_i values are all in the micromolar range. The irreversible constant K_i for covalent hMAO-B inhibitors is in general 5-fold the reversible K_i ; however, the k_{inact}/K_i indicated comparable inhibitory potencies of the hMAO-B inhibitors to L-deprenyl.

Structure of hMAO-B in Complex with Inhibitors. Structural studies were performed by cocrystallization of hMAO-B with the inhibitors selected for the kinetic analyses, using previously published procedures.²⁶ Structures for inhibitors **1**, **84**, and **97** were solved at resolution ranging

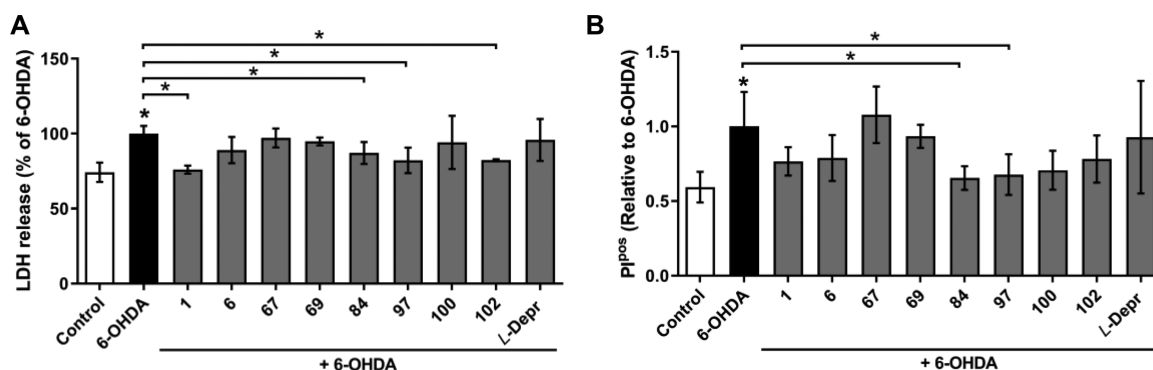


Figure 8. Effects of inhibitors on 6-OHDA-induced cell death in SH-SY5Y cells. (A, B) SH-SY5Y cells were pretreated with the compounds (5 μ M) for 30 min (as indicated) and then treated with 6-OHDA (100 μ M). After 24 h, LDH assays (A) and PI staining (B) were performed. Data are mean values \pm standard deviation ($n \geq 2$; each in duplicate): *, $p < 0.05$ (one-way ANOVA, with Bonferroni correction, followed by t -tests).

from 2.3 to 1.7 Å (Figure 6). The crystallographic statistics are reported in Table S1. Crystallographic studies on hMAO-B in complex with **1**, **84**, and **97** showed that these inhibitor molecules are certain to be bound to the enzyme active site (Figure 6). Ligand binding does not cause any major conformational changes to the overall protein dimeric structure (Figure S4). As for all of the inhibitors, the structure of the active site is identical in the two monomers present in the asymmetric unit that forms the protein dimer, and here we will refer to chain A of each structure in the following discussion. The electron density map clearly showed that all of these inhibitors form a covalent adduct with the flavin (Figure 6).

All of these inhibitors bind to the hMAO-B active site in a similar fashion, from the covalent adduct with the flavin to the 4-substituted phenyl ring at the other end of the molecule (Figure 6). They adopt an extended conformation, as they occupy both the substrate and the cavity spaces (Ile199 in the open conformation). The 4-substituted phenyl ring is constrained by the flat hydrophobic shape of the hMAO-B cavity in a position perpendicular to the flavin plane, as for other well-known inhibitors, such as L-deprenyl and safinamide (Figure 7A). The site occupied by the halogen substituent on the aromatic ring of **1** is also conserved, which is a common feature of many hMAO-B inhibitors.²⁷ The more polar substituents that have lower inhibitory activities (e.g., **82**, **105**) would be much less favored in their binding to this highly hydrophobic site. The enzyme active site architecture does not undergo any conformational change with respect to that of other hMAO-B structures except for minor modifications to the side chains of Cys172 and Tyr188 (Figure 7A). This is due to the position adopted by the piperidine ring that represents the hallmark of this series of inhibitors. Despite the flat shape of the hMAO-B cavity, the nonplanar conformation of the piperidine and its pyramidal nitrogen that is involved in the covalent adduct constrain the piperidine ring to bind perpendicular to the plane of the cavity (Figure 6). Instead, with other inhibitors such as L-deprenyl and safinamide, there is an aromatic ring that binds coplanar with the cavity plane and with any substituted aromatic at the other end of the molecule, if present (Figure 7A). Therefore, the position of the piperidine in the upper part of the cavity allows Cys172 and Tyr188 to move slightly upward. In the structure of the complex with **97**, the conformation of the Cys172 and Tyr188 is conserved to some extent with respect to the previous structures. This is due to the linker that is devoid of the double bond, and the consequent tetrahedral conformation of its carbon atoms

results in a more contracted conformation of the inhibitor molecule with respect to **84** (Figure 7B) and **1**. As a result, the piperidine collapses toward the bottom of the cavity, and the covalent linkage is forced to adopt a slightly different conformation with respect to the other propargyl inhibitors (Figure 7).

Cell-Based Assays. Following the chemical-space exploration and kinetic and structural evaluations, several of these structurally diverse hMAO-A and hMAO-B inhibitors were also tested *in vitro* in cell models. First, their cytotoxicity profiles were defined using the SH-SY5Y human neuroblastoma cell line. By use of the MTS assay, no significant cytotoxic effects were seen for 24 h treatments of these cells with the compounds **1**, **6**, **67**, **69**, **84**, **97**, **100**, and **102** at concentrations of 5 μ M and 10 μ M (Figure S5). Indeed, at 50 μ M, the cell viabilities remained >80% for almost all of the compounds, which is roughly 3 log units higher than the concentrations needed to achieve 50% *in vitro* inhibition of either of the two MAO isoforms.

The experimental *in vitro* cell model with the neurotoxin 6-hydroxydopamine (6-OHDA) is commonly used to study neurodegenerative processes, as it induces toxicity that mimics the biochemistry and neuropathology of Parkinson's disease.²⁸ To determine the possibility that MAO inhibitors can abrogate 6-OHDA-induced toxicity, we examined lactate dehydrogenase (LDH) release and propidium iodide (PI) staining in the SH-SY5Y cells after 30 min pretreatment with the compounds at the noncytotoxic concentration of 5 μ M, followed by 6-OHDA treatment for 24 h (Figure 8). The active treatment with 6-OHDA significantly increased LDH release (135% vs control), while pretreatment with compounds **1**, **84**, **97**, and **102** protected against this increased LDH release (76%, 87%, 82%, 82% vs 6-OHDA, respectively), thus indicating improved cell viability. In the confirmation using flow cytometry, the proportion of PI-positive cells increased after the active 24 h treatment with 6-OHDA and was significantly reduced following the pretreatments with the hMAO-B inhibitors **84** and **97** (0.65 and 0.68, respectively), compared to the 6-OHDA-treated cells. Altogether, this indicates that the selective hMAO-B inhibitors **84** and **97** reduced the 6-OHDA-induced cytotoxicity and increased the viability of these SH-SY5Y neuronal-like cells.

In Vivo MAO Inhibition in Mouse Brain Homogenates and in Vitro Permeability. The inhibition of the MAOs in mouse brain homogenates was also investigated both *in vitro* and *ex vivo* (Table 3). Here, the more potent of the inhibitors

Table 3. *In Vitro* and *ex Vivo* Mouse Brain Homogenate Residual Activities of **69** and **100** at 60 mg/kg ip on MAO-A and MAO-B According to Substrate^a

compd	residual activity (%)					
	MAO-A substrate		MAO-A/B substrate		MAO-B substrate	
	5-HT (0.25 mM)		p-tyramine (0.5 mM)		benzylamine (0.5 mM)	
	<i>in vitro</i> ^b	<i>ex vivo</i> ^c	<i>in vitro</i> ^b	<i>ex vivo</i> ^c	<i>in vitro</i> ^b	<i>ex vivo</i> ^c
69	−1.3 ± 0.1	1.6 ± 0.02	31.3 ± 0.2	14.2 ± 0.2	nd	nd
100	nd	nd	59.4 ± 0.2	77.2 ± 0.2	−7.7 ± 0.2	24.3 ± 0.5

^aData are mean values ± SD (*n* = 1, in triplicate). nd, not determined. ^b*In vitro*: 50 μM compounds (final concentrations) versus 0.9% saline with mouse brain homogenate from nontreated mice. ^c*Ex vivo*: brain homogenates from mice treated (*n* = 3, per group) with 60 mg/kg ip compounds or 0.9% saline 30 min before brain homogenate preparation.

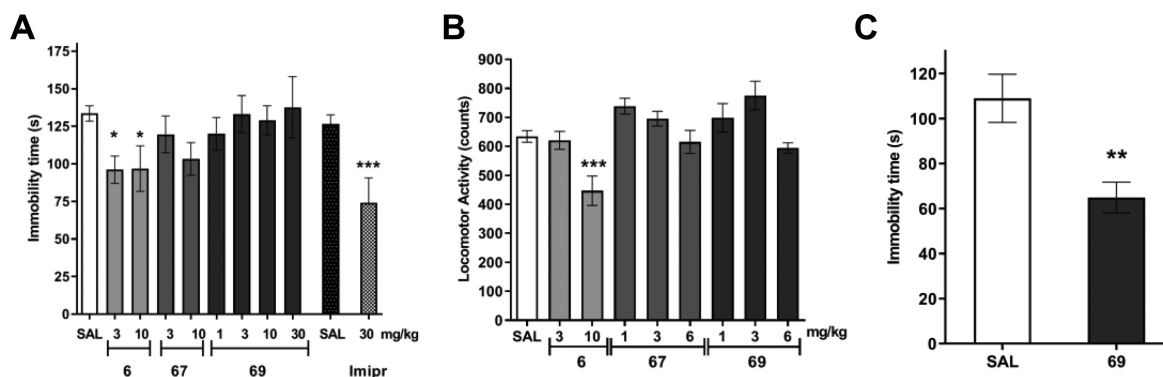


Figure 9. *In vivo* evaluation in mice of antidepressant-like activity of the selective MAO-A inhibitors **6**, **67**, and **69**. (A) Effects of acute ip treatment with **6** (3, 10 mg/kg, *n* = 13, 9), **67** (3, 10 mg/kg, *n* = 6, 10), and **69** (1, 3, 10, 30 mg/kg, *n* = 8, 7, 8, 6) and imipramine (30 mg/kg, *n* = 8) in the tail suspension test. Data are mean values ± SEM of immobility time in comparison to control mice (SAL, *n* = 23): *, *p* < 0.05; ***, *p* < 0.001 (one-way ANOVA, followed by Dunnett's tests). (B) Effects of acute ip treatment with **6** (3, 10 mg/kg, *n* = 8, 8), **67** (1, 3, 6 mg/kg; *n* = 5, 5, 5), and **69** (1, 3, 6 mg/kg, *n* = 10, 5, 5) on locomotor activity of the mice. Data are mean values ± SEM of spontaneous locomotor activity counts recorded in 5 min sessions: ***, *p* < 0.001 (one-way ANOVA, followed by Dunnett's tests). (C) Effects of 10-day chronic ip treatment with **69** (0.3 mg/kg, daily; *n* = 10) in the tail suspension test. Data are mean values ± SEM of the immobility time, compared to control mice (*n* = 8): **, *p* < 0.01 (unpaired *t*-test).

against hMAO-A (i.e., **69**) and hMAO-B (i.e., **100**) were tested based on their IC₅₀ values and structural features. Brain homogenates from male Swiss mice were first characterized in terms of their MAOs activity and substrate specificity (Table S2, Figure S6).

Compound **69** completely abolished MAO-A activity *in vitro* at 50 μM when 5-HT was used as the selective MAO-A substrate. Compound **100** at 50 μM inhibited mice MAO-B when benzylamine was used as the selective MAO-B substrate (Table 3). When the dual hMAO-A/B substrate *p*-tyramine was used, the inhibition was lower (i.e., higher residual activities; RAs). The same profile of inhibition was established *ex vivo* for brain homogenates from mice treated with these compounds, which were injected intraperitoneally (ip) 30 min before preparation of the brain homogenates. Again, more potent inhibition was seen in these brain homogenates when the isoenzyme-selective substrates were used. Selective MAO-A inhibitor **69** was the most active compound when administered at 60 mg/kg ip (RA, 1.6% ± 0.02%), while 60 mg/kg ip **100** resulted in similar MAO-B inhibition (RA, 24.3% ± 0.5%). Compounds **69** and **100** showed dose-dependent inhibition of these corresponding MAO isoforms (ED₅₀ of 0.43 ± 0.26 mg/kg and 1.38 ± 0.87 mg/kg, respectively).

MAO inhibitors are in clinical use for treatment of psychiatric and neurological disorders, where they are used in chronic, low-dose regimes.²⁹ These MAO-A and MAO-B activities in *ex vivo* mouse brain homogenates were therefore

studied after chronic 10-day administration to the mice of **69** and **100** at the low dose of 0.3 mg/kg ip. This chronic administration of selective MAO-A inhibitor **69** significantly reduced MAO-A activity compared to 0.9% saline ip in the control mice. After the single administration of **69** at 0.3 mg/kg ip, the *ex vivo* MAO-A RA was reduced to 67.8% ± 31.2% (i.e., compared to 0.9% saline), whereas the 10-day treatment resulted in MAO-A RA of 9.5% ± 23.4%. Similar to **69**, one single ip injection of **100** at 0.3 mg/kg showed MAO-B RA of 83.4% ± 19.2%, while chronic 10-day treatment resulted in RA of 28.3% ± 13.8%, which demonstrated accumulation of inhibition over time.

The *ex vivo* inhibitory activity of inhibitors **69** and **100** was also demonstrated in the mouse brain homogenates prepared 90 min after acute oral administration to the mice, via oral gavage at 30 mg/kg. Inhibitors **69** and **100** showed RAs of 45.3% ± 14.6% (vs 0.9% saline-treated mice) and 30.5% ± 10.4% (vs 0.9% saline treated mice), respectively. This prompted us to also study gut permeability of these representative inhibitors (i.e., **69**, **84**, and **100**) *in vitro* on rat intestine. The apparent bidirectional permeability coefficient for the rat intestine *in vitro* was determined for **69**. This was 108 ± 13 nm/s (as mean ± SEM) in the absorptive direction and 354 ± 99 nm/s in the eliminatory direction. For comparison, the apparent permeability coefficients of the internal low- and high-permeability standards furosemide and metoprolol in the absorptive direction were 64 ± 11 nm/s and 140 ± 18 nm/s, respectively.

Behavioral Studies with the Selective MAO-A and MAO-B Inhibitors. MAO-A inhibitors are currently used in the therapy of treatment-resistant major depressive disorder and some specific types of depression.³⁰ Symptoms of depression correlate highly with those of anxiety.³¹ These have been shown to be associated with 5-HT_{1A} receptors,³² which are presynaptic and postsynaptic G-protein-coupled receptors that are involved in neuromodulation. 5-HT_{1A} receptor agonists, such as buspirone, show efficacy for the relief of anxiety and depression.³² The binding affinities (K_i values) for this 5-HT_{1A} receptor subtype were thus determined for these MAO inhibitors to potentially further explain their behavioral effects. These ranged from low micromolar to submicromolar K_i values (Table S3). Following treatments with the selective irreversible MAO-A inhibitors **6**, **67**, and **69**, the Swiss mice were subjected to the different behavioral tasks to determine whether these compounds have any antidepressant-like activity, any activity in an anxiety model and whether they affect locomotor activity.³³

The antidepressant-like activity was screened with the widely used tail suspension test. At 30 min before the behavioral assays, the mice were treated with **6**, **67**, and **69** at 3 mg/kg and 10 mg/kg ip, with **69** also at 1 mg/kg and 30 mg/kg ip, or were injected with 0.9% saline as control. Imipramine (30 mg/kg ip) was used as the reference drug. Compounds **67** and **69** did not decrease the immobility time, whereas selective MAO-A inhibitor **6** and imipramine significantly reduced it, which demonstrated the antidepressant-like effects of these compounds under acute treatment (Figure 9A).

The performance of mice in the “elevated plus maze test” was used here as a rodent model of anxiety, which was carried out 30 min after the ip treatments with **6**, **67**, and **69** (Table S4). Compound **6** at the dose of 10 mg/kg ip induced a significant decrease compared to mice injected with 0.9% saline, for both the number of total arm entries (9.7 ± 2.9 vs 22.0 ± 1.5 ; $p < 0.001$) and the proportion of time spent in the center of the apparatus (13.4 ± 2.3 vs 43.5 ± 2.8 ; $p < 0.001$), and also an increase in the proportion of open-arm entries (2.0-fold; $p < 0.001$). Meanwhile, **69** at 3 mg/kg ip produced a significant increase in the proportion of open-arm entries (2.0-fold; $p < 0.001$) and in the time spent in those entries (2.1-fold; $p < 0.001$), similar to diazepam (reference drug) at 1 mg/kg ip (2.1-fold, 2.4-fold, respectively; $p < 0.001$ for both).

The locomotor activity of the mice was also determined, as it can affect the data obtained in these behavioral assays. It was shown that **6** at 10 mg/kg ip significantly decreased spontaneous locomotor activity (Figure 9B), which is correlated with the decrease in the total arm entries in the elevated plus maze test. This indicates that the effects of **6** after acute 10 mg/kg ip treatment are not associated with antidepressant-like or anxiolytic effects but rather with a decrease in the locomotion of the mice. On the other hand, the increased open arm parameters in the elevated plus maze for **69** (3 mg/kg ip) appear to be correlated with an anxiolytic-like effect, which would be mediated through the 5-HT_{1A} receptor, as locomotion was not altered at this dose of **69**. Importantly, chronic 10-day treatment with **69** at a low dose (i.e., 0.3 mg/kg ip, daily) significantly decreased the immobility time in the treated group (Figure 9C). No significant effects were seen for this chronic low dose of **69** in the elevated plus maze and locomotor activity tests (Table S5). This confirmed the antidepressant-like effects of **69** when administered chronically, which were not seen for the acute treatment regime.

Behavioral studies of the selective hMAO-B inhibitors were performed with compound **100** (irreversible MAO-B inhibitor). Although *trans* derivative **84** also showed potent irreversible MAO-B inhibition ($IC_{50} = 18.6 \pm 3.3$ nM; equipotent to **100**), it was not studied here *in vivo* due to its poor permeability in the rat gut (see above) and its low binding potential for the 5-HT_{1A} receptor (Table S3).

The hole-board test is commonly used to study stress-related changes in exploratory behavior of animals.³⁴ This was combined here with the locomotor activity test. At acute ip doses of ≥ 10 mg/kg of **100** in the mice, the hole-board test parameters and locomotor activities were reduced (Table S6, Figure S7A–C). Due to the locomotor impairment at high doses, compound **100** was further studied in the haloperidol-induced catalepsy test at lower doses (see Supplementary Results and Discussion). Compound **100** was also tested in the same battery of behavioral tests after 10 days of low-dose ip treatment (0.3 mg/kg, daily), where it did not affect the locomotor activity of the mice (Figure S7D) or the parameters of the hole-board test (Figure S8). During these 10-day treatments (i.e., **69**, **100** at 0.3 mg/kg ip, daily), the body mass of the mice was also monitored (Figure S9). No significant differences were seen for the proportions of body mass variations versus the control mice (0.9% saline treated). Also, all of these mice survived these 10-day treatments without any apparent signs of changes in behavior, which supports the general safety of these compounds.

DISCUSSION AND CONCLUSIONS

Biological receptors differ greatly in shape, polarity, and conformational dynamics.¹ However, it is a challenging task to obtain selectivity between structurally related targets such as isoenzymes, which requires different ligand-design approaches. MAO-A and MAO-B are two closely related isoenzymes where numerous selective inhibitors have been described in the literature, with some now used in the clinical setting for treatment of neurological disorders.³⁵

Selective hMAO-B inhibitor **6** was identified in a screening campaign, and chemistry-driven exploration of the chemical space revealed that the *trans* isomers selectively inhibit hMAO-B over hMAO-A. On the other hand, *cis* isomers were identified as selective hMAO-A inhibitors. The inhibitory potencies in the SARs exploration phase are generally expressed as IC_{50} values (Table 1), although these derivatives are irreversible. The IC_{50} values are thus dependent on the assay conditions and particularly on the preincubation period.³⁶ Despite these limitations, the measured IC_{50} values still allow relatively simple, yet not the most precise, comparisons between such compounds in a series.¹¹ The inhibitory activity against hMAO-B was increased by introducing bulkier and more lipophilic substituents onto position 4 of the phenyl ring, as previously reported in the literature.³⁷ A similar trend was also observed for the turnover of variously substituted substrates of the benzylamine and phenethylamine classes,³⁸ where the binding affinity improved with increasing hydrophobicity of the substituent.

Further examination of the binding kinetics for the selected compounds here using purified enzyme samples confirmed the variable nature of these IC_{50} values. The overall higher affinity inferred from the IC_{50} values (Table 1) compared to K_i (Table 2) is related to the covalent nature of these inhibitors, which fully inactivate the enzyme during the preincubation step in the absence of substrate (not included in competitive steady-state

experiments used to determine IC_{50}). For the same reason, the variability of the IC_{50} values among the different inhibitors that was not seen for K_i has to be interpreted in light of the time-dependent inactivation process that showed different kinetics depending on the inhibitor (Table 2). For example, **84** showed an IC_{50} that is 0.05-fold that of **1** and a similar reversible K_i , while its inactivation rate was 4-fold that of **1**, which results in a k_{inact}/K_i ratio that is comparable between these two inhibitors. Similar observations can be reasoned for the other covalent analogues and for L-deprenyl.

Crystallographic studies confirmed the covalent adduct formation with flavin for the inhibitors investigated here. A similar binding mode for all of these inhibitors was seen, with only minor modifications of the active site arrangements in comparison to other hMAO-B structures reported in the literature. These changes were most prominent with the *trans* inhibitors **1** and **84**, which imposed a slight upward shift of Cys172 and Tyr188. This is related to the conformation adopted by the piperidine ring, which represents the hallmark of this class of inhibitors, as a novel element with respect to previous propargyl inhibitors (i.e., where the nitrogen atom is within a linear molecular structure rather than part of a ring).

The inhibitor series studied here were not cytotoxic to SH-SY5Y cells up to treatments of 50 μ M. Remarkably, only the selective hMAO-B inhibitors decreased the LDH release induced by the neurotoxin 6-OHDA. The reduced proportion of PI-positive SH-SY5Y cells was also confirmed for the two MAO-B-selective ligands during 6-OHDA-induced toxicity. This indicated their neuroprotective nature, which might also be attributed, among others possibilities, to their selective MAO-B inhibition. Following ip and peroral administration, these compounds inhibited MAO-A and MAO-B activities *ex vivo* in the mouse brain homogenates. The extent of their inhibition varied depending on the inhibitor selectivity and the substrate used. Selective MAO-A inhibitor **69** completely inhibited MAO-A *ex vivo* when the MAO-A substrate 5-HT was used (RA, 1.6%), while its inhibition was lower when using *p*-tyramine (RA, 14.2%), which is a dual MAO-A/B substrate. The difference is even more evident for the MAO-B inhibitors, with decreased inhibition when switching from the MAO-B substrate benzylamine to dual substrate *p*-tyramine. Both MAO-A and MAO-B can metabolize *p*-tyramine; however, only one of them was inhibited by the selective inhibitor, which explained the impaired inhibition. This additionally confirmed the *in vitro* selectivity of these inhibitors not only on the isolated human enzymes but also in complex matrices, such as mouse brain homogenates. The MAO inhibition in these mouse brain homogenates after peroral single-dose administration also indicated the oral bioavailability of these analogues. The *in vitro* permeability of **69** studied for rat intestine was between that of the low-permeability and high-permeability standards, and as such, **69** should be classified with an intermediate/moderate permeability, with the possibility of interference by the intestinal efflux mechanisms, as seen by the higher apparent permeability coefficient determined for the eliminatory direction. The permeabilities of **84** and **100** were not determinable *in vitro* due to their high tissue binding. These findings do not correlate directly with the *ex vivo* effects; however, the *ex vivo* effects show that both **69** and **100** reached the brain tissue and inhibited the MAO activity after their oral administration.

Under the acute treatment regime in these mice, the selective MAO-A inhibitor **69** did not affect the immobility

time of the mice in the tail suspension test. The observed anxiolytic-like activity with acute treatment with **69**, which can be attributed to 5-HT_{1A} binding, prompted us to also study **69** in a 10-day treatment regime. The antidepressant-like effects of **69** in this setup, together with no significant toxic effects, confirmed the therapeutic potential for this class of selective hMAO-A inhibitors. On the other hand, the selective MAO-B inhibitor **100** did not produce the expected results for haloperidol-induced catalepsy, in terms of what would be expected for a MAO-B inhibitor.³⁹ Nonetheless, the general safety of these compounds has been established in the chronic low-dose treatment regime.

In summary, we have generated the first example of selective hMAO-A and hMAO-B inhibitors where this selectivity is conferred by the configurational *cis/trans* isomerism of a double bond. *Cis* isomers with fluorine or unsubstituted benzene ring selectively inhibit hMAO-A. On the other hand, *trans* derivatives and their corresponding reduced ethyl analogues with small lipophilic substituents on benzene ring selectively inhibit hMAO-B. In addition, we provide the first in depth, and we believe critical, kinetic and structural characterization of these 1-propargyl-4-styrylpiperidines as potential fragments in the design of pharmaceuticals that can be used to target the MAOs.

EXPERIMENTAL SECTION

Chemistry. General Information. The reagents and solvents used were obtained from commercial sources (i.e., Acros Organics, Sigma-Aldrich, TCI Europe, Merck, Carlo Erba, Apollo Scientific) and were used as provided. Anhydrous THF was prepared by distillation over sodium and benzophenone under Ar(g). Analytical thin-layer chromatography was performed on silica gel aluminum sheets (60 F254, 0.20 mm; Merck). Flash column chromatography was performed on silica gel 60 (particle size 0.040–0.063 mm, Merck). ¹H NMR and ¹³C spectra were recorded at 400 and 100 MHz, respectively, on a Bruker Avance III NMR spectrometer (Bruker, MA, USA) at 295 K. The chemical shifts (δ) are reported in ppm and are referenced to the deuterated solvent used. HRMS measurements were performed (Autospec Q Micromass MS; Fisons, VG Analytical, Manchester, U.K.) at the Jozef Stefan Institute, Ljubljana, Slovenia, and on a LC–MS/MS system (Q Executive Plus; Thermo Scientific, MA, USA). MS measurements were performed on an Expression CMS mass spectrometer (Advion, NY, USA). Infrared spectra were obtained on a Thermo Nicolet FT-IR spectrometer using the ATR technique. Analytical reversed-phase HPLC analyses were performed on a modular system (1100LC; Agilent Technologies, CA, USA, and Thermo Scientific Dionex UltiMate 3000; Thermo Fisher Scientific Inc., MA, USA). Method: C18 column (Eclipse Plus; 5 μ m, 4.6 mm \times 150 mm; Agilent), *T* = 25 $^{\circ}$ C; sample 0.2 mg/mL in MeCN; flow rate = 1.0 mL/min; detector λ = 220 nm; mobile phase A (0.1% TFA [v/v] in water), mobile phase B (MeCN). Gradient (for mobile phase B): 0–12 min, 10–90%; 12–14 min, 90%; 14–15 min, 90–10%. Purities of the tested compounds were established to be \geq 95%, as determined by HPLC. All compounds described in Table 1 were checked by SwissADME⁴⁰ for the presence of PAINS substructures,⁴¹ and no PAINS substructures were identified.

General Synthetic Chemistry Experimental Protocols. General Procedure A: Synthesis of Wittig Reagents. Appropriate benzyl halide (25.0 mmol, 1.0 equiv) was dissolved in MeCN (25–50 mL), and triphenylphosphine (6.56 g, 25.0 mmol, 1.0 equiv) was added at room temperature. The reaction mixture was stirred at 85 $^{\circ}$ C for 16–24 h. The solvent was evaporated, and CH₂Cl₂ (10 mL) and Et₂O (50 mL) were added to the residue. The precipitated solid was filtered off, washed with Et₂O (20 mL), and dried overnight at room temperature. The crude product was used in the following reaction step without further purification.

General Procedure B: Wittig Reaction. Appropriate Wittig reagent synthesized according to general procedure A (1.1 equiv) was dissolved in anhydrous THF (30 mL) under argon atmosphere. NaHMDS (2 N in THF, 1.2 equiv) or KHMDs (0.5 M in toluene, 1.1 equiv) was added to the resulting suspension at room temperature. The orange-red colored reaction mixture was then stirred for 30 min under argon, followed by a dropwise addition of *N*-Boc protected 3- or 4- formylpiperidine (1.0 equiv) solution in anhydrous THF (10 mL). The reaction mixture was stirred at room temperature overnight (16–24 h) and then quenched by adding saturated aqueous NaHCO₃ solution (10–15 mL). The solvent was evaporated, and the white residue was resuspended in EtOAc (50 mL) and saturated aqueous NaHCO₃ solution (50 mL) and transferred into a separating funnel. The phases were separated, and the aqueous phase was additionally extracted with EtOAc (2 × 50 mL). Combined organic phases were washed with saturated brine (100 mL), dried over Na₂SO₄, and evaporated. The crude product was purified by flash column chromatography to yield (in a majority of cases) both pure *cis* and *trans* isomers.

General Procedure C: Reduction of the Double Bond. Alkene derivative (Wittig reaction product-mixture of *cis* and *trans* isomer, 1.0 equiv) was dissolved in EtOH (50 mL) and purged under a stream of argon for 10 min. Catalytic amount of Pd/C (10% load on carbon, 10–20% [w/w] calculated to the starting material) was added, and the resulting suspension mixture was stirred under H₂(g) atmosphere at room temperature for 16–24 h. The catalyst was removed by filtration through Celite and evaporated to obtain crude product. The product was used without further purification unless stated otherwise.

General Procedure D: Boc Protection Removal (HCl Method). To the solution of Boc-protected derivative (1.0 equiv) in 1,4-dioxane or EtOH (30 mL), concentrated HCl (10.0 equiv) was added at room temperature. The reaction mixture was stirred at 80 °C for 2 h. The solvent was evaporated under reduced pressure, and the crude product was used in the next step without further purification.

General Procedure E: Alkylation of Piperidine. Piperidine intermediate (in the form of the salt with HCl) was dissolved in MeCN (20–30 mL) or DMF (5–10 mL) at 0 °C under an argon atmosphere. K₂CO₃ or Cs₂CO₃ (3.0 equiv) was added, followed by dropwise addition of propargyl bromide (80% solution in toluene, 1.2 equiv). The resulting suspension was stirred at room temperature (unless specified otherwise) for 16–72 h. The solvent was evaporated, the residue dissolved in a mixture of CH₂Cl₂ (50 mL) and saturated aqueous NaHCO₃ solution (50 mL) and transferred into a separating funnel. The organic phase was further washed with saturated brine solution (50 mL), dried over Na₂SO₄, and evaporated. The crude product was purified by flash column chromatography.

General Procedure F: Hydrolysis of Nitrile. The starting nitrile (1.0 equiv) was dissolved in *tert*-butanol (20–50 mL), followed by the addition of powdered KOH (3.0 equiv). The resulting suspension was stirred at 90 °C for 12–24 h, and then the solvent was evaporated. The residue was dissolved in a mixture of CH₂Cl₂ (50 mL) and saturated aqueous NaHCO₃ (50 mL) and transferred into a separating funnel. The water layer was additionally extracted with CH₂Cl₂ (50 mL). The combined organic layers were washed with saturated brine (50 mL), dried over Na₂SO₄, and evaporated. The crude product was purified by flash column chromatography.

Synthesis of Intermediates and Inhibitors. (E)-4-(4-Fluorostyryl)-1-(prop-2-yn-1-yl)piperidine (1). Synthesized from **5** (0.157 g, 0.514 mmol, 1.0 equiv) via general procedures D and E. Column chromatography, EtOAc/*n*-hex = 1/1 (v/v). Yield: 26% (33 mg); yellow oil. ¹H NMR (400 MHz, CDCl₃): δ 1.57 (dt, *J* = 12.3, 3.4 Hz, 1H), 1.60 (dt, *J* = 12.0, 3.7 Hz, 1H), 1.77–1.83 (m, 2H), 2.08–2.18 (m, 1H), 2.27 (t, *J* = 2.4 Hz, 1H), 2.30 (dd, *J* = 11.7, 2.0 Hz, 2H), 2.95 (td, *J* = 11.1, 2.8 Hz, 2H), 3.34 (d, *J* = 2.4 Hz, 2H), 6.07 (dd, *J* = 16.0, 7.0 Hz, 1H), 6.34 (d, *J* = 16.0 Hz, 1H), 6.95–7.00 (m, 2H), 7.28–7.33 (m, 2H). ¹³C NMR (100 MHz, CDCl₃): δ 31.89, 38.71, 47.20, 52.19, 73.26, 78.73, 115.31 (d, *J*_{C,F} = 21.4 Hz), 127.14, 127.41 (d, *J*_{C,F} = 7.7 Hz), 133.70 (d, *J*_{C,F} = 3.3 Hz), 134.49, 161.94 (d, *J*_{C,F} = 245.9 Hz). HRMS (ESI⁺): *m/z* calcd for C₁₆H₁₉FN [M + H]⁺ 244.1502; found 244.1508. IR (ATR): 3287, 2925, 2804, 1599, 1507,

1425, 1314, 1222, 1124, 966, 855, 669, 631 cm⁻¹. HPLC purity, 96.2% (*t*_R = 9.11 min).

***tert*-Butyl 4-(Methoxy(methyl)carbamoyl)piperidine-1-carboxylate (2).** Piperidine-4-carboxylic acid (15.00 g, 116.1 mmol, 1.0 equiv) was dissolved in a mixture of 1,4-dioxane (75 mL) and 1 M NaOH (116.1 mL, 116.1 mmol, 1.0 equiv) and cooled to 0 °C. A solution of Boc₂O (30.41 g, 139.3 mmol, 1.2 equiv) in 1,4-dioxane (100 mL) was added dropwise over 30 min. The resulting suspension was stirred at room temperature for 1 h. The organic solvent was evaporated, and the aqueous residue was transferred into a separating funnel and extracted with Et₂O (2 × 100 mL). The aqueous layer was acidified with 2 M HCl to pH 2–3. The precipitated solid was filtered under suction, washed with cold water (100 mL), and dried at 50 °C overnight to obtain 1-(*tert*-butoxycarbonyl)piperidine-4-carboxylic acid. Yield: 91% (24.22 g); white crystals, mp 158–160 °C. ¹H NMR (400 MHz, CDCl₃): δ 1.46 (s, 9H), 1.62–1.69 (m, 2H), 1.88–1.94 (m, 2H), 2.48 (tt, *J* = 10.9, 3.9 Hz, 1H), 2.82–2.89 (m, 2H), 4.03 (td, *J* = 13.6, 3.7 Hz, 2H), 9.13 (bs, 1H).

1-(*tert*-Butoxycarbonyl)piperidine-4-carboxylic acid (10.00 g, 43.61 mmol, 1.0 equiv) was suspended in CH₂Cl₂ (150 mL) and cooled to 0 °C. Then Et₃N (15.11 mL, 109.03 mmol, 2.5 equiv) was added, followed by TBTU (14.70 g, 45.78 mmol, 1.05 equiv). After stirring for 30 min at 0 °C, *N,O*-dimethylhydroxylamine hydrochloride (5.10 g, 52.32 mmol, 1.2 equiv) was added, and the mixture was stirred overnight at room temperature. The resulting solution was transferred into a separating funnel and washed with saturated aqueous NaHCO₃ solution (2 × 100 mL), 1 M HCl (100 mL), saturated brine solution (100 mL), dried over Na₂SO₄, and evaporated. Column chromatography, EtOAc/*n*-hex = 1/2 (v/v). Yield: 76% (9.03 g); white crystals, mp 68–72 °C. ¹H NMR (400 MHz, CDCl₃): δ 1.45 (s, 9H), 1.61–1.74 (m, 4H), 2.72–2.83 (m, 3H), 3.17 (s, 3H), 3.70 (s, 3H), 4.17 (td, *J* = 13.4, 2.9 Hz, 2H).

***tert*-Butyl 4-Formylpiperidine-1-carboxylate (3).** *tert*-Butyl 4-(methoxy(methyl)carbamoyl)piperidine-1-carboxylate **2** (9.03 g, 33.16 mmol, 1.0 equiv) was dissolved in anhydrous THF (75 mL) and cooled to 0 °C. After stirring 10 min under an argon atmosphere, LiAlH₄ (1.89 g, 49.73 mmol, 1.5 equiv) was added. The mixture was stirred at 0 °C for 2 h and afterward quenched by adding saturated aqueous NaHCO₃ solution (30 mL). The suspension formed was transferred into a separating funnel and extracted with EtOAc (3 × 100 mL). Combined organic phases were washed with saturated aqueous NaHCO₃ solution (100 mL), 1 M HCl (100 mL), saturated brine solution (100 mL), dried over Na₂SO₄, and evaporated. The crude product was used without further purification. Yield: 83% (5.87 g); pale yellow oil.

***tert*-Butyl 4-(4-Fluorostyryl)piperidine-1-carboxylate [Isomers (Z)-4 and (E)-5].** Synthesized from aldehyde **3** (2.0 g, 9.38 mmol, 1.0 equiv), (4-fluorobenzyl)triphenylphosphonium bromide (4.66 g, 10.3 mmol, 1.1 equiv) and NaHMDS (2 N in THF, 5.63 mL, 11.26 mmol, 1.2 equiv) via general procedure B. Column chromatography, petroleum ether/Et₂O = 10/1 (v/v). Overall yield of reaction: 52% (mass of both *Z* and *E* isomers, 1.5 g); isolated pure *Z* isomer, 55 mg; isolated pure *E* isomer, 155 mg; mixture of *E/Z* isomers, 1.29 g.

4: *R*_f = 0.82 (EtOAc/*n*-hex = 1/2, v/v); white crystals, mp 80–82 °C. ¹H NMR (400 MHz, CDCl₃): δ 1.34 (dt, *J* = 12.4, 4.6 Hz, 1H), 1.37 (dt, *J* = 12.7, 4.7 Hz, 1H), 1.45 (s, 9H), 1.59–1.66 (m, 2H), 2.58–2.66 (m, 1H), 2.72 (t, *J* = 11.7 Hz, 2H), 4.08 (d, *J* = 12.5 Hz, 2H), 5.44 (dd, *J* = 11.6, 10.1 Hz, 1H), 6.34 (d, *J* = 11.6 Hz, 1H), 6.99–7.05 (m, 2H), 7.16–7.21 (m, 2H). HRMS (ESI⁺): *m/z* calcd for C₁₈H₂₄FNO₂Na [M + Na]⁺ 328.1689; found 328.1688.

5: *R*_f = 0.79 (EtOAc/*n*-hex = 1/2, v/v); yellow oil. ¹H NMR (400 MHz, CDCl₃): δ 1.30–1.42 (m, 2H), 1.46 (s, 9H), 1.51–1.57 (m, 1H), 1.71–1.77 (m, 2H), 2.77 (dt, *J* = 13.2, 2.7 Hz, 2H), 4.13 (d, *J* = 13.0 Hz, 2H), 6.05 (dd, *J* = 15.9, 6.9 Hz, 1H), 6.34 (d, *J* = 16.2 Hz, 1H), 6.95–7.01 (m, 2H), 7.27–7.32 (m, 2H). HRMS (ESI⁺): *m/z* calcd for C₁₈H₂₄FNO₂Na [M + Na]⁺ 328.1689; found 328.1686.

(Z)-4-(4-Fluorostyryl)-1-(prop-2-yn-1-yl)piperidine (6). Synthesized from **4** (57 mg, 0.187 mmol, 1.0 equiv) via general procedures D and E. Column chromatography, EtOAc/*n*-hex = 1/1

(v/v). Yield: 72% (33 mg); white crystals, mp 45–46 °C. ¹H NMR (400 MHz, CDCl₃): δ 1.51–1.61 (m, 2H), 1.69–1.76 (m, 2H), 2.21–2.28 (m, 3H), 2.45–2.55 (m, 1H), 2.90 (dt, *J* = 9.0, 2.7 Hz, 2H), 3.32 (d, *J* = 2.4 Hz, 2H), 5.48 (dd, *J* = 11.5, 10.1 Hz, 1H), 6.33 (d, *J* = 11.6 Hz, 1H), 6.99–7.05 (m, 2H), 7.17–7.21 (m, 2H). ¹³C NMR (100 MHz, CDCl₃): δ 32.16, 34.31, 47.22, 51.85, 73.21, 78.77, 115.12 (d, *J*_{C,F} = 21.3 Hz), 127.07, 130.00 (d, *J*_{C,F} = 7.9 Hz), 133.58 (d, *J*_{C,F} = 3.3 Hz), 137.05, 161.52 (d, *J*_{C,F} = 246.1 Hz). HRMS (ESI⁺): *m/z* calcd for C₁₆H₁₉FN [M + H]⁺ 244.1502; found 244.1503. IR (ATR): 3299, 2930, 1601, 1508, 1446, 1225, 1157, 972, 845, 657 cm⁻¹. HPLC purity, 99.5% (*t*_R = 9.03 min).

(±)-tert-Butyl 3-(Methoxy(methyl)carbamoyl)piperidine-1-carboxylate (7). Synthesis of (±)-1-(tert-butoxycarbonyl)-piperidine-3-carboxylic acid was carried out following the procedure described for the synthesis of compound 2, starting from (±)-piperidine-3-carboxylic acid (7.75 g, 60.0 mmol, 1.0 equiv). Yield: 86% (11.83 g); white crystals, mp 164–165 °C. ¹H NMR (400 MHz, CDCl₃): δ 1.43–1.53 (m, 1H), 1.45 (s, 9H), 1.59–1.75 (m, 2H), 2.03–2.09 (m, 1H), 2.48 (tt, *J* = 10.2, 4.0 Hz, 1H), 2.82–2.89 (m, 1H), 3.03 (dd, *J* = 12.7, 10.6 Hz, 1H), 3.88 (td, *J* = 13.3, 4.0 Hz, 1H), 4.08–4.15 (m, 1H), 8.67 (bs, 1H).

(±)-1-(tert-butoxycarbonyl)piperidine-3-carboxylic acid (10.00 g, 43.61 mmol, 1.0 equiv) was transformed to Weinreb amide 7 following the procedure described for compound 2. Yield: 82% (9.74 g); white crystals, mp 89–91 °C. ¹H NMR (400 MHz, CDCl₃): δ 1.41–1.52 (m, 1H), 1.44 (s, 9H), 1.58–1.73 (m, 2H), 1.87–1.94 (m, 1H), 2.68 (tt, *J* = 12.8, 2.9 Hz, 1H), 2.72–2.82 (m, 1H), 2.86 (t, *J* = 11.7 Hz, 1H), 3.17 (s, 3H), 3.72 (s, 3H), 4.05–4.15 (m, 2H).

(±)-tert-Butyl 3-Formylpiperidine-1-carboxylate (8). Synthesis of aldehyde 8 was carried out following the procedure described for compound 3, starting from amide 7 (9.74 g, 35.76 mmol, 1.0 equiv). Yield: 79% (6.03 g); pale yellow oil.

(±)-tert-Butyl 3-(4-Fluorostyryl)piperidine-1-carboxylate [Isomers (Z)-9 and (E)-10]. Synthesized from 8 (1.02 g, 4.78 mmol, 1.0 equiv), (4-fluorobenzyl)triphenylphosphonium bromide (2.59 g, 5.74 mmol, 1.2 equiv), and NaHMDS (2 N in THF, 2.87 mL, 5.74 mmol, 1.2 equiv) via general procedure B. Column chromatography, petroleum ether/Et₂O = 10/1 (v/v) yielding pure *trans* isomer 10 (<8% *cis* isomer 9 was present in the mixture as estimated from ¹H NMR). Overall yield of reaction (mixture of *E/Z* isomers): 56% (0.817 g).

10: *R*_f = 0.38 (Et₂O/petroleum ether = 1/10, v/v); yellow oil. ¹H NMR (400 MHz, CDCl₃, *E* isomer): δ 1.31–1.41 (m, 1H), 1.47 (s, 9H), 1.68–1.73 (m, 1H), 1.90–1.94 (m, 1H), 2.26–2.34 (m, 1H), 2.60–2.71 (m, 1H), 2.78 (dd, *J* = 13.2, 11.5 Hz, 2H), 3.97 (d, *J* = 13.1 Hz, 2H), 5.99 (dd, *J* = 16.0, 7.0 Hz, 1H), 6.40 (d, *J* = 16.0 Hz, 1H), 6.95–7.02 (m, 2H), 7.27–7.32 (m, 2H). HRMS (ESI⁺): *m/z* calcd for C₁₈H₂₄FNO₂Na [M + Na]⁺ 328.1689; found 328.1682.

(±)-tert-Butyl 3-(2,4,5-Trifluorostyryl)piperidine-1-carboxylate [Isomers (Z)-11 and (E)-12]. Synthesized from 8 (0.79 g, 3.71 mmol, 1.0 equiv), (2,4,5-trifluorobenzyl)triphenylphosphonium bromide (2.23 g, 4.58 mmol, 1.2 equiv), and NaHMDS (2 N in THF, 2.29 mL, 4.58 mmol, 1.2 equiv) via general procedure B. Column chromatography, petroleum ether/Et₂O = 10/1 (v/v) to obtain a mixture of *cis/trans* isomers (ratio ~40/60, estimated from ¹H NMR). Overall yield of reaction: 47% (mass of both *Z* and *E* isomers, 0.595 g).

11 and 12 (mixture of both isomers): *R*_f = 0.34 (petroleum ether/Et₂O = 10/1, v/v); yellow oil. ¹H NMR (400 MHz, CDCl₃): δ 1.30–1.40 (m, 3.4H), 1.45 (1.46) (s + s, 15.3H), 1.62–1.73 (m, 1.7H), 1.88–1.94 (m, 0.7H), 2.30–2.38 (m, 0.7H), 2.43–2.53 (m, 1H), 2.62–2.84 (m, 3.4H), 3.92–4.08 (m, 3.4H), 5.58 (dd, *J* = 11.5, 10.4 Hz, 0.7H), 6.07 (dd, *J* = 16.2, 7.1 Hz, 1H), 6.32 (d, *J* = 11.5 Hz, 0.7H), 6.49 (d, *J* = 16.3 Hz, 1H), 6.85–6.96 (m, 1.7H), 7.11 (ddd, *J* = 10.6, 8.8, 6.9 Hz, 1H), 7.21 (ddd, *J* = 11.2, 8.7, 7.0 Hz, 0.7H). HRMS (ESI⁺): *m/z* calcd for C₁₈H₂₂F₃NO₂Na [M + Na]⁺ 364.1500; found 364.1491.

tert-Butyl 4-(2,4,5-Trifluorostyryl)piperidine-1-carboxylate [Isomers (Z)-13 and (E)-14]. Synthesized from aldehyde 3 (0.575 g, 2.70 mmol, 1.0 equiv), (2,4,5-trifluorobenzyl)triphenyl-

phosphonium bromide (1.59 g, 3.25 mmol, 1.2 equiv) and NaHMDS (2 N solution in THF, 1.63 mL, 3.25 mmol, 1.2 equiv) via general procedure B. Column chromatography, petroleum ether/Et₂O = 10/1 (v/v). Overall yield of reaction: 52% (mass of both *Z* and *E* isomers, 0.48 g); isolated pure *Z* isomer, 165 mg; isolated pure *E* isomer, 135 mg; mixture of *E/Z* isomers, 180 mg.

13: *R*_f = 0.80 (EtOAc/n-hex = 1/2, v/v); yellow crystals, mp 86–87 °C. ¹H NMR (400 MHz, CDCl₃): δ 1.30–1.40 (m, 2H), 1.46 (s, 9H), 1.58–1.64 (m, 2H), 2.37–2.48 (m, 1H), 2.70 (dt, *J* = 13.4, 2.7 Hz, 2H), 4.08 (td, *J* = 13.4, 2.7 Hz, 2H), 5.55 (dd, *J* = 11.4, 10.3 Hz, 1H), 6.17 (d, *J* = 11.6 Hz, 1H), 6.93 (ddd, *J* = 10.1, 9.2, 6.7 Hz, 1H), 7.01 (ddd, *J* = 10.6, 8.7, 6.9 Hz, 1H). HRMS (ESI⁺): *m/z* calcd for C₁₈H₂₂F₃NO₂Na [M + Na]⁺ 364.1500; found 364.1503.

14: *R*_f = 0.78 (EtOAc/n-hex = 1/2, v/v); pale yellow crystals, mp 60–63 °C. ¹H NMR (400 MHz, CDCl₃): δ 1.36 (dt, *J* = 12.4, 4.2 Hz, 1H), 1.39 (dt, *J* = 12.3, 4.3 Hz, 1H), 1.47 (s, 9H), 1.71–1.79 (m, 2H), 2.25–2.36 (m, 1H), 2.78 (t, *J* = 12.0 Hz, 2H), 4.14 (bs, 2H), 6.13 (dd, *J* = 16.1, 6.9 Hz, 1H), 6.44 (d, *J* = 16.1 Hz, 1H), 6.88 (dt, *J* = 9.9, 6.6 Hz, 1H), 7.01 (ddd, *J* = 11.1, 8.8, 7.0 Hz, 1H). HRMS (ESI⁺): *m/z* calcd for C₁₈H₂₂F₃NO₂Na [M + Na]⁺ 364.1500; found 364.1497.

(±)-tert-Butyl 3-(4-Fluorophenethyl)piperidine-1-carboxylate (15). Synthesized from a mixture of 9 and 10 (0.55 g, 1.80 mmol, 1.0 equiv) via general procedure C. Yield: quantitative (0.55 g); yellow oil. ¹H NMR (400 MHz, CDCl₃): δ 1.08–1.13 (m, 1H), 1.35–1.56 (m, 3H), 1.45 (s, 9H), 1.59–1.66 (m, 1H), 1.80–1.87 (m, 1H), 2.41–2.56 (m, 1H), 2.61 (t, *J* = 12.2 Hz, 2H), 2.79 (dt, *J* = 12.2, 2.5 Hz, 2H), 3.89 (td, *J* = 13.1, 3.9 Hz, 1H), 4.04 (bs, 1H), 6.92–6.98 (m, 2H), 7.09–7.14 (m, 2H). HRMS (ESI⁺): *m/z* calcd for C₁₈H₂₆FNO₂Na [M + Na]⁺ 330.1845; found 330.1842.

(±)-tert-Butyl 3-(2,4,5-Trifluorophenethyl)piperidine-1-carboxylate (16). Synthesized from a mixture of 11 and 12 (0.30 g, 0.88 mmol, 1.0 equiv) via general procedure C. Yield: 97% (0.29 g); yellow oil. ¹H NMR (400 MHz, CDCl₃): δ 1.09–1.18 (m, 1H), 1.37–1.55 (m, 4H), 1.47 (s, 9H), 1.62–1.69 (m, 1H), 1.83–1.90 (m, 1H), 2.55 (dd, *J* = 13.0, 9.3 Hz, 1H), 2.62 (t, *J* = 7.6 Hz, 2H), 2.82 (ddd, *J* = 13.2, 11.2, 3.2 Hz, 1H), 3.89 (td, *J* = 13.2, 4.1 Hz, 1H), 3.97 (d, *J* = 12.6 Hz, 1H), 6.88 (ddd, *J* = 10.1, 9.3, 6.7 Hz, 1H), 7.00 (ddd, *J* = 10.6, 8.7, 6.9 Hz, 1H). HRMS (ESI⁺): *m/z* calcd for C₁₈H₂₄F₃NO₂Na [M + Na]⁺ 366.1657; found 366.1653.

tert-Butyl 4-(4-Fluorophenethyl)piperidine-1-carboxylate (17). Synthesized from a mixture of 4 and 5 (0.152 g, 0.50 mmol, 1.0 equiv) via general procedure C. Yield: quantitative (0.155 g); yellow oil. ¹H NMR (400 MHz, CDCl₃): δ 1.11 (dt, *J* = 12.4, 4.2 Hz, 1H), 1.14 (dt, *J* = 12.5, 4.2 Hz, 1H), 1.35–1.44 (m, 1H), 1.45 (s, 9H), 1.51–1.56 (m, 2H), 1.60–1.62 (m, 1H), 1.65–1.72 (m, 2H), 2.57–2.62 (m, 1H), 2.66 (t, *J* = 11.5 Hz, 2H), 4.07 (bs, 2H), 6.93–6.99 (m, 2H), 7.09–7.14 (m, 2H). HRMS (ESI⁺): *m/z* calcd for C₁₈H₂₆FNO₂Na [M + Na]⁺ 330.1845; found 330.1848.

tert-Butyl 4-(2,4,5-Trifluorophenethyl)piperidine-1-carboxylate (18). Synthesized from a mixture of 13 and 14 (0.152 g, 0.45 mmol, 1.0 equiv) via general procedure C. Yield: quantitative (0.155 g); yellow oil. ¹H NMR (400 MHz, CDCl₃): δ 1.11 (dt, *J* = 12.4, 4.3 Hz, 1H), 1.14 (dt, *J* = 12.7, 4.2 Hz, 1H), 1.35–1.44 (m, 1H), 1.45 (s, 9H), 1.49–1.54 (m, 2H), 1.66–1.73 (m, 2H), 2.59 (t, *J* = 8.0 Hz, 2H), 2.66 (dt, *J* = 13.2, 2.5 Hz, 2H), 4.09 (d, *J* = 13.2 Hz, 2H), 6.87 (ddd, *J* = 10.0, 9.4, 6.7 Hz, 1H), 6.97 (ddd, *J* = 10.6, 8.8, 7.1 Hz, 1H). HRMS (ESI⁺): *m/z* calcd for C₁₈H₂₄F₃NO₂Na [M + Na]⁺ 366.1657; found 366.1652.

(±)-(E)-3-(4-Fluorostyryl)-1-(prop-2-yn-1-yl)piperidine (19). Synthesized from a mixture of 9 and 10 (0.190 g, 2.11 mmol, 1.0 equiv) via general procedures D and E. Column chromatography, EtOAc/n-hex = 1/1 (v/v) yielding pure *trans* isomer 19. Yield: 45% (68 mg); yellow oil. ¹H NMR (400 MHz, CDCl₃): δ 1.17 (dt, *J* = 12.3, 4.1 Hz, 1H), 1.61–1.72 (m, 1H), 1.74–1.80 (m, 1H), 1.81–1.87 (m, 1H), 2.09 (t, *J* = 10.8 Hz, 1H), 2.19 (dt, *J* = 11.4, 3.0 Hz, 1H), 2.25 (t, *J* = 2.4 Hz, 1H), 2.41–2.50 (m, 1H), 2.82–2.87 (m, 1H), 2.89–2.93 (m, 1H), 3.34 (d, *J* = 2.5 Hz, 2H), 6.04 (dd, *J* = 16.0, 7.2 Hz, 1H), 6.38 (d, *J* = 16.0 Hz, 1H), 6.95–7.01 (m, 2H), 7.28–7.33 (m, 2H). ¹³C NMR (100 MHz, CDCl₃): δ 24.64, 29.94, 39.41,

47.18, 52.23, 57.76, 73.97, 77.87, 115.34 (d, $J_{\text{C,F}} = 21.7$ Hz), 127.47 (d, $J_{\text{C,F}} = 8.0$ Hz), 128.41, 131.95, 133.50 (d, $J_{\text{C,F}} = 3.3$ Hz), 162.03 (d, $J_{\text{C,F}} = 246.0$ Hz). HRMS (ESI+): m/z calcd for $\text{C}_{16}\text{H}_{19}\text{FN}$ [$\text{M} + \text{H}$] $^+$ 244.1502; found 244.1509. IR (ATR): 3433, 3196, 2934, 2544, 2124, 1507, 1225, 1159, 1012, 858, 750, 647 cm^{-1} . HPLC purity, 99.4% ($t_{\text{R}} = 9.10$ min).

(±)-(E)-1-(Prop-2-yn-1-yl)-3-(2,4,5-trifluorostyryl)piperidine (20). Synthesized from a mixture of **11** and **12** (0.219 g, 0.64 mmol, 1.0 equiv) via general procedures D and E. Column chromatography, EtOAc/n-hex = 1/1 (v/v) to obtain pure *trans* isomer **20**. Yield: 34% (61 mg); yellow oil. ^1H NMR (400 MHz, CDCl_3): δ 1.21 (ddd, $J = 15.8, 12.1, 4.1$ Hz, 1H), 1.63–1.87 (m, 3H), 2.13 (t, $J = 10.7$ Hz, 1H), 2.24 (dt, $J = 11.2, 2.6$ Hz, 1H), 2.27 (t, $J = 2.4$ Hz, 1H), 2.47–2.56 (m, 1H), 2.84–2.87 (m, 1H), 2.90–2.94 (m, 1H), 3.36 (d, $J = 2.4$ Hz, 2H), 6.12 (dd, $J = 16.1, 7.2$ Hz, 1H), 6.46 (d, $J = 16.2$ Hz, 1H), 6.88 (dt, $J = 9.9, 6.7$ Hz, 1H), 7.22 (ddd, $J = 11.1, 8.8, 7.0$ Hz, 1H). ^{13}C NMR (100 MHz, CDCl_3): δ 24.77, 29.89, 39.90, 47.28, 52.32, 57.64, 73.44, 78.51, 105.56 (dd, $J_{\text{C,F}} = 28.4, 21.0$ Hz), 114.14 (dd, $J_{\text{C,F}} = 19.8, 5.1$ Hz), 120.01–120.02 (m), 121.74–121.93 (m), 136.12–136.16 (m), 146.93 (ddd, $J_{\text{C,F}} = 243.9, 13.2, 3.6$ Hz), 148.83 (ddd, $J_{\text{C,F}} = 251.2, 14.8, 12.4$ Hz), 154.78 (ddd, $J_{\text{C,F}} = 248.0, 9.0, 2.1$ Hz). IR (ATR): 3304, 2932, 2798, 1621, 1512, 1427, 1336, 1154, 1106, 969, 879, 850, 665 cm^{-1} . HRMS (ESI+): m/z calcd for $\text{C}_{16}\text{H}_{17}\text{F}_3\text{N}$ [$\text{M} + \text{H}$] $^+$ 280.1313; found 280.1316. HPLC purity, 99.1% ($t_{\text{R}} = 9.57$ min).

(Z)-1-(Prop-2-yn-1-yl)-4-(2,4,5-trifluorostyryl)piperidine (21). Synthesized from **13** (165 mg, 0.483 mmol, 1.0 equiv) via general procedures D and E. Column chromatography, EtOAc/n-hex = 1/1 (v/v). Yield: 68% (92 mg); white crystals, mp 72–74 $^{\circ}\text{C}$. ^1H NMR (400 MHz, CDCl_3): δ 1.55 (dt, $J = 12.5, 3.8$ Hz, 1H), 1.58 (dt, $J = 11.7, 3.8$ Hz, 1H), 1.66–1.71 (m, 2H), 2.20–2.35 (m, 3H), 2.25 (t, $J = 2.5$ Hz, 1H), 2.90 (dt, $J = 11.6, 2.8$ Hz, 2H), 3.32 (d, $J = 2.4$ Hz, 2H), 5.64 (dd, $J = 11.3, 10.4$ Hz, 1H), 6.23 (d, $J = 11.6$ Hz, 1H), 6.92 (ddd, $J = 10.0, 9.3, 6.7$ Hz, 1H), 7.01 (ddd, $J = 10.6, 8.8, 6.9$ Hz, 1H). ^{13}C NMR (100 MHz, CDCl_3): δ 31.77, 34.96, 47.19, 51.71, 73.33, 78.62, 105.51 (dd, $J_{\text{C,F}} = 28.7, 20.7$ Hz), 117.62 (dd, $J_{\text{C,F}} = 19.4, 4.6$ Hz), 119.00, 121.36 (ddd, $J_{\text{C,F}} = 17.7, 5.8, 4.4$ Hz), 140.20, 146.36 (ddd, $J_{\text{C,F}} = 243.7, 12.6, 3.6$ Hz), 148.88 (ddd, $J_{\text{C,F}} = 248.8, 14.4, 12.6$ Hz), 154.97 (ddd, $J_{\text{C,F}} = 246.8, 9.0, 2.7$ Hz). HRMS (ESI+): m/z calcd for $\text{C}_{16}\text{H}_{17}\text{F}_3\text{N}$ [$\text{M} + \text{H}$] $^+$ 280.1313; found 280.1317. IR (ATR): 3293, 2905, 2824, 1618, 1503, 1423, 1310, 1192, 1151, 1133, 972, 882, 779, 679, 653 cm^{-1} . HPLC purity, 100% ($t_{\text{R}} = 9.47$ min).

(E)-1-(Prop-2-yn-1-yl)-4-(2,4,5-trifluorostyryl)piperidine (22). Synthesized from **14** (0.135 g, 0.395 mmol, 1.0 equiv) via general procedures D and E. Column chromatography, EtOAc/n-hex = 1/1 (v/v). Yield: 74% (82 mg); yellow oil. ^1H NMR (400 MHz, CDCl_3): δ 1.56 (dt, $J = 12.4, 3.4$ Hz, 1H), 1.59 (dt, $J = 12.0, 3.7$ Hz, 1H), 1.78–1.84 (m, 2H), 2.11–2.20 (m, 1H), 2.26 (t, $J = 2.4$ Hz, 1H), 2.30 (dt, $J = 11.7, 2.3$ Hz, 2H), 2.95 (dt, $J = 11.6, 2.8$ Hz, 2H), 3.34 (d, $J = 2.4$ Hz, 2H), 6.13 (dd, $J = 16.1, 7.0$ Hz, 1H), 6.43 (d, $J = 16.1$ Hz, 1H), 6.87 (dt, $J = 9.9, 6.7$ Hz, 1H), 7.23 (ddd, $J = 11.1, 8.8, 7.0$ Hz, 1H). ^{13}C NMR (100 MHz, CDCl_3): δ 31.69, 39.02, 47.17, 52.07, 73.23, 78.73, 105.51 (dd, $J_{\text{C,F}} = 28.5, 20.9$ Hz), 114.06 (dd, $J_{\text{C,F}} = 19.6, 5.2$ Hz), 118.96–119.03 (m), 121.95 (ddd, $J_{\text{C,F}} = 14.8, 5.8, 4.4$ Hz), 138.10–138.17 (m), 146.93 (ddd, $J_{\text{C,F}} = 243.5, 12.9, 3.4$ Hz), 148.76 (ddd, $J_{\text{C,F}} = 251.1, 14.9, 12.6$ Hz), 154.73 (ddd, $J_{\text{C,F}} = 247.4, 9.1, 2.3$ Hz). HRMS (ESI+): m/z calcd for $\text{C}_{16}\text{H}_{17}\text{F}_3\text{N}$ [$\text{M} + \text{H}$] $^+$ 280.1313; found 280.1318. IR (ATR): 3305, 3180, 2931, 2804, 2513, 1619, 1510, 1426, 1335, 1150, 1107, 970, 878, 706, 630 cm^{-1} . HPLC purity, 100% ($t_{\text{R}} = 9.57$ min).

(±)-3-(4-Fluorophenethyl)-1-(prop-2-yn-1-yl)piperidine (23). Synthesized from **15** (0.193 g, 0.628 mmol, 1.0 equiv) via general procedures D and E. Column chromatography, EtOAc/n-hex = 1/1 (v/v). Yield: 33% (51 mg); yellow oil. ^1H NMR (400 MHz, CDCl_3): δ 0.85–0.95 (m, 1H), 1.46–1.54 (m, 2H), 1.55–1.65 (m, 2H), 1.66–1.74 (m, 1H), 1.75–1.82 (m, 1H), 1.88 (t, $J = 10.6$ Hz, 1H), 2.14 (dt, $J = 11.4, 3.0$ Hz, 1H), 2.24 (t, $J = 2.4$ Hz, 1H), 2.60 (t, $J = 7.9$ Hz, 2H), 2.79–2.83 (m, 1H), 2.84–2.89 (m, 1H), 3.30 (d, $J = 2.4$ Hz, 2H), 6.91–6.97 (m, 2H), 7.09–7.14 (m, 2H). ^{13}C NMR (100 MHz, CDCl_3): δ 25.03, 30.25, 32.26, 35.55, 36.44, 47.29, 52.72, 58.53, 73.49, 78.45, 115.00 (d, $J_{\text{C,F}} = 21.0$ Hz), 129.54 (d, $J_{\text{C,F}} = 7.9$

Hz), 138.00 (d, $J_{\text{C,F}} = 3.2$ Hz), 161.13 (d, $J_{\text{C,F}} = 243.3$ Hz). HRMS (ESI+): m/z calcd for $\text{C}_{16}\text{H}_{21}\text{FN}$ [$\text{M} + \text{H}$] $^+$ 246.1658; found 246.1652. IR (ATR): 3302, 2929, 2853, 2797, 1601, 1509, 1452, 1222, 1157, 1106, 828, 661 cm^{-1} . HPLC purity, 98.5% ($t_{\text{R}} = 9.16$ min).

(±)-3-(2,4,5-Trifluorophenethyl)-1-(prop-2-yn-1-yl)piperidine (24). Synthesized from **16** (0.181 g, 0.527 mmol, 1.0 equiv) via general procedures D and E. Column chromatography, EtOAc/n-hex = 1/2 (v/v). Yield: 26% (39 mg); yellow oil. ^1H NMR (400 MHz, CDCl_3): δ 0.88–0.98 (m, 1H), 1.45–1.56 (m, 2H), 1.58–1.77 (m, 3H), 1.78–1.85 (m, 1H), 1.91–2.00 (m, 1H), 2.17–2.25 (m, 1H), 2.26–2.29 (m, 1H), 2.54–2.66 (m, 2H), 2.88 (t, $J = 12.6$ Hz, 2H), 3.35 (d, $J = 2.5$ Hz, 2H), 6.86 (ddd, $J = 10.0, 9.5, 6.7$ Hz, 1H), 6.98 (ddd, $J = 10.6, 8.8, 6.9$ Hz, 1H). ^{13}C NMR (100 MHz, CDCl_3): δ 25.08, 25.67, 30.21, 34.61, 35.62, 47.33, 52.76, 58.46, 73.28, 78.69, 105.20 (dd, $J_{\text{C,F}} = 28.6, 20.6$ Hz), 117.71 (dd, $J_{\text{C,F}} = 18.7, 6.2$ Hz), 125.50 (td, $J_{\text{C,F}} = 18.1, 4.4$ Hz), 146.57 (ddd, $J_{\text{C,F}} = 243.7, 12.4, 3.7$ Hz), 148.14 (ddd, $J_{\text{C,F}} = 248.6, 14.3, 12.5$ Hz), 155.73 (ddd, $J_{\text{C,F}} = 243.8, 9.2, 2.7$ Hz). HRMS (ESI+): m/z calcd for $\text{C}_{16}\text{H}_{19}\text{F}_3\text{N}$ [$\text{M} + \text{H}$] $^+$ 282.1470; found 282.1464. IR (ATR): 3306, 2931, 2798, 1515, 1422, 1331, 1209, 1150, 1100, 843, 659 cm^{-1} . HPLC purity, 100% ($t_{\text{R}} = 9.57$ min).

4-(4-Fluorophenethyl)-1-(prop-2-yn-1-yl)piperidine (25). Synthesized from **17** (0.130 g, 0.423 mmol, 1.0 equiv) via general procedures D and E. Column chromatography, EtOAc/n-hex = 1/1 (v/v). Yield: 85% (88 mg); colorless oil. ^1H NMR (400 MHz, CDCl_3): δ 1.21–1.40 (m, 3H), 1.52–1.57 (m, 2H), 1.73–1.79 (m, 2H), 2.19–2.24 (m, 2H), 2.25 (t, $J = 2.4$ Hz, 1H), 2.57–2.61 (m, 2H), 2.89–2.93 (m, 2H), 3.33 (d, $J = 2.4$ Hz, 2H), 6.92–6.98 (m, 2H), 7.09–7.14 (m, 2H). ^{13}C NMR (100 MHz, CDCl_3): δ 32.07, 32.21, 34.61, 38.35, 47.16, 52.48, 73.09, 78.90, 114.99 (d, $J_{\text{C,F}} = 21.1$ Hz), 129.54 (d, $J_{\text{C,F}} = 7.9$ Hz), 138.16 (d, $J_{\text{C,F}} = 3.1$ Hz), 161.11 (d, $J_{\text{C,F}} = 243.2$ Hz). HRMS (ESI+): m/z calcd for $\text{C}_{16}\text{H}_{21}\text{FN}$ [$\text{M} + \text{H}$] $^+$ 246.1658; found 246.1657. IR (ATR): 3300, 2923, 1601, 1508, 1453, 1218, 1156, 824, 642 cm^{-1} . HPLC purity, 97.5% ($t_{\text{R}} = 9.15$ min).

1-(Prop-2-yn-1-yl)-4-(2,4,5-trifluorophenethyl)piperidine (26). Synthesized from **18** (0.175 g, 0.509 mmol, 1.0 equiv) via general procedures D and E. Column chromatography, EtOAc/n-hex = 1/1 (v/v). Yield: 32% (45 mg); yellow oil. ^1H NMR (400 MHz, CDCl_3): δ 1.22–1.39 (m, 3H), 1.49–1.55 (m, 2H), 1.72–1.79 (m, 2H), 2.17–2.23 (m, 2H), 2.23–2.25 (m, 1H), 2.59 (t, $J = 7.8$ Hz, 2H), 2.88–2.93 (m, 2H), 3.30–3.32 (m, 2H), 6.86 (ddd, $J = 10.0, 9.5, 6.7$ Hz, 1H), 6.97 (ddd, $J = 10.7, 8.8, 6.5$ Hz, 1H). ^{13}C NMR (100 MHz, CDCl_3): δ 25.56, 31.94, 34.68, 36.55, 47.13, 52.40, 73.16, 78.81, 105.18 (dd, $J_{\text{C,F}} = 28.7, 20.6$ Hz), 117.66 (dd, $J_{\text{C,F}} = 19.1, 6.5$ Hz), 125.50–125.82 (m), 146.57 (ddd, $J_{\text{C,F}} = 243.6, 12.6, 3.2$ Hz), 148.09 (ddd, $J_{\text{C,F}} = 249.2, 13.4, 11.5$ Hz), 155.72 (ddd, $J_{\text{C,F}} = 243.4, 9.3, 2.7$ Hz). HRMS (ESI+): m/z calcd for $\text{C}_{16}\text{H}_{19}\text{F}_3\text{N}$ [$\text{M} + \text{H}$] $^+$ 282.1470; found 282.1471. IR (ATR): 3306, 2920, 2803, 1517, 1423, 1334, 1210, 1151, 1108, 876, 660 cm^{-1} . HPLC purity, 100% ($t_{\text{R}} = 9.63$ min).

Wittig Salts (27a–I). Synthesized according to general procedure A. The product was used in next reaction step without purification.

tert-Butyl 4-Styrylpiperidine-1-carboxylate [Isomers (Z)-28 and (E)-29]. Synthesized from aldehyde **3** (2.00 g, 9.38 mmol, 1.0 equiv), benzyltriphenylphosphonium chloride (4.01 g, 10.32 mmol, 1.1 equiv), and NaHMDS (2 N in THF, 5.63 mL, 11.26 mmol, 1.2 equiv) via general procedure B. Column chromatography, petroleum ether/Et₂O = 9/1 (v/v). Overall yield of reaction: 66% (mass of both Z and E isomers, 1.78 g); isolated pure Z isomer, 95 mg; isolated pure E isomer, 285 mg; mixture of E/Z isomers, 1.4 g.

28: $R_{\text{f}} = 0.31$ (petroleum ether/Et₂O = 9/1, v/v); colorless oil. ^1H NMR (400 MHz, CDCl_3): δ 1.36 (ddd, $J = 17.1, 13.9, 5.3$ Hz, 2H), 1.46 (s, 9H), 1.65–1.68 (m, 2H), 2.68–2.76 (m, 3H), 4.08 (bs, 2H), 5.45 (dd, $J = 11.7, 10.0$ Hz, 1H), 6.39 (d, $J = 11.7$ Hz, 1H), 7.21–7.25 (m, 3H), 7.31–7.35 (m, 2H). MS (ESI+): m/z [$\text{M} + \text{Na}$] $^+$ 310.18; found 310.17.

29: $R_{\text{f}} = 0.28$ (petroleum ether/Et₂O = 9/1, v/v); colorless oil. ^1H NMR (400 MHz, CDCl_3): δ 1.36 (ddd, $J = 16.6, 12.6, 4.5$ Hz, 2H), 1.47 (s, 9H), 1.73–1.76 (m, 2H), 2.22–2.31 (m, 1H), 2.77 (t, $J =$

11.5 Hz, 2H), 4.12 (bs, 2H), 6.13 (dd, $J = 17.0, 6.9$ Hz, 1H), 6.38 (d, $J = 16.0$ Hz, 1H), 7.17–7.21 (m, 1H), 7.27–7.35 (m, 4H). MS (ESI⁺): m/z [M + Na]⁺ 310.18; found 310.12.

tert-Butyl 4-(3-Fluorostyryl)piperidine-1-carboxylate [Isomers (Z)-30 and (E)-31]. Synthesized from aldehyde 3 (2.00 g, 9.38 mmol, 1.0 equiv), 27a (4.20 g, 10.32 mmol, 1.1 equiv), and NaHMDS (2 N in THF, 5.63 mL, 11.26 mmol, 1.2 equiv) via general procedure B. Column chromatography, petroleum ether/Et₂O = 10/1 (v/v). Overall yield of reaction: 56% (mass of both Z and E isomers, 1.60 g); isolated pure Z isomer, 120 mg; isolated pure E isomer, 355 mg; mixture of E/Z isomers, 1.125 g.

30: $R_f = 0.70$ (EtOAc/n-hex = 1/2, v/v); pale yellow oil. ¹H NMR (400 MHz, CDCl₃): δ 1.35 (dt, $J = 12.4, 3.9$ Hz, 1H), 1.38 (dt, $J = 12.2, 3.7$ Hz, 1H), 1.46 (s, 9H), 1.60–1.69 (m, 2H), 2.62–2.77 (m, 3H), 4.09 (bs, 2H), 5.50 (dd, $J = 11.6, 10.2$ Hz, 1H), 6.35 (d, $J = 11.6$ Hz, 1H), 6.91–6.97 (m, 2H), 6.99–7.01 (m, 1H), 7.27–7.32 (m, 1H). MS (ESI⁺): m/z [M + Na]⁺ 328.17; found 328.42.

31: $R_f = 0.67$ (EtOAc/n-hex = 1/2, v/v); white crystals, mp 45–46 °C. ¹H NMR (400 MHz, CDCl₃): δ 1.31–1.44 (m, 2H), 1.47 (s, 9H), 1.71–1.78 (m, 2H), 2.23–2.33 (m, 1H), 2.78 (t, $J = 12.2$ Hz, 2H), 4.13 (bs, 2H), 6.15 (dd, $J = 16.0, 6.8$ Hz, 1H), 6.35 (d, $J = 16.0$ Hz, 1H), 6.89 (ddt, $J = 8.4, 2.6, 0.9$ Hz, 1H), 7.02–7.06 (m, 1H), 7.07–7.11 (m, 1H), 7.25 (td, $J = 8.0, 5.8$ Hz, 1H). MS (ESI⁺): m/z [M + Na]⁺ 328.17; found 328.40.

tert-Butyl 4-(2-Fluorostyryl)piperidine-1-carboxylate [Isomers (Z)-32 and (E)-33]. Synthesized from aldehyde 3 (1.50 g, 7.04 mmol, 1.0 equiv), 27b (3.49 g, 7.74 mmol, 1.1 equiv), and NaHMDS (2 N in THF, 4.22 mL, 8.45 mmol, 1.2 equiv) via general procedure B. Column chromatography, petroleum ether/Et₂O = 10/1 (v/v). Overall yield of reaction: 58% (mass of both Z and E isomers, 1.25 g); isolated pure Z isomer, 252 mg; isolated pure E isomer, 194 mg; mixture of E/Z isomers, 0.804 g.

32: $R_f = 0.16$ (petroleum ether/Et₂O = 10/1, v/v); colorless oil. ¹H NMR (400 MHz, CDCl₃): δ 1.27–1.40 (m, 2H), 1.43 (s, 9H), 1.56–1.62 (m, 2H), 2.44–2.54 (m, 1H), 2.61–2.70 (m, 2H), 4.09 (bs, 2H), 5.53 (dd, $J = 11.6, 10.2$ Hz, 1H), 6.33 (d, $J = 11.6$ Hz, 1H), 6.96 (ddd, $J = 10.8, 8.2, 1.3$ Hz, 1H), 7.00–7.10 (m, 2H), 7.17–7.22 (m, 1H). MS (ESI⁺): m/z [M + Na]⁺ 328.17; found 328.42.

33: $R_f = 0.14$ (petroleum ether/Et₂O = 10/1, v/v); colorless oil. ¹H NMR (400 MHz, CDCl₃): δ 1.36 (dt, $J = 12.3, 4.2$ Hz, 1H), 1.39 (dt, $J = 12.3, 4.2$ Hz, 1H), 1.46 (s, 9H), 1.70–1.77 (m, 2H), 2.23–2.33 (m, 1H), 2.76 (t, $J = 11.0$ Hz, 2H), 4.12 (bs, 2H), 6.20 (dd, $J = 16.1, 7.0$ Hz, 1H), 6.53 (d, $J = 16.1$ Hz, 1H), 6.99 (ddd, $J = 10.8, 8.1, 1.2$ Hz, 1H), 7.05 (dt, $J = 7.6, 1.2$ Hz, 1H), 7.12–7.18 (m, 1H), 7.41 (dt, $J = 7.7, 1.8$ Hz, 1H). MS (ESI⁺): m/z [M + Na]⁺ 328.17; found 328.42.

tert-Butyl 4-(2-Chloro-4-fluorostyryl)piperidine-1-carboxylate [Isomers (Z)-34 and (E)-35]. Synthesized from aldehyde 3 (1.50 g, 7.03 mmol, 1.0 equiv), 27c (3.76 g, 7.74 mmol, 1.1 equiv) and NaHMDS (2 N in THF, 4.22 mL, 8.44 mmol, 1.2 equiv) via general procedure B. Column chromatography, petroleum ether/Et₂O = 10/1 (v/v). Overall yield of reaction: 52% (mass of both Z and E isomers, 1.24 g); isolated pure Z isomer, 114 mg; isolated pure E isomer, 285 mg; mixture of E/Z isomers, 0.841 g.

34: $R_f = 0.73$ (EtOAc/n-hex = 1/2, v/v); colorless oil. ¹H NMR (400 MHz, CDCl₃): δ 1.27 (dt, $J = 12.9, 4.4$ Hz, 1H), 1.30 (dt, $J = 12.3, 4.0$ Hz, 1H), 1.39 (s, 9H), 1.50–1.58 (m, 2H), 2.60–2.40 (m, 1H), 2.60 (t, $J = 11.4$ Hz, 2H), 4.01 (bs, 2H), 5.51 (dd, $J = 11.4, 10.2$ Hz, 1H), 6.29 (d, $J = 11.5$ Hz, 1H), 6.89 (dt, $J = 8.5, 3.0$ Hz, 1H), 7.06 (dd, $J = 8.5, 2.6$ Hz, 1H), 7.13 (dd, $J = 8.6, 6.2$ Hz, 1H). MS (ESI⁺): m/z [M + K]⁺ 378.10; found 378.66.

35: $R_f = 0.68$ (EtOAc/n-hex = 1/2, v/v); white crystals, mp 90–92 °C. ¹H NMR (400 MHz, CDCl₃): δ 1.36 (dt, $J = 12.4, 4.1$ Hz, 1H), 1.39 (dt, $J = 12.3, 4.2$ Hz, 1H), 1.46 (s, 9H), 1.72–1.79 (m, 2H), 2.27–2.36 (m, 1H), 2.77 (t, $J = 11.4$ Hz, 2H), 4.13 (bs, 2H), 6.04 (dd, $J = 15.9, 6.9$ Hz, 1H), 6.67 (d, $J = 15.9$ Hz, 1H), 6.92 (dt, $J = 8.4, 2.6$ Hz, 1H), 7.07 (dd, $J = 8.5, 2.6$ Hz, 1H), 7.44 (dd, $J = 8.8, 6.1$ Hz, 1H). MS (ESI⁺): m/z [M + Na]⁺ 362.13; found 362.40.

tert-Butyl 4-(4-Methylstyryl)piperidine-1-carboxylate [Isomers (Z)-36 and (E)-37]. Synthesized from aldehyde 3 (1.49 g, 7.00

mmol, 1.0 equiv), 27d (3.13 g, 7.00 mmol, 1.0 equiv), and KHMDS (0.5 M in toluene, 15.40 mL, 7.70 mmol, 1.1 equiv) via general procedure B. Column chromatography, EtOAc/n-hex = 1/5 (v/v). Overall yield of reaction: 45% (mass of both Z and E isomers, 0.94 g); isolated pure Z isomer, 159 mg; isolated pure E isomer, 155 mg; mixture of E/Z isomers, 0.626 g.

36: $R_f = 0.75$ (EtOAc/n-hex = 1/5, v/v); colorless oil. ¹H NMR (400 MHz, CDCl₃): δ 1.29–1.41 (m, 2H), 1.46 (s, 9H), 1.64–1.70 (m, 2H), 2.35 (s, 3H), 2.66–2.77 (m, 3H), 4.08 (bs, 2H), 5.41 (dd, $J = 11.6, 10.0$ Hz, 1H), 6.36 (d, $J = 11.5$ Hz, 1H), 7.12–7.17 (m, 4H). MS (ESI⁺): m/z [M + Na]⁺ 324.19; found 324.63.

37: $R_f = 0.72$ (EtOAc/n-hex = 1/5, v/v); colorless oil. ¹H NMR (400 MHz, CDCl₃): δ 1.36 (dt, $J = 12.2, 4.2$ Hz, 1H), 1.39 (dt, $J = 12.4, 4.3$ Hz, 1H), 1.47 (s, 9H), 1.71–1.78 (m, 2H), 2.22–2.31 (m, 1H), 2.32 (s, 3H), 2.77 (t, $J = 12.6$ Hz, 2H), 4.12 (bs, 2H), 6.09 (dd, $J = 16.0, 6.9$ Hz, 1H), 6.35 (d, $J = 15.8$ Hz, 1H), 7.09–7.12 (m, 2H), 7.22–7.25 (m, 2H). MS (ESI⁺): m/z [M + H]⁺ 302.21; found 302.60.

tert-Butyl 4-(4-Isopropylstyryl)piperidine-1-carboxylate [Isomers (Z)-38 and (E)-39]. Synthesized from aldehyde 3 (1.30 g, 6.10 mmol, 1.0 equiv), 27e (3.19 g, 6.71 mmol, 1.1 equiv), and NaHMDS (2 N in THF, 3.66 mL, 7.32 mmol, 1.2 equiv) via general procedure B. Column chromatography, petroleum ether/Et₂O = 9/1 (v/v). Overall yield of reaction: 65% (mass of both Z and E isomers, 1.78 g); isolated pure Z isomer, 194 mg; isolated pure E isomer, 235 mg; mixture of E/Z isomers, 1.351 g.

38: $R_f = 0.31$ (petroleum ether/Et₂O = 10/1, v/v); colorless oil. ¹H NMR (400 MHz, CDCl₃): δ 1.28 (d, $J = 7.0$ Hz, 6H), 1.36 (dd, $J = 11.9, 3.3$ Hz, 1H), 1.39 (dd, $J = 11.8, 3.0$ Hz, 1H), 1.49 (s, 9H), 1.68–1.75 (m, 2H), 2.72–2.81 (m, 3H), 2.92 (sept, $J = 6.9$ Hz, 1H), 4.11 (bs, 2H), 5.42 (dd, $J = 11.7, 10.0$ Hz, 1H), 6.36 (d, $J = 11.7$ Hz, 1H), 7.18–7.23 (m, 4H). MS (ESI⁺): m/z [M + Na]⁺ 352.22; found 352.00.

39: $R_f = 0.24$ (petroleum ether/Et₂O = 10/1, v/v); colorless oil. ¹H NMR (400 MHz, CDCl₃): δ 1.25 (d, $J = 7.0$ Hz, 6H), 1.37 (dd, $J = 12.8, 4.1$ Hz, 1H), 1.40 (dd, $J = 12.1, 3.9$ Hz, 1H), 1.49 (s, 9H), 1.71–1.79 (m, 2H), 2.22–2.30 (m, 1H), 2.78 (t, $J = 11.4$ Hz, 2H), 2.89 (sept, $J = 7.0$ Hz, 1H), 4.14 (bs, 2H), 6.11 (dd, $J = 16.0, 6.9$ Hz, 1H), 6.38 (d, $J = 15.9$ Hz, 1H), 7.16–7.18 (m, 2H), 7.28–7.30 (m, 2H). MS (ESI⁺): m/z [M + Na]⁺ 352.22; found 352.01.

tert-Butyl 4-(4-Chlorostyryl)piperidine-1-carboxylate [Isomers (Z)-40 and (E)-41]. Synthesized from aldehyde 3 (2.00 g, 9.38 mmol, 1.0 equiv), 27f (4.37 g, 10.32 mmol, 1.1 equiv), and NaHMDS (2 N in THF, 5.63 mL, 11.26 mmol, 1.2 equiv) via general procedure B. Column chromatography, petroleum ether/Et₂O = 10/1 (v/v). Overall yield of reaction: 63% (mass of both Z and E isomers, 1.78 g); isolated pure Z isomer, 202 mg; isolated pure E isomer, 221 mg; mixture of E/Z isomers, 1.357 g.

40: $R_f = 0.15$ (petroleum ether/Et₂O = 10/1, v/v); white crystals, mp 69–70 °C. ¹H NMR (400 MHz, CDCl₃): δ 1.38 (ddd, $J = 17.4, 13.3, 4.7$ Hz, 2H), 1.46 (s, 9H), 1.61–1.67 (m, 2H), 2.58–2.76 (m, 3H), 4.08 (bs, 2H), 5.47 (dd, $J = 11.6, 10.1$ Hz, 1H), 6.36 (d, $J = 11.7$ Hz, 1H), 7.14–7.17 (m, 2H), 7.28–7.32 (m, 2H). MS (ESI⁺): m/z [M + Na]⁺ 344.14; found 344.54.

41: $R_f = 0.10$ (petroleum ether/Et₂O = 10/1, v/v); white crystals, mp 60–62 °C. ¹H NMR (400 MHz, CDCl₃): δ 1.35 (dd, $J = 12.4, 4.1$ Hz, 1H), 1.38 (dd, $J = 12.2, 4.1$ Hz, 1H), 1.46 (s, 9H), 1.71–1.77 (m, 2H), 2.22–2.31 (m, 1H), 2.77 (t, $J = 11.5$ Hz, 2H), 4.14 (bs, 2H), 6.11 (dd, $J = 16.0, 6.9$ Hz, 1H), 6.32 (d, $J = 16.0, 1.2$ Hz, 1H), 7.52 (s, 4H). MS (ESI⁺): m/z [M + Na]⁺ 344.14; found 344.48.

tert-Butyl 4-(4-Bromostyryl)piperidine-1-carboxylate [Isomers (Z)-42 and (E)-43]. Synthesized from aldehyde 3 (2.00 g, 9.38 mmol, 1.0 equiv), 27g (5.28 g, 10.31 mmol, 1.1 equiv), and NaHMDS (2 N in THF, 5.63 mL, 11.26 mmol, 1.2 equiv) via general procedure B. Column chromatography, EtOAc/n-hex = 1/2 (v/v). Overall yield of reaction: 48% (mass of both Z and E isomers, 1.66 g); pure Z isomer was not isolated; isolated pure E isomer, 325 mg; mixture of E/Z isomers, 1.335 g.

43: $R_f = 0.40$ (EtOAc/n-hex = 1/2, v/v); white crystals, mp 65–67 °C. ¹H NMR (400 MHz, CDCl₃): δ 1.36 (dt, $J = 12.4, 4.2$ Hz, 1H),

1.39 (dt, $J = 12.4, 4.5$ Hz, 1H), 1.47 (s, 9H), 1.71–1.78 (m, 2H), 2.22–2.32 (m, 1H), 2.74–2.81 (m, 2H), 4.12 (bs, 2H), 6.13 (dd, $J = 16.0, 6.8$ Hz, 1H), 6.32 (d, $J = 16.0$ Hz, 1H), 7.19–7.22 (m, 2H), 7.39–7.43 (m, 2H).

tert-Butyl 4-(4-Methoxystyryl)piperidine-1-carboxylate [Isomers (Z)-44 and (E)-45]. Synthesized from aldehyde 3 (1.87 g, 8.77 mmol, 1.0 equiv), 27h (4.04 g, 9.65 mmol, 1.1 equiv), and NaHMDS (2 N in THF, 5.26 mL, 10.52 mmol, 1.2 equiv) via general procedure B. Column chromatography, EtOAc/n-hex = 1/9 (v/v) yielding a mixture of *cis/trans* isomers (ratio 20/80, estimated from ^1H NMR). Overall yield of reaction: 40% (mass of both *Z* and *E* isomers, 1.12 g); pure *Z* and *E* isomers were not isolated.

44 and 45 (mixture of both isomers): $R_f = 0.13$ (EtOAc/n-hex = 1/9, v/v); colorless oil. ^1H NMR (400 MHz, CDCl_3): δ 1.31–1.41 (m, 2.6H), 1.46–1.47 (m, 11.5H), 1.63–1.75 (m, 2.6H), 2.20–2.29 (m, 1H), 2.69–2.82 (m, 2.6H), 3.78 (s, 3H), 3.78 (s, 0.7H), 4.12 (bs, 2.6H), 5.36 (dd, $J = 11.6, 10.0$ Hz, 0.2H), 5.99 (dd, $J = 16.0, 6.9$ Hz, 1H), 6.30–6.34 (m, 1.2H), 6.81–6.85 (m, 2H), 6.85–6.89 (m, 0.5H), 7.16–7.19 (m, 0.5H), 7.24–7.29 (m, 2H). MS (ESI+): m/z $[\text{M} + \text{Na}]^+$ 340.19; found 340.04.

tert-Butyl 4-(4-(Trifluoromethyl)styryl)piperidine-1-carboxylate [Isomers (Z)-46 and (E)-47]. Synthesized from aldehyde 3 (2.00 g, 9.38 mmol, 1.0 equiv), 27i (5.56 g, 10.32 mmol, 1.1 equiv), and NaHMDS (2 N in THF, 5.63 mL, 11.26 mmol, 1.2 equiv) via general procedure B. Column chromatography, petroleum ether/Et₂O = 9/1 (v/v). Overall yield of reaction: 66% (mass of both *Z* and *E* isomers, 2.18 g); isolated pure *Z* isomer, 85 mg; isolated pure *E* isomer, 780 mg; mixture of *E/Z* isomers, 1.305 g.

46: $R_f = 0.23$ (petroleum ether/Et₂O = 9/1, v/v); colorless oil. ^1H NMR (400 MHz, CDCl_3): δ 1.32–1.42 (m, 2H), 1.45 (s, 9H), 1.62–1.67 (m, 2H), 2.59–2.68 (m, 1H), 2.71 (t, $J = 12.8$ Hz, 2H), 4.09 (bs, 2H), 5.56 (dd, $J = 11.7, 10.2$ Hz, 1H), 6.36 (d, $J = 11.7$ Hz, 1H), 7.32 (d, $J = 8.5$ Hz, 2H), 7.58 (d, $J = 8.1$ Hz, 2H).

47: $R_f = 0.18$ (petroleum ether/Et₂O = 9/1, v/v); white crystals, mp 46–48 °C. ^1H NMR (400 MHz, CDCl_3): δ 1.35 (dd, $J = 12.2, 4.1$ Hz, 1H), 1.39 (dd, $J = 12.5, 4.1$ Hz, 1H), 1.46 (s, 9H), 1.71–1.77 (m, 2H), 2.24–2.33 (m, 1H), 2.76 (t, $J = 11.4$ Hz, 2H), 4.14 (bs, 2H), 6.22 (dd, $J = 16.0, 6.8$ Hz, 1H), 6.38 (d, $J = 16.1$ Hz, 1H), 7.40 (d, $J = 8.4$ Hz, 2H), 7.51 (d, $J = 8.2$ Hz, 2H).

tert-Butyl 4-(3-(Trifluoromethyl)styryl)piperidine-1-carboxylate [Isomers (Z)-48 and (E)-49]. Synthesized from aldehyde 3 (1.49 g, 7.00 mmol, 1.0 equiv), 27j (3.51 g, 7.00 mmol, 1.0 equiv), and KHMDS (0.5 M in toluene, 15.40 mL, 7.70 mmol, 1.1 equiv) via general procedure B. Column chromatography, petroleum ether/Et₂O = 8/1, (v/v). Overall yield of reaction: 62% (mass of both *Z* and *E* isomers, 1.53 g); isolated pure *Z* isomer, 51 mg; isolated pure *E* isomer, 404 mg; mixture of *E/Z* isomers, 1.075 g.

48: $R_f = 0.20$ (petroleum ether/Et₂O = 8/1, v/v); colorless oil. ^1H NMR (400 MHz, CDCl_3): δ 1.35 (dt, $J = 12.6, 4.0$ Hz, 1H), 1.36–1.43 (m, 1H), 1.45 (s, 9H), 1.61–1.68 (m, 2H), 2.56–2.66 (m, 1H), 2.71 (t, $J = 11.2$ Hz, 2H), 4.08 (bs, 2H), 5.55 (dd, $J = 11.6, 10.2$ Hz, 1H), 6.40 (d, $J = 11.6$ Hz, 1H), 7.38–7.50 (m, 4H). MS (ESI+): m/z $[\text{M} + \text{Na}]^+$ 378.17; found 378.76.

49: $R_f = 0.15$ (petroleum ether/Et₂O = 8/1, v/v); colorless oil. ^1H NMR (400 MHz, CDCl_3): δ 1.37 (dt, $J = 12.4, 4.3$ Hz, 1H), 1.40 (dt, $J = 12.2, 4.1$ Hz, 1H), 1.47 (s, 9H), 1.73–1.80 (m, 2H), 2.26–2.36 (m, 1H), 2.78 (t, $J = 12.0$ Hz, 2H), 4.14 (bs, 2H), 6.22 (dd, $J = 16.0, 6.9$ Hz, 1H), 6.41 (d, $J = 16.0$ Hz, 1H), 7.38–7.46 (m, 2H), 7.48–7.51 (m, 1H), 7.57–7.59 (m, 1H). MS (ESI+): m/z $[\text{M} + \text{Na}]^+$ 378.17; found 378.69.

tert-Butyl 4-(4-Cyanostyryl)piperidine-1-carboxylate [Isomers (Z)-50 and (E)-51]. Synthesized from aldehyde 3 (2.35 g, 11.02 mmol, 1.0 equiv), 27k (5.56 g, 12.12 mmol, 1.1 equiv), and NaHMDS (2 N in THF, 6.61 mL, 13.22 mmol, 1.2 equiv) via general procedure B. Column chromatography, petroleum ether/Et₂O = 3/1 (v/v). Overall yield of reaction: 39% (mass of both *Z* and *E* isomers, 1.35 g); isolated pure *Z* isomer, 370 mg; isolated pure *E* isomer, 320 mg; mixture of *E/Z* isomers, 0.66 g.

50: $R_f = 0.20$ (petroleum ether/Et₂O = 3/1, v/v); white crystals, mp 65–68 °C. ^1H NMR (400 MHz, CDCl_3): δ 1.31–1.40 (m, 2H),

1.43 (s, 9H), 1.57–1.64 (m, 2H), 2.54–2.64 (m, 1H), 2.70 (t, $J = 11.7$ Hz, 2H), 4.05 (bs, 2H), 5.58 (dd, $J = 11.7, 10.2$ Hz, 1H), 6.36 (d, $J = 11.8$ Hz, 1H), 7.28–7.31 (m, 2H), 7.58–7.61 (m, 2H). MS (ESI+): m/z $[\text{M} + \text{Na}]^+$ 335.17; found 335.31.

51: $R_f = 0.14$ (petroleum ether/Et₂O = 3/1, v/v); white crystals, mp 88–90 °C. ^1H NMR (400 MHz, CDCl_3): δ 1.30–1.40 (m, 2H), 1.43 (s, 9H), 1.70–1.75 (m, 2H), 2.25–2.34 (m, 1H), 2.75 (t, $J = 10.7$ Hz, 2H), 4.11 (bs, 2H), 6.26 (dd, $J = 16.0, 6.6$ Hz, 1H), 6.36 (d, $J = 16.0$ Hz, 1H), 7.37–7.39 (m, 2H), 7.52–7.55 (m, 2H). MS (ESI+): m/z $[\text{M} - \text{H}]^-$ 311.17; found 311.37.

tert-Butyl 4-(4-(Methylsulfonyl)styryl)piperidine-1-carboxylate [Isomers (Z)-52 and (E)-53]. Synthesized from aldehyde 3 (0.94 g, 4.10 mmol, 1.0 equiv), 27l (1.94 g, 4.50 mmol, 1.1 equiv), and NaHMDS (2 N in THF, 2.45 mL, 4.90 mmol, 1.2 equiv) via general procedure B. Column chromatography, EtOAc/n-hex = 1/2 (v/v). Overall yield of reaction: 30% (mass of both *Z* and *E* isomers, 0.46 g); isolated pure *Z* isomer, 180 mg; isolated pure *E* isomer, 260 mg; mixture of *E/Z* isomers, 0.02 g.

52: $R_f = 0.27$ (EtOAc/n-hex = 1/2, v/v); colorless oil. ^1H NMR (400 MHz, CDCl_3): δ 1.34–1.45 (m, 2H), 1.47 (s, 9H), 1.62–1.69 (m, 2H), 2.58–2.68 (m, 1H), 2.72 (t, $J = 12.0$ Hz, 2H), 3.08 (s, 3H), 4.11 (bs, 2H), 5.62 (dd, $J = 11.6, 10.4$ Hz, 1H), 6.44 (d, $J = 11.6$ Hz, 1H), 7.40–7.43 (m, 2H), 7.90–7.93 (m, 2H). MS (ESI+): m/z $[\text{M} + \text{Na}]^+$ 388.16; found 387.91.

53: $R_f = 0.22$ (EtOAc/n-hex = 1/2, v/v); white crystals, mp 93–97 °C. ^1H NMR (400 MHz, CDCl_3): δ 1.38 (dt, $J = 12.4, 4.1$ Hz, 1H), 1.41 (dd, $J = 12.4, 4.0$ Hz, 1H), 1.47 (s, 9H), 1.75–1.83 (m, 2H), 2.30–2.39 (m, 1H), 2.79 (t, $J = 10.7$ Hz, 2H), 3.05 (s, 3H), 4.15 (bs, 2H), 6.33 (dd, $J = 16.0, 6.7$ Hz, 1H), 6.45 (d, $J = 16.0$ Hz, 1H), 7.50–7.53 (m, 2H), 7.85–7.88 (m, 2H). MS (ESI+): m/z $[\text{M} + \text{Na}]^+$ 388.16; found 387.91.

tert-Butyl 4-(4-Cyclopropylstyryl)piperidine-1-carboxylate [Isomers (Z)-54 and (E)-55]. To the solution of 42 and 43 (0.733 g, 2.0 mmol, 1.0 equiv), cyclopropylboronic acid (0.224 g, 2.60 mmol, 1.3 equiv), K₃PO₄ (1.48 g, 7.00 mmol, 3.5 equiv) and tricyclohexylphosphine (20% solution in toluene, 0.316 mL, 0.20 mmol, 0.1 equiv) in toluene (10 mL) and water (0.4 mL), Pd(OAc)₂ (23 mg, 0.1 mmol, 0.05 equiv) was added under an argon atmosphere. The reaction mixture was stirred at 100 °C for 3 h and then allowed to cool down to room temperature. Water (20 mL) was added to the mixture, which was then transferred into a separating funnel, and extracted with EtOAc (2 × 50 mL). Combined organic layers were washed with saturated brine (20 mL), dried over Na₂SO₄, and evaporated. Column chromatography, petroleum ether/Et₂O = 10/1 (v/v). Overall yield of reaction: 78% (mass of both *Z* and *E* isomers, 0.511 g); isolated pure *Z* isomer, 85 mg; isolated pure *E* isomer, 210 mg; mixture of *E/Z* isomers, 0.216 g.

54: $R_f = 0.29$ (petroleum ether/Et₂O = 10/1, v/v); colorless oil. ^1H NMR (400 MHz, CDCl_3): δ 0.68–0.73 (m, 2H), 0.94–1.00 (m, 2H), 1.30–1.41 (m, 2H), 1.47 (s, 9H), 1.63–1.70 (m, 2H), 1.86–1.93 (m, 1H), 2.67–2.79 (m, 3H), 4.09 (bs, 2H), 5.40 (dd, $J = 11.6, 10.0$ Hz, 1H), 6.35 (d, $J = 11.6$ Hz, 1H), 7.03–7.06 (m, 2H), 7.12–7.16 (m, 2H).

55: $R_f = 0.22$ (petroleum ether/Et₂O = 10/1, v/v); colorless oil. ^1H NMR (400 MHz, CDCl_3): δ 0.66–0.70 (m, 2H), 0.92–0.97 (m, 2H), 1.36 (dt, $J = 12.7, 4.4$ Hz, 1H), 1.39 (dt, $J = 12.3, 4.1$ Hz, 1H), 1.48 (s, 9H), 1.70–1.78 (m, 2H), 1.83–1.90 (m, 1H), 2.21–2.31 (m, 1H), 2.78 (t, $J = 11.6$ Hz, 2H), 4.13 (bs, 2H), 6.08 (dd, $J = 16.0, 6.9$ Hz, 1H), 6.34 (d, $J = 16.0$ Hz, 1H), 6.98–7.02 (m, 2H), 7.22–7.25 (m, 2H).

tert-Butyl 4-Phenethylpiperidine-1-carboxylate (56). Synthesized from a mixture of 28 and 29 (1.139 g, 4.84 mmol, 1.0 equiv) via general procedure C. Yield: quantitative (1.39 g); colorless oil. ^1H NMR (400 MHz, CDCl_3): δ 1.21 (ddd, $J = 16.5, 12.5, 4.3$ Hz, 2H), 1.35–1.43 (m, 1H), 1.45 (s, 9H), 1.53–1.59 (m, 2H), 1.68–1.71 (m, 2H), 2.60–2.69 (m, 4H), 4.07 (bs, 2H), 7.15–7.19 (m, 3H), 7.24–7.29 (m, 2H). MS (ESI+): m/z $[\text{M} + \text{Na}]^+$ 312.19; found 311.91.

tert-Butyl 4-(3-Fluorophenethyl)piperidine-1-carboxylate (57). Synthesized from a mixture of 30 and 31 (0.452 g, 1.48 mmol, 1.0 equiv) via general procedure C. Yield: 95% (0.432 g); pale

yellow oil. ^1H NMR (400 MHz, CDCl_3): δ 1.11 (dt, J = 12.3, 4.1 Hz, 1H), 1.14 (dt, J = 12.5, 4.2 Hz, 1H), 1.35–1.44 (m, 1H), 1.45 (s, 9H), 1.50–1.59 (m, 2H), 1.65–1.72 (m, 2H), 2.59–2.72 (m, 4H), 4.08 (bs, 2H), 6.84–6.89 (m, 2H), 6.91–6.95 (m, 1H), 7.22 (ddd, J = 8.9, 7.6, 6.1 Hz, 1H). MS (ESI+): m/z $[\text{M} + \text{Na}]^+$ 330.18; found 330.42.

tert-Butyl 4-(2-Fluorophenethyl)piperidine-1-carboxylate (58). Synthesized from a mixture of **32** and **33** (0.252 g, 0.83 mmol, 1.0 equiv) via general procedure C. Yield: 95% (0.242 g); pale yellow oil. ^1H NMR (400 MHz, CDCl_3): δ 1.12 (dt, J = 12.4, 4.1 Hz, 1H), 1.15 (dt, J = 12.4, 4.2 Hz, 1H), 1.37–1.44 (m, 1H), 1.46 (s, 9H), 1.52–1.59 (m, 2H), 1.69–1.76 (m, 2H), 2.58–2.72 (m, 4H), 4.08 (bs, 2H), 6.97–7.02 (m, 1H), 7.03–7.04 (m, 1H), 7.13–7.19 (m, 2H). MS (ESI+): m/z $[\text{M} + \text{Na}]^+$ 330.18; found 330.41.

tert-Butyl 4-(4-Methylphenethyl)piperidine-1-carboxylate (59). Synthesized from a mixture of **36** and **37** (0.28 g, 0.93 mmol, 1.0 equiv) via general procedure C. Yield: quantitative; yellow oil. ^1H NMR (400 MHz, CDCl_3): δ 1.11 (dt, J = 12.3, 4.1 Hz, 1H), 1.14 (dt, J = 12.4, 4.1 Hz, 1H), 1.36–1.44 (m, 1H), 1.45 (s, 9H), 1.51–1.57 (m, 2H), 1.65–1.73 (m, 2H), 2.32 (s, 3H), 2.56–2.61 (m, 2H), 2.63–2.70 (m, 2H), 4.07 (bs, 2H), 7.04–7.10 (m, 4H). MS (ESI+): m/z $[\text{M} + \text{Na}]^+$ 326.21; found 326.73.

tert-Butyl 4-(4-Isopropylphenethyl)piperidine-1-carboxylate (60). Synthesized from a mixture of **38** and **39** (0.870 g, 2.64 mmol, 1.0 equiv) via general procedure C. Yield: 83% (0.727 g); colorless oil. ^1H NMR (400 MHz, CDCl_3): δ 1.16 (ddd, J = 16.9, 12.9, 5.5 Hz, 2H), 1.27 (d, J = 7.0 Hz, 6H), 1.40–1.47 (m, 1H), 1.49 (s, 9H), 1.54–1.61 (m, 2H), 1.70–1.76 (m, 2H), 2.61–2.64 (m, 2H), 2.70 (t, J = 11.5 Hz, 2H), 2.91 (sept, J = 6.9 Hz, 1H), 4.10 (bs, 2H), 7.11–7.13 (m, 2H), 7.16–7.18 (m, 2H). MS (ESI+): m/z $[\text{M} + \text{Na}]^+$ 354.24; found 354.05.

tert-Butyl 4-(4-Chlorophenethyl)piperidine-1-carboxylate (61). Synthesized from a mixture of **40** and **41** (0.850 g, 2.64 mmol, 1.0 equiv) via general procedure C. Column chromatography, petroleum ether/ Et_2O = 3/1 (v/v). Yield: 86% (0.736 g); colorless oil. ^1H NMR (400 MHz, CDCl_3): δ 1.08 (dd, J = 12.3, 4.2 Hz, 1H), 1.11 (dd, J = 12.8, 3.9 Hz, 1H), 1.33–1.40 (m, 1H), 1.44 (s, 9H), 1.48–1.53 (m, 2H), 1.63–1.68 (m, 2H), 2.55–2.59 (m, 2H), 2.64 (t, J = 11.6 Hz, 2H), 4.07 (bs, 2H), 7.05–7.08 (m, 2H), 7.18–7.22 (m, 2H). MS (ESI+): m/z $[\text{M} + \text{Na}]^+$ 346.15; found 346.55.

tert-Butyl 4-(4-Methoxyphenethyl)piperidine-1-carboxylate (62). Synthesized from a mixture of **44** and **45** (0.250 g, 0.79 mmol, 1.0 equiv) via general procedure C. Yield: 86% (0.245 g); colorless oil. ^1H NMR (400 MHz, CDCl_3): δ 1.12 (ddd, J = 16.3, 12.5, 4.3 Hz, 2H), 1.35–1.43 (m, 1H), 1.45 (s, 9H), 1.50–1.56 (m, 2H), 1.64–1.71 (m, 2H), 2.55–2.59 (m, 2H), 2.66 (t, J = 11.8 Hz, 2H), 3.79 (s, 3H), 4.07 (bs, 2H), 6.81–6.84 (m, 2H), 7.07–7.10 (m, 2H). MS (ESI+): m/z $[\text{M} + \text{Na}]^+$ 342.20; found 342.59.

tert-Butyl 4-(4-(Trifluoromethyl)phenethyl)piperidine-1-carboxylate (63). Synthesized from a mixture of **46** and **47** (0.24 g, 0.68 mmol, 1.0 equiv) via general procedure C. Yield: quantitative; yellow oil. ^1H NMR (400 MHz, CDCl_3): δ 1.12 (dt, J = 12.4, 4.2 Hz, 1H), 1.15 (dt, J = 12.3, 4.3 Hz, 1H), 1.36–1.44 (m, 1H), 1.45 (s, 9H), 1.53–1.61 (m, 2H), 1.65–1.73 (m, 2H), 2.60–2.70 (m, 4H), 4.08 (bs, 2H), 7.25–7.28 (m, 2H), 7.50–7.53 (m, 2H).

tert-Butyl 4-(3-(Trifluoromethyl)phenethyl)piperidine-1-carboxylate (64). Synthesized from a mixture of **48** and **49** (0.27 g, 0.76 mmol, 1.0 equiv) via general procedure C. Yield: quantitative; colorless oil. ^1H NMR (400 MHz, CDCl_3): δ 1.13 (dt, J = 12.2, 4.2 Hz, 1H), 1.16 (dt, J = 12.4, 4.2 Hz, 1H), 1.37–1.45 (m, 1H), 1.46 (s, 9H), 1.55–1.61 (m, 2H), 1.67–1.74 (m, 2H), 2.63–2.72 (m, 4H), 4.09 (bs, 2H), 7.34–7.45 (m, 4H). MS (ESI+): m/z $[\text{M} + \text{Na}]^+$ 380.18; found 380.77.

tert-Butyl 4-(4-Cyanophenethyl)piperidine-1-carboxylate (65). Synthesized from a mixture of **50** and **51** (0.658 g, 2.11 mmol, 1.0 equiv) via general procedure C. Column chromatography, petroleum ether/ Et_2O = 3/1 (v/v). Yield: 95% (0.632 g); colorless oil. ^1H NMR (400 MHz, CDCl_3): δ 1.09 (dd, J = 12.4, 4.2 Hz, 1H), 1.12 (dd, J = 12.5, 4.3 Hz, 1H), 1.34–1.40 (m, 1H), 1.42 (s, 9H), 1.51–1.58 (m, 2H), 1.63–1.68 (m, 2H), 2.61–2.68 (m, 4H), 4.06

(bs, 2H), 7.23–7.25 (m, 2H), 7.51–7.54 (m, 2H). MS (ESI+): m/z $[\text{M} + \text{Na}]^+$ 337.19; found 337.07.

tert-Butyl 4-(4-Propylphenethyl)piperidine-1-carboxylate (66). Synthesized from a mixture of **54** and **55** (0.216 g, 0.660 mmol, 1.0 equiv) via general procedure C. The reaction conditions applied resulted in cyclopropyl ring opening to yield the titled compound. Yield: 92% (0.200 g); colorless oil. ^1H NMR (400 MHz, CDCl_3): δ 0.95 (t, J = 7.3 Hz, 3H), 1.07–1.17 (m, 2H), 1.37–1.45 (m, 1H), 1.45 (s, 9H), 1.52–1.67 (m, 6H), 2.53–2.61 (m, 4H), 2.67 (t, J = 13.0 Hz, 2H), 4.07 (bs, 2H), 7.06–7.11 (m, 4H). ^{13}C NMR (100 MHz, CDCl_3): δ 13.89, 24.63, 28.47, 32.11, 32.48, 35.53, 37.64, 38.41, 43.98, 79.17, 128.10, 128.40, 139.65, 140.03, 154.89. HRMS (ESI+): m/z calcd for $\text{C}_{21}\text{H}_{33}\text{O}_2\text{NNa}$ $[\text{M} + \text{Na}]^+$ 354.2404; found 354.2401.

(Z)-1-(Prop-2-yn-1-yl)-4-styrylpiperidine (67). Synthesized from **28** (0.100 g, 0.348 mmol, 1.0 equiv) via general procedures D and E. Column chromatography, $\text{EtOAc}/n\text{-hex}$ = 1/1 (v/v). Yield: 82% (64 mg); white crystals, mp 42–43 °C. ^1H NMR (400 MHz, CDCl_3): δ 1.50–1.60 (m, 2H), 1.74 (bd, J = 16.0 Hz, 2H), 2.19–2.26 (m, 3H), 2.52–2.62 (m, 1H), 2.86–2.90 (m, 2H), 3.29 (d, J = 2.4 Hz, 2H), 5.49 (dd, J = 11.4, 10.3 Hz, 1H), 6.38 (d, J = 11.7 Hz, 1H), 7.21–7.25 (m, 3H), 7.31–7.35 (m, 2H). ^{13}C NMR (100 MHz, CDCl_3): δ 32.29, 34.38, 47.23, 51.87, 72.93, 79.03, 126.55, 128.03, 128.18, 128.45, 137.19, 137.57. HRMS (ESI+): m/z calcd for $\text{C}_{16}\text{H}_{20}\text{N}$ $[\text{M} + \text{H}]^+$ 226.1596; found 226.1598. IR (ATR): 3210, 2988, 2945, 2917, 2800, 1498, 1446, 1425, 1330, 1311, 1127, 1103, 1073, 969, 904, 799, 775, 727, 696, 670, 560 cm^{-1} . HPLC purity, 99.9% (t_R = 8.86 min).

(E)-1-(Prop-2-yn-1-yl)-4-styrylpiperidine (68). Synthesized from **29** (0.196 g, 0.682 mmol, 1.0 equiv) via general procedures D and E. Column chromatography, $\text{EtOAc}/n\text{-hex}$ = 1/1 (v/v). Yield: 89% (137 mg); white crystals, mp 44–46 °C. ^1H NMR (400 MHz, CDCl_3): δ 1.56 (dd, J = 11.9, 3.9 Hz, 1H), 1.59 (dd, J = 11.9, 3.9 Hz, 1H), 1.79–1.84 (m, 2H), 2.09–2.19 (m, 1H), 2.25–2.31 (m, 3H), 2.94 (td, J = 11.1, 2.4 Hz, 2H), 3.33 (d, J = 2.5 Hz, 2H), 6.18 (dd, J = 16.0, 7.0 Hz, 1H), 6.39 (d, J = 16.5 Hz, 1H), 7.18–7.22 (m, 1H), 7.26–7.32 (m, 2H), 7.34–7.37 (m, 2H). ^{13}C NMR (100 MHz, CDCl_3): δ 31.91, 38.71, 47.13, 52.13, 72.91, 78.98, 125.87, 126.85, 128.10, 128.35, 134.76, 137.47. HRMS (ESI+): m/z calcd for $\text{C}_{16}\text{H}_{20}\text{N}$ $[\text{M} + \text{H}]^+$ 226.1596; found 226.1594. IR (ATR): 3264, 2929, 2909, 2805, 1446, 1429, 1315, 1223, 1135, 1106, 976, 962, 897, 744, 686, 670, 619, 519 cm^{-1} . HPLC purity, 99.2% (t_R = 8.90 min).

(Z)-4-(3-Fluorostyryl)-1-(prop-2-yn-1-yl)piperidine (69). Synthesized from **30** (110 mg, 0.360 mmol, 1.0 equiv) via general procedures D and E. Column chromatography, $\text{EtOAc}/n\text{-hex}$ = 1/2 (v/v). Yield: 12% (11 mg); yellow crystals, mp 51–53 °C. ^1H NMR (400 MHz, CDCl_3): δ 1.49–1.60 (m, 2H), 1.69–1.76 (m, 2H), 2.23 (dt, J = 11.7, 2.5 Hz, 2H), 2.24 (t, J = 2.4 Hz, 1H), 2.48–2.58 (m, 1H), 2.86–2.91 (m, 2H), 3.30 (d, J = 2.4 Hz, 2H), 5.53 (dd, J = 11.6, 10.2 Hz, 1H), 6.33 (d, J = 11.7 Hz, 1H), 6.90–6.95 (m, 2H), 6.99–7.01 (m, 1H), 7.26–7.31 (m, 1H). ^{13}C NMR (100 MHz, CDCl_3): δ 32.16, 34.45, 47.23, 51.81, 73.02, 78.96, 113.44 (d, J_{CF} = 21.2 Hz), 115.17 (d, J_{CF} = 21.3 Hz), 124.22 (d, J_{CF} = 2.8 Hz), 127.01 (d, J_{CF} = 2.1 Hz), 129.62 (d, J_{CF} = 8.6 Hz), 138.29, 139.76 (d, J_{CF} = 7.9 Hz), 162.66 (d, J_{CF} = 245.2 Hz). HRMS (ESI+): m/z calcd for $\text{C}_{16}\text{H}_{19}\text{FN}$ $[\text{M} + \text{H}]^+$ 244.1502; found 244.1504. IR (ATR): 3304, 2924, 2851, 2805, 2755, 1611, 1580, 1513, 1487, 1465, 1444, 1386, 1364, 1335, 1311, 1272, 1247, 1231, 1138, 1124, 1105, 1073, 1018, 973, 937, 923, 878, 792, 764, 752, 694, 667, 634 cm^{-1} . HPLC purity, 97.9% (t_R = 9.10 min).

(E)-4-(3-Fluorostyryl)-1-(prop-2-yn-1-yl)piperidine (70). Synthesized from **31** (0.300 g, 0.982 mmol, 1.0 equiv) via general procedures D and E. Column chromatography, $\text{EtOAc}/n\text{-hex}$ = 1/2 (v/v). Yield: 38% (91 mg); pale yellow oil. ^1H NMR (400 MHz, CDCl_3): δ 1.57 (dt, J = 12.0, 3.9 Hz, 1H), 1.60 (dt, J = 11.9, 3.9 Hz, 1H), 1.78–1.84 (m, 2H), 2.10–2.19 (m, 1H), 2.27 (t, J = 2.5 Hz, 1H), 2.31 (dt, J = 11.7, 2.5 Hz, 2H), 2.93–2.98 (m, 2H), 3.35 (d, J = 2.5 Hz, 2H), 6.17 (dd, J = 16.0, 6.9 Hz, 1H), 6.34 (d, J = 16.0 Hz, 1H), 6.88 (ddt, J = 8.4, 2.6, 0.9 Hz, 1H), 7.02–7.06 (m, 1H), 7.07–7.11 (m, 1H), 7.21–7.27 (m, 1H). ^{13}C NMR (100 MHz, CDCl_3): δ

31.71, 38.64, 47.15, 52.10, 73.32, 78.62, 112.39 (d, $J_{\text{C,F}} = 22.0$ Hz), 113.73 (d, $J_{\text{C,F}} = 21.3$ Hz), 121.87 (d, $J_{\text{C,F}} = 2.9$ Hz), 127.33 (d, $J_{\text{C,F}} = 2.9$ Hz), 129.84 (d, $J_{\text{C,F}} = 8.7$ Hz), 136.10, 139.94 (d, $J_{\text{C,F}} = 7.3$ Hz), 163.06 (d, $J_{\text{C,F}} = 244.9$ Hz). HRMS (ESI+): m/z calcd for $\text{C}_{16}\text{H}_{19}\text{FN}$ $[\text{M} + \text{H}]^+$ 244.1502; found 244.1504. IR (ATR): 3303, 2931, 2808, 2751, 1651, 1611, 1583, 491, 1466, 1445, 1385, 1364, 1336, 1312, 1267, 1245, 1140, 1106, 1074, 962, 939, 897, 873, 829, 809, 777, 684, 631, 590 cm^{-1} . HPLC purity, 99.6% ($t_{\text{R}} = 9.15$ min).

(Z)-4-(2-Fluorostyryl)-1-(prop-2-yn-1-yl)piperidine (71). Synthesized from 32 (225 mg, 0.737 mmol, 1.0 equiv) via general procedures D and E. Column chromatography, EtOAc/n-hex = 1/2 (v/v). Yield: 5% (9 mg); colorless oil. ^1H NMR (400 MHz, CDCl_3): δ 1.49–1.59 (m, 2H), 1.68–1.75 (m, 2H), 2.16–2.23 (m, 2H), 2.23 (t, $J = 2.4$ Hz, 1H), 2.33–2.43 (m, 1H), 2.85–2.90 (m, 2H), 3.30 (d, $J = 2.4$ Hz, 2H), 5.62 (dd, $J = 11.6$, 10.2 Hz, 1H), 6.37 (d, $J = 11.4$ Hz, 1H), 7.03–7.08 (m, 1H), 7.09–7.13 (m, 1H), 7.21–7.26 (m, 2H). ^{13}C NMR (100 MHz, CDCl_3): δ 32.11, 34.98, 47.28, 51.89, 72.94, 79.08, 115.43 (d, $J_{\text{C,F}} = 22.3$ Hz), 120.66 (d, $J_{\text{C,F}} = 3.0$ Hz), 123.66 (d, $J_{\text{C,F}} = 3.6$ Hz), 125.22 (d, $J_{\text{C,F}} = 15.0$ Hz), 128.45 (d, $J_{\text{C,F}} = 8.2$ Hz), 130.28 (d, $J_{\text{C,F}} = 3.7$ Hz), 139.25, 160.03 (d, $J_{\text{C,F}} = 246.6$ Hz). HRMS (ESI+): m/z calcd for $\text{C}_{16}\text{H}_{19}\text{FN}$ $[\text{M} + \text{H}]^+$ 244.1502; found 244.1505. IR (ATR): 3300, 2918, 2802, 2754, 1485, 1451, 1334, 1310, 1272, 1232, 1134, 1095, 972, 835, 780, 758, 634 cm^{-1} . HPLC purity, 97.1% ($t_{\text{R}} = 9.04$ min).

(E)-4-(2-Fluorostyryl)-1-(prop-2-yn-1-yl)piperidine (72). Synthesized from 33 (0.180 g, 0.589 mmol, 1.0 equiv) via general procedures D and E. Column chromatography, EtOAc/n-hex = 1/2 (v/v). Yield: 58% (83 mg); pale yellow oil. ^1H NMR (400 MHz, CDCl_3): δ 1.56 (dt, $J = 12.0$, 3.9 Hz, 1H), 1.59 (dt, $J = 12.0$, 3.9 Hz, 1H), 1.79–1.85 (m, 2H), 2.12–2.20 (m, 1H), 2.25 (t, $J = 2.4$ Hz, 1H), 2.28 (dt, $J = 11.7$, 2.5 Hz, 2H), 2.91–2.96 (m, 2H), 3.33 (d, $J = 2.4$ Hz, 2H), 6.23 (dd, $J = 16.1$, 7.1 Hz, 1H), 6.55 (d, $J = 16.1$ Hz, 1H), 7.00 (ddd, $J = 10.8$, 8.1, 1.2 Hz, 1H), 7.07 (dt, $J = 7.4$, 1.0 Hz, 1H), 7.14–7.19 (m, 1H), 7.44 (dt, $J = 7.7$, 1.7 Hz, 1H). ^{13}C NMR (100 MHz, CDCl_3): δ 31.93, 39.22, 47.24, 52.21, 72.97, 79.06, 115.58 (d, $J_{\text{C,F}} = 22.3$ Hz), 120.59 (d, $J_{\text{C,F}} = 3.8$ Hz), 123.95 (d, $J_{\text{C,F}} = 3.6$ Hz), 125.32 (d, $J_{\text{C,F}} = 12.3$ Hz), 126.88 (d, $J_{\text{C,F}} = 12.3$ Hz), 128.14 (d, $J_{\text{C,F}} = 8.5$ Hz), 137.41 (d, $J_{\text{C,F}} = 4.2$ Hz), 159.94 (d, $J_{\text{C,F}} = 248.4$ Hz). HRMS (ESI+): m/z calcd for $\text{C}_{16}\text{H}_{19}\text{FN}$ $[\text{M} + \text{H}]^+$ 244.1502; found 244.1500. IR (ATR): 3183, 2947, 2921, 2802, 2756, 1576, 1485, 1455, 1445, 1389, 1371, 1360, 1331, 1301, 1277, 1263, 1230, 1213, 1194, 1183, 1141, 1108, 1091, 1031, 1020, 983, 968, 946, 842, 811, 777, 754, 713 cm^{-1} . HPLC purity, 99.5% ($t_{\text{R}} = 9.09$ min).

(Z)-4-(2-Chloro-4-fluorostyryl)-1-(prop-2-yn-1-yl)piperidine (73). Synthesized from 34 (110 mg, 0.324 mmol, 1.0 equiv) via general procedures D and E. Column chromatography, EtOAc/n-hex = 1/2 (v/v). Yield: 6% (5 mg); white-yellow crystals, mp 51–53 °C. ^1H NMR (400 MHz, CDCl_3): δ 1.48–1.58 (m, 2H), 1.64–1.69 (m, 2H), 2.13–2.30 (m, 3H), 2.23 (t, $J = 2.4$ Hz, 1H), 2.83–2.88 (m, 2H), 3.28 (d, $J = 2.4$ Hz, 2H), 5.61 (dd, $J = 10.8$, 10.4 Hz, 1H), 6.35 (d, $J = 11.5$ Hz, 1H), 6.96 (dt, $J = 8.4$, 2.4 Hz, 1H), 7.14 (dd, $J = 8.4$, 2.4 Hz, 1H), 7.19 (dd, $J = 8.2$, 6.4 Hz, 1H). ^{13}C NMR (100 MHz, CDCl_3): δ 32.09, 34.57, 47.23, 51.78, 72.99, 78.97, 113.64 (d, $J_{\text{C,F}} = 20.7$ Hz), 116.70 (d, $J_{\text{C,F}} = 24.8$ Hz), 124.51, 130.93 (d, $J_{\text{C,F}} = 8.3$ Hz), 132.06 (d, $J_{\text{C,F}} = 3.7$ Hz), 134.16 (d, $J_{\text{C,F}} = 10.2$ Hz), 138.65, 161.35 (d, $J_{\text{C,F}} = 248.6$ Hz). HRMS (ESI+): m/z calcd for $\text{C}_{16}\text{H}_{18}\text{FCIN}$ $[\text{M} + \text{H}]^+$ 278.1112; found 244.1105. IR (ATR): 3166, 3010, 2932, 2789, 2758, 1601, 1574, 1485, 1467, 1445, 1403, 1390, 1367, 1331, 1307, 1295, 1271, 1257, 1230, 1221, 1210, 1169, 1142, 1121, 1109, 1064, 1041, 1016, 1006, 973, 951, 901, 875, 863, 821, 790, 768, 747, 704, 687, 643, 615, 583, 547 cm^{-1} . HPLC purity, 99.7% ($t_{\text{R}} = 9.85$ min).

(E)-4-(2-Chloro-4-fluorostyryl)-1-(prop-2-yn-1-yl)piperidine (74). Synthesized from 35 (0.263 g, 0.774 mmol, 1.0 equiv) via general procedures D and E. Column chromatography, EtOAc/n-hex = 1/2 (v/v). Yield: 58% (125 mg); pale yellow oil. ^1H NMR (400 MHz, CDCl_3): δ 1.56 (dt, $J = 12.0$, 3.9 Hz, 1H), 1.59 (dt, $J = 11.9$, 3.9 Hz, 1H), 1.77–1.85 (m, 2H), 2.12–2.23 (m, 1H), 2.25 (t, $J = 2.4$ Hz, 1H), 2.28 (dt, $J = 11.7$, 2.5 Hz, 2H), 2.91–2.96 (m, 2H), 3.32 (d, $J = 2.4$ Hz, 2H), 6.07 (dd, $J = 15.9$, 7.1 Hz, 1H), 6.68 (d, $J = 15.9$ Hz,

1H), 6.90–6.95 (m, 1H), 7.08 (dd, $J = 8.5$, 2.6 Hz, 1H), 7.47 (dt, $J = 8.8$, 6.1 Hz, 1H). ^{13}C NMR (100 MHz, CDCl_3): δ 31.88, 38.93, 47.18, 52.10, 72.95, 78.98, 114.11 (d, $J_{\text{C,F}} = 21.3$ Hz), 116.56 (d, $J_{\text{C,F}} = 24.7$ Hz), 123.61 (d, $J_{\text{C,F}} = 1.1$ Hz), 127.48 (d, $J_{\text{C,F}} = 8.8$ Hz), 131.97 (d, $J_{\text{C,F}} = 3.7$ Hz), 133.00 (d, $J_{\text{C,F}} = 10.2$ Hz), 137.51 (d, $J_{\text{C,F}} = 1.7$ Hz), 161.32 (d, $J_{\text{C,F}} = 249.4$ Hz). HRMS (ESI+): m/z calcd for $\text{C}_{16}\text{H}_{18}\text{FCIN}$ $[\text{M} + \text{H}]^+$ 278.1112; found 278.1120. IR (ATR): 3303, 2933, 2803, 2753, 1650, 1600, 1574, 1466, 1445, 1396, 1364, 1336, 1312, 1269, 1258, 1237, 1183, 1137, 1122, 1040, 966, 904, 858, 805, 776, 760, 686, 627, 579 cm^{-1} . HPLC purity, 100% ($t_{\text{R}} = 9.86$ min).

(Z)-4-(4-Methylstyryl)-1-(prop-2-yn-1-yl)piperidine (75). Synthesized from 36 (0.07 g, 0.23 mmol, 1.0 equiv) via general procedures D and E. Column chromatography, EtOAc/n-hex = 1/2 (v/v). Yield: 49% (27 mg); yellow crystals, mp 85–86 °C. ^1H NMR (400 MHz, CDCl_3): δ 1.49–1.57 (m, 2H), 1.72–1.76 (m, 2H), 2.20–2.26 (m, 3H), 2.35 (s, 3H), 2.52–2.62 (m, 1H), 2.86–2.91 (m, 2H), 3.30 (d, $J = 2.4$ Hz, 2H), 5.45 (dd, $J = 11.6$, 10.0 Hz, 1H), 6.35 (d, $J = 11.6$ Hz, 1H), 7.15 (s, 4H). ^{13}C NMR (100 MHz, CDCl_3): δ 21.16, 32.36, 34.45, 47.29, 51.96, 72.94, 79.10, 127.94, 128.43, 128.94, 134.74, 136.33, 136.62. HRMS (ESI+): m/z calcd for $\text{C}_{17}\text{H}_{22}\text{N}$ $[\text{M} + \text{H}]^+$ 240.1752; found 240.1756. IR (ATR): 3210, 2934, 2858, 2798, 2756, 1466, 1450, 1432, 1335, 1272, 1143, 1109, 1067, 972, 946, 836, 824, 810, 785, 738, 687, 560 cm^{-1} . HPLC purity, 100% ($t_{\text{R}} = 9.62$ min).

(E)-4-(4-Methylstyryl)-1-(prop-2-yn-1-yl)piperidine (76). Synthesized from 37 (0.42 g, 1.39 mmol, 1.0 equiv) via general procedures D and E. Column chromatography, EtOAc/n-hex = 1/3 (v/v). Yield: 36% (121 mg); orange crystals, mp 65–67 °C. ^1H NMR (400 MHz, CDCl_3): δ 1.62–1.72 (m, 2H), 1.89–1.95 (m, 2H), 2.18–2.28 (m, 1H), 2.34–2.41 (m, 3H), 2.43 (s, 3H), 3.01–3.06 (m, 2H), 3.43 (d, $J = 2.5$ Hz, 2H), 6.22 (dd, $J = 16.0$, 7.0 Hz, 1H), 6.46 (d, $J = 15.9$ Hz, 1H), 7.21 (d, $J = 7.9$ Hz, 2H), 7.36 (d, $J = 8.3$ Hz, 2H). ^{13}C NMR (100 MHz, CDCl_3): δ 21.09, 32.04, 38.77, 47.21, 52.25, 72.92, 79.07, 125.83, 127.98, 129.13, 133.84, 134.78, 136.62. HRMS (ESI+): m/z calcd for $\text{C}_{17}\text{H}_{22}\text{N}$ $[\text{M} + \text{H}]^+$ 240.1752; found 240.1756. IR (ATR): 3209, 2933, 2858, 2800, 2756, 1513, 1450, 1427, 1335, 1311, 1271, 1134, 1109, 1067, 1019, 972, 910, 824, 795, 785, 739, 685, 642, 561, 518 cm^{-1} . HPLC purity, 97.7% ($t_{\text{R}} = 9.65$ min).

(Z)-4-(4-Isopropylstyryl)-1-(prop-2-yn-1-yl)piperidine (77). Synthesized from 38 (0.180 g, 0.546 mmol, 1.0 equiv) via general procedures D and E. Column chromatography, EtOAc/n-hex = 1/2 (v/v). Yield: 79% (115 mg); colorless oil. ^1H NMR (400 MHz, CDCl_3): δ 1.27 (d, $J = 6.9$ Hz, 6H), 1.50–1.60 (m, 2H), 1.74–1.78 (m, 2H), 2.21–2.28 (m, 2H), 2.24 (t, $J = 2.4$ Hz, 1H), 2.56–2.66 (m, 1H), 2.87–2.95 (m, 3H), 3.31 (d, $J = 2.5$ Hz, 2H), 5.45 (dd, $J = 11.7$, 10.0 Hz, 1H), 6.35 (d, $J = 11.7$ Hz, 1H), 7.17–7.23 (m, 4H). ^{13}C NMR (100 MHz, CDCl_3): δ 23.95, 32.36, 33.77, 34.44, 47.28, 51.95, 72.93, 79.10, 126.29, 127.90, 128.49, 135.09, 136.56, 147.27. HRMS (ESI+): m/z calcd for $\text{C}_{19}\text{H}_{26}\text{N}$ $[\text{M} + \text{H}]^+$ 268.2065; found 268.2061. IR (ATR): 3295, 2958, 2937, 2801, 1508, 1335, 1311, 1136, 973, 849, 676 cm^{-1} . HPLC purity, 99.1% ($t_{\text{R}} = 10.83$ min).

(E)-4-(4-Isopropylstyryl)-1-(prop-2-yn-1-yl)piperidine (78). Synthesized from 39 (0.207 g, 0.628 mmol, 1.0 equiv) via general procedures D and E. Column chromatography, EtOAc/n-hex = 1/1 (v/v). Yield: 45% (76 mg); pale yellow crystals, mp 60–64 °C. ^1H NMR (400 MHz, CDCl_3): δ 1.24 (d, $J = 6.9$ Hz, 6H), 1.52–1.61 (m, 2H), 1.78–1.83 (m, 2H), 2.05–2.20 (m, 1H), 2.24–2.31 (m, 2H), 2.26 (t, $J = 2.5$ Hz, 1H), 2.83–2.95 (m, 3H), 3.32 (d, $J = 2.5$ Hz, 2H), 6.13 (dd, $J = 16.0$, 7.0 Hz, 1H), 6.37 (d, $J = 16.6$ Hz, 1H), 7.15–7.17 (m, 2H), 7.28–7.30 (m, 2H). ^{13}C NMR (100 MHz, CDCl_3): δ 23.93, 32.05, 33.76, 38.76, 47.23, 52.25, 72.90, 79.08, 125.89, 126.549, 127.96, 134.01, 135.21, 147.73. HRMS (ESI+): m/z calcd for $\text{C}_{19}\text{H}_{26}\text{N}$ $[\text{M} + \text{H}]^+$ 268.2065; found 268.2062. IR (ATR): 3299, 2959, 2936, 2908, 2802, 1514, 1457, 1425, 1384, 1310, 1131, 1103, 1053, 977, 899, 855, 812, 762, 685, 654, 639, 553 cm^{-1} . HPLC purity, 98.5% ($t_{\text{R}} = 10.89$ min).

(Z)-4-(4-Chlorostyryl)-1-(prop-2-yn-1-yl)piperidine (79). Synthesized from 40 (0.150 g, 0.466 mmol, 1.0 equiv) via general procedures D and E. Column chromatography, EtOAc/n-hex = 1/2

(v/v). Yield: 67% (81 mg); white crystals, mp 97–99 °C. ^1H NMR (400 MHz, CDCl_3): δ 1.49–1.59 (m, 2H), 1.68–1.74 (m, 2H), 2.18–2.25 (m, 2H), 2.23 (t, J = 2.5 Hz, 1H), 2.44–2.54 (m, 1H), 2.85–2.90 (m, 2H), 3.30 (d, J = 2.5 Hz, 2H), 5.51 (dd, J = 11.6, 10.1 Hz, 1H), 6.32 (d, J = 11.7 Hz, 1H), 7.14–7.17 (m, 2H), 7.28–7.31 (m, 2H). ^{13}C NMR (100 MHz, CDCl_3): δ 32.20, 34.45, 47.24, 51.83, 73.01, 78.97, 126.92, 128.37, 129.74, 132.30, 135.99, 137.88. HRMS (ESI+): m/z calcd for $\text{C}_{16}\text{H}_{19}\text{ClN}$ [$\text{M} + \text{H}$] $^+$ 260.1206; found 260.1201. IR (ATR): 3198, 2936, 2800, 2757, 1487, 1452, 1335, 1272, 1144, 1120, 1090, 1068, 971, 836, 797, 756, 716, 695, 586, 557 cm^{-1} . HPLC purity, 98.6% (t_R = 9.78 min).

(E)-4-(4-Chlorostyryl)-1-(prop-2-yn-1-yl)piperidine (80). Synthesized from **41** (0.165 g, 0.513 mmol, 1.0 equiv) via general procedures D and E. Column chromatography, EtOAc/n-hex = 1/2 (v/v). Yield: 45% (87 mg); white crystals, mp 83–85 °C. ^1H NMR (400 MHz, CDCl_3): δ 1.49–1.59 (m, 2H), 1.76–1.82 (m, 2H), 2.06–2.16 (m, 1H), 2.23–2.29 (m, 2H), 2.25 (t, J = 2.4 Hz, 1H), 2.92 (td, J = 11.1, 2.4 Hz, 2H), 3.31 (d, J = 2.5 Hz, 2H), 6.13 (dd, J = 16.0, 7.0 Hz, 1H), 6.31 (dd, J = 16.0, 1.1 Hz, 1H), 7.22–7.27 (m, 4H). ^{13}C NMR (100 MHz, CDCl_3): δ 31.89, 38.77, 47.18, 52.15, 72.95, 79.00, 127.00, 127.13, 128.51, 132.39, 135.55, 136.04. HRMS (ESI+): m/z calcd for $\text{C}_{16}\text{H}_{19}\text{ClN}$ [$\text{M} + \text{H}$] $^+$ 260.1206; found 260.1207. IR (ATR): 3154, 2931, 2916, 2797, 1489, 1441, 1422, 1329, 1313, 1135, 1089, 1010, 971, 907, 850, 801, 722, 594, 519 cm^{-1} . HPLC purity, 99.6% (t_R = 9.81 min).

(E)-4-(4-Bromostyryl)-1-(prop-2-yn-1-yl)piperidine (81). Synthesized from **43** (0.36 g, 0.98 mmol, 1.0 equiv) via general procedures D and E. Column chromatography, EtOAc/n-hex = 1/2 (v/v). Yield: 34% (102 mg); white crystals, mp 103–106 °C. ^1H NMR (400 MHz, CDCl_3): δ 1.50–1.60 (m, 2H), 1.77–1.83 (m, 2H), 2.08–2.17 (m, 1H), 2.24–2.30 (m, 3H), 2.91–2.95 (m, 2H), 3.32 (d, J = 2.2 Hz, 2H), 6.15 (dd, J = 16.0, 6.9 Hz, 1H), 6.31 (d, J = 16.2 Hz, 1H), 7.19–7.22 (m, 2H), 7.39–7.42 (m, 2H). ^{13}C NMR (100 MHz, CDCl_3): δ 31.93, 38.85, 47.25, 52.22, 72.96, 79.06, 120.59, 127.15, 127.56, 131.53, 135.78, 136.59. HRMS (ESI+): m/z calcd for $\text{C}_{16}\text{H}_{19}\text{BrN}$ [$\text{M} + \text{H}$] $^+$ 304.0701; found 304.0706. IR (ATR): 3150, 2929, 2850, 2798, 2745, 1485, 1466, 1423, 1328, 1310, 1135, 1117, 1098, 1069, 1007, 970, 906, 848, 822, 798, 754, 715, 579, 516 cm^{-1} . HPLC purity, 100% (t_R = 10.00 min).

(E)-4-(4-Methoxystyryl)-1-(prop-2-yn-1-yl)piperidine (82). Synthesized from a mixture of **44** and **45** (0.810 g, 2.552 mmol, 1.0 equiv) via general procedures D and E. Column chromatography EtOAc/n-hex = 1/1 (v/v), yielding only *trans* isomer **82**. Yield: 32% (192 mg); white crystals, mp 59–61 °C. ^1H NMR (400 MHz, CDCl_3): δ 1.50–1.60 (m, 2H), 1.76–1.82 (m, 2H), 2.06–2.15 (m, 1H), 2.23–2.30 (m, 2H), 2.25 (t, J = 2.4 Hz, 1H), 2.90–2.95 (m, 2H), 3.32 (d, J = 2.4 Hz, 2H), 3.79 (s, 3H), 6.02 (dd, J = 15.9, 7.0 Hz, 1H), 6.32 (d, J = 15.9 Hz, 1H), 6.81–6.85 (m, 2H), 7.26–7.30 (m, 2H). ^{13}C NMR (100 MHz, CDCl_3): δ 32.13, 38.77, 47.23, 52.28, 55.23, 72.90, 79.11, 113.85, 127.02, 127.49, 130.39, 132.77, 158.69. HRMS (ESI+): m/z calcd for $\text{C}_{17}\text{H}_{22}\text{NO}$ [$\text{M} + \text{H}$] $^+$ 256.1701; found 256.1706. IR (ATR): 3270, 2940, 2907, 2825, 1604, 1509, 1467, 1313, 1241, 1176, 1128, 1029, 968, 959, 906, 854, 831, 801, 769, 719, 645, 622, 529 cm^{-1} . HPLC purity, 97.7% (t_R = 8.92 min).

(Z)-1-(Prop-2-yn-1-yl)-4-(4-(trifluoromethyl)styryl)piperidine (83). Synthesized from **46** (0.075 g, 0.211 mmol, 1.0 equiv) via general procedures D and E. Column chromatography, EtOAc/n-hex = 2/1 (v/v). Yield: 81% (45 mg); pale yellow oil. ^1H NMR (400 MHz, CDCl_3): δ 1.51–1.61 (m, 2H), 1.70–1.74 (m, 2H), 2.19–2.25 (m, 2H), 2.24 (t, J = 2.5 Hz, 1H), 2.45–2.55 (m, 1H), 2.87–2.91 (m, 2H), 3.30 (d, J = 2.5 Hz, 2H), 5.60 (dd, J = 11.7, 10.2 Hz, 1H), 6.39 (d, J = 11.7 Hz, 1H), 7.33 (d, J = 8.6 Hz, 2H), 7.59 (d, J = 8.2 Hz, 2H). ^{13}C NMR (100 MHz, CDCl_3): δ 32.18, 34.55, 47.24, 51.78, 73.05, 78.92, 124.19 (q, $J_{\text{C,F}}$ = 271.8 Hz), 125.17 (q, $J_{\text{C,F}}$ = 3.9 Hz), 126.89, 128.58 (t, $J_{\text{C,F}}$ = 32.3 Hz), 128.67, 139.22, 141.18 (q, $J_{\text{C,F}}$ = 1.4 Hz). HRMS (ESI+): m/z calcd for $\text{C}_{17}\text{H}_{19}\text{F}_3\text{N}$ [$\text{M} + \text{H}$] $^+$ 294.1470; found 294.1469. IR (ATR): 3305, 2933, 2805, 1615, 1331, 1167, 1129, 1068, 1017, 973, 851, 634, 603 cm^{-1} . HPLC purity, 100% (t_R = 10.21 min).

(E)-1-(Prop-2-yn-1-yl)-4-(4-(trifluoromethyl)styryl)piperidine (84). Synthesized from **47** (0.580 g, 1.632 mmol, 1.0 equiv) via general procedures D and E. Column chromatography, EtOAc/n-hex = 2/1 (v/v). Yield: 85% (376 mg); white crystals, mp 72–74 °C. ^1H NMR (400 MHz, CDCl_3): δ 1.52–1.62 (m, 2H), 1.80–1.85 (m, 2H), 2.12–2.20 (m, 1H), 2.26 (t, J = 2.4 Hz, 1H), 2.25–2.32 (m, 2H), 2.92–2.96 (m, 2H), 3.33 (d, J = 2.5 Hz, 2H), 6.27 (dd, J = 16.0, 6.9 Hz, 1H), 6.41 (d, J = 16.0 Hz, 1H), 7.43 (d, J = 8.4 Hz, 2H), 7.54 (d, J = 8.2 Hz, 2H). ^{13}C NMR (100 MHz, CDCl_3): δ 31.78, 38.84, 47.17, 52.11, 72.97, 78.95, 124.20 (q, $J_{\text{C,F}}$ = 271.8 Hz), 125.34 (q, $J_{\text{C,F}}$ = 3.9 Hz), 126.07, 127.02, 128.69 (q, $J_{\text{C,F}}$ = 32.4 Hz), 137.62, 141.07 (q, $J_{\text{C,F}}$ = 1.4 Hz). HRMS (ESI+): m/z calcd for $\text{C}_{17}\text{H}_{19}\text{F}_3\text{N}$ [$\text{M} + \text{H}$] $^+$ 294.1470; found 294.1464. IR (ATR): 3157, 2933, 2917, 2806, 1613, 1312, 1160, 1109, 1066, 1055, 972, 866, 831, 736, 600, 579, 517 cm^{-1} . HPLC purity, 99.9% (t_R = 10.19 min).

(Z)-1-(Prop-2-yn-1-yl)-4-(3-(trifluoromethyl)styryl)piperidine (85). Synthesized from **48** (0.05 g, 0.14 mmol, 1.0 equiv) via general procedures D and E. Column chromatography, EtOAc/n-hex = 1/3 (v/v). Yield: 27% (11 mg); yellow oil. ^1H NMR (400 MHz, CDCl_3): δ 1.59–1.77 (m, 2H), 1.75 (dd, J = 12.8, 2.2 Hz, 2H), 2.26–2.32 (m, 3H), 2.44–2.54 (m, 1H), 2.92–2.98 (m, 2H), 3.35 (d, J = 2.4 Hz, 2H), 5.60 (dd, J = 11.6, 10.2 Hz, 1H), 5.41 (d, J = 11.7 Hz, 1H), 7.39–7.51 (m, 4H). ^{13}C NMR (100 MHz, CDCl_3): δ 31.83, 34.35, 47.10, 51.69, 73.79, 78.08, 123.37 (q, $J_{\text{C,F}}$ = 3.8 Hz), 124.10 (q, $J_{\text{C,F}}$ = 272.3 Hz), 125.21 (q, $J_{\text{C,F}}$ = 3.7 Hz), 127.08, 128.72, 130.64 (q, $J_{\text{C,F}}$ = 32.2 Hz), 131.60, 138.20, 138.45. HRMS (ESI+): m/z calcd for $\text{C}_{17}\text{H}_{19}\text{NF}_3$ [$\text{M} + \text{H}$] $^+$ 294.1470; found 294.1466. IR (ATR): 3306, 2933, 2850, 2804, 2757, 1688, 1444, 1327, 1162, 1122, 1092, 1072, 972, 905, 807, 703, 696, 656, 628 cm^{-1} . HPLC purity, 95.9% (t_R = 10.13 min).

(E)-1-(Prop-2-yn-1-yl)-4-(3-(trifluoromethyl)styryl)piperidine (86). Synthesized from **49** (0.19 g, 0.53 mmol, 1.0 equiv) via general procedures D and E. Column chromatography, EtOAc/n-hex = 1/3 (v/v). Yield: 70% (109 mg); green oil. ^1H NMR (400 MHz, CDCl_3): δ 1.52–1.62 (m, 2H), 1.78–1.84 (m, 2H), 2.11–2.20 (m, 1H), 2.26 (t, J = 2.4 Hz, 1H), 2.29 (dt, J = 11.8, 2.3 Hz, 2H), 2.91–2.97 (m, 2H), 3.33 (d, J = 2.4 Hz, 2H), 6.24 (dd, J = 16.0, 6.9 Hz, 1H), 6.41 (d, J = 16.0 Hz, 1H), 7.38–7.45 (m, 2H), 7.51 (d, J = 7.5 Hz, 1H), 7.58 (s, 1H). ^{13}C NMR (100 MHz, CDCl_3): δ 31.87, 38.86, 47.24, 52.18, 73.01, 79.02, 122.64 (q, $J_{\text{C,F}}$ = 3.9 Hz), 123.50 (q, $J_{\text{C,F}}$ = 3.9 Hz), 124.16 (q, $J_{\text{C,F}}$ = 272.3 Hz), 127.03, 128.88, 129.18, 130.85 (q, $J_{\text{C,F}}$ = 32.1 Hz), 136.91, 138.39. HRMS (ESI+): m/z calcd for $\text{C}_{17}\text{H}_{19}\text{NF}_3$ [$\text{M} + \text{H}$] $^+$ 294.1470; found 294.1465. IR (ATR): 3306, 2934, 2849, 2804, 2755, 1444, 1329, 1201, 1162, 1120, 1094, 1071, 965, 900, 792, 696, 662, 628 cm^{-1} . HPLC purity, 99.8% (t_R = 10.16 min).

(Z)-4-(2-(1-(Prop-2-yn-1-yl)piperidin-4-yl)vinyl)benzonitrile (87). Synthesized from **50** (0.350 g, 1.120 mmol, 1.0 equiv) via general procedures D and E. Column chromatography, EtOAc/ CH_2Cl_2 = 3/7 (v/v). Yield: 50% (125 mg); white crystals, mp 118–121 °C. ^1H NMR (400 MHz, CDCl_3): δ 1.51–1.61 (m, 2H), 1.68–1.74 (m, 2H), 2.19–2.25 (m, 2H), 2.24 (t, J = 2.4 Hz, 1H), 2.42–2.50 (m, 1H), 2.86–2.91 (m, 2H), 3.30 (d, J = 2.5 Hz, 2H), 5.64 (dd, J = 11.7, 10.2 Hz, 1H), 6.37 (d, J = 11.8 Hz, 1H), 7.30–7.33 (m, 2H), 7.61–7.63 (m, 2H). ^{13}C NMR (100 MHz, CDCl_3): δ 32.01, 34.61, 47.15, 51.64, 73.05, 78.81, 110.05, 118.88, 126.58, 129.00, 132.02, 140.13, 142.21. HRMS (ESI+): m/z calcd for $\text{C}_{17}\text{H}_{19}\text{N}_2$ [$\text{M} + \text{H}$] $^+$ 251.1548; found 251.1550. IR (ATR): 3199, 2930, 2812, 2793, 2771, 2225, 1602, 1500, 1451, 1396, 1337, 1274, 1226, 1143, 1110, 970, 850, 729, 697, 569, 528 cm^{-1} . HPLC purity, 98.3% (t_R = 8.39 min).

(E)-4-(2-(1-(Prop-2-yn-1-yl)piperidin-4-yl)vinyl)benzonitrile (88). Synthesized from **51** (0.300 g, 0.960 mmol, 1.0 equiv) via general procedures D and E. Column chromatography, $\text{CH}_2\text{Cl}_2/\text{MeOH}$ = 50/1 (v/v). Yield: 54% (130 mg); white crystals, mp 59–62 °C. ^1H NMR (400 MHz, CDCl_3): δ 1.47–1.58 (m, 2H), 1.74–1.80 (m, 2H), 2.09–2.18 (m, 1H), 2.21–2.27 (m, 2H), 2.23 (t, J = 2.4 Hz, 1H), 2.87–2.92 (m, 2H), 3.28 (d, J = 2.5 Hz, 2H), 6.27 (dd, J = 16.0, 6.5 Hz, 1H), 6.35 (d, J = 16.1 Hz, 1H), 7.36–7.39 (m, 2H), 7.51–7.54 (m, 2H). ^{13}C NMR (100 MHz, CDCl_3): δ 31.58, 38.79, 47.06, 51.95, 72.96, 78.83, 109.93, 118.93, 126.35, 126.77, 132.16, 138.94,

141.99. HRMS (ESI+): m/z calcd for $C_{17}H_{19}N_2$ $[M + H]^+$ 251.1548; found 251.1549. IR (ATR): 3284, 2941, 2916, 2802, 2224, 1646, 1602, 1503, 1423, 1382, 1338, 1315, 1223, 1138, 1104, 984, 970, 900, 855, 831, 762, 692, 630, 551 cm^{-1} . HPLC purity, 99.3% (t_R = 8.34 min).

(Z)-4-(4-(Methylsulfonyl)styryl)-1-(prop-2-yn-1-yl)piperidine (89). Synthesized from **52** (0.126 g, 0.346 mmol, 1.0 equiv) via general procedures D and E. Column chromatography, EtOAc/n-hex = 2/1 (v/v). Yield: 76% (80 mg); white crystals, mp 71–74 °C. 1H NMR (400 MHz, $CDCl_3$): δ 1.49–1.60 (m, 2H), 1.67–1.73 (m, 2H), 2.20 (dt, J = 11.7, 2.5 Hz, 2H), 2.23 (t, J = 2.4 Hz, 1H), 2.41–2.51 (m, 1H), 2.86 (td, J = 8.9, 2.7 Hz, 2H), 3.05 (s, 3H), 3.28 (d, J = 2.5 Hz, 2H), 5.64 (dd, J = 11.7, 10.3 Hz, 1H), 6.39 (d, J = 11.7 Hz, 1H), 7.37–7.40 (m, 2H), 7.86–7.90 (m, 2H). ^{13}C NMR (100 MHz, $CDCl_3$): δ 32.03, 34.60, 44.46, 47.16, 51.64, 73.08, 78.82, 126.42, 127.32, 129.17, 138.28, 140.29, 143.22. HRMS (ESI+): m/z calcd for $C_{17}H_{22}NO_2S$ $[M + H]^+$ 304.1371; found 304.1370. IR (ATR): 3273, 2937, 2799, 2757, 1640, 1593, 1463, 1415, 1296, 1141, 1078, 955, 848, 774, 723, 679, 615, 593, 525 cm^{-1} . HPLC purity, 98.3% (t_R = 4.60 min).

(E)-4-(4-(Methylsulfonyl)styryl)-1-(prop-2-yn-1-yl)piperidine (90). Synthesized from **53** (0.205 g, 0.56 mmol, 1.0 equiv) via general procedures D and E. Column chromatography, EtOAc/n-hex = 2/1 (v/v). Yield: 85% (145 mg); white crystals, mp 101–105 °C. 1H NMR (400 MHz, $CDCl_3$): δ 1.52–1.62 (m, 2H), 1.80–1.85 (m, 2H), 2.14–2.23 (m, 1H), 2.25–2.32 (m, 3H), 2.92–2.97 (m, 2H), 3.04 (s, 3H), 3.33 (d, J = 2.2 Hz, 2H), 6.34 (dd, J = 16.0, 6.6 Hz, 1H), 6.43 (d, J = 16.1 Hz, 1H), 7.51 (d, J = 8.1 Hz, 2H), 7.85 (d, J = 8.0 Hz, 2H). ^{13}C NMR (100 MHz, $CDCl_3$): δ 31.73, 38.98, 44.60, 47.22, 52.11, 73.05, 78.94, 126.66, 126.74, 127.68, 138.37, 139.35, 143.16. HRMS (ESI+): m/z calcd for $C_{17}H_{22}NO_2S$ $[M + H]^+$ 304.1371; found 304.1372. IR (ATR): 3282, 2927, 2797, 2750, 1647, 1595, 1466, 1404, 1303, 1146, 1091, 960, 858, 767, 705, 684, 649, 595, 544, 526 cm^{-1} . HPLC purity, 95.1% (t_R = 5.06 min).

(Z)-4-(4-Cyclopropylstyryl)-1-(prop-2-yn-1-yl)piperidine (91). Synthesized from **54** (0.080 g, 0.244 mmol, 1.0 equiv) via general procedures D and E. Column chromatography, EtOAc/n-hex = 1/2 (v/v). Yield: 20% (16 mg); colorless oil. 1H NMR (400 MHz, $CDCl_3$): δ 0.68–0.72 (m, 2H), 0.94–0.99 (m, 2H), 1.49–1.59 (m, 2H), 1.71–1.77 (m, 2H), 1.86–1.92 (m, 1H), 2.20–2.26 (m, 3H), 2.52–2.62 (m, 1H), 2.86–2.91 (m, 2H), 3.30 (d, J = 2.5 Hz, 2H), 5.43 (dd, J = 11.6, 10.0 Hz, 1H), 6.33 (d, J = 11.6 Hz, 1H), 7.02–7.06 (m, 2H), 7.12–7.16 (m, 2H). ^{13}C NMR (100 MHz, $CDCl_3$): δ 9.31, 15.16, 32.35, 34.45, 47.28, 51.95, 72.96, 79.08, 125.44, 127.88, 128.47, 134.75, 136.53, 142.48. HRMS (ESI+): m/z calcd for $C_{19}H_{24}N$ $[M + H]^+$ 266.1909; found 266.1905. IR (ATR): 3355, 2973, 2916, 2849, 1739, 1654, 1468, 1373, 1239, 1086, 1045, 879, 719 cm^{-1} . HPLC purity, 95.9% (t_R = 10.27 min).

(E)-4-(4-Cyclopropylstyryl)-1-(prop-2-yn-1-yl)piperidine (92). Synthesized from **55** (0.200 g, 0.611 mmol, 1.0 equiv) via general procedures D and E. Column chromatography, EtOAc/n-hex = 1/2 (v/v). Yield: 40% (65 mg); pale yellow crystals, mp 66–68 °C. 1H NMR (400 MHz, $CDCl_3$): δ 0.66–0.70 (m, 2H), 0.92–0.97 (m, 2H), 1.50–1.61 (dt, 2H), 1.77–1.83 (m, 2H), 1.85–1.90 (m, 1H), 2.07–2.17 (m, 1H), 2.26 (t, J = 2.4 Hz, 1H), 2.27 (dt, J = 11.7, 2.5 Hz, 2H), 2.90–2.95 (m, 2H), 3.32 (d, J = 2.4 Hz, 2H), 6.10 (dd, J = 15.9, 7.0 Hz, 1H), 6.34 (d, J = 15.9 Hz, 1H), 6.98–7.01 (m, 2H), 7.23–7.26 (m, 2H). ^{13}C NMR (100 MHz, $CDCl_3$): δ 9.17, 15.12, 32.04, 38.75, 47.20, 52.23, 72.91, 79.06, 125.66, 125.84, 127.90, 133.77, 134.82, 142.79. HRMS (ESI+): m/z calcd for $C_{19}H_{24}N$ $[M + H]^+$ 266.1909; found 266.1908. IR (ATR): 3007, 2932, 2919, 2854, 2805, 2748, 1607, 1514, 1424, 1385, 1312, 1135, 1103, 1041, 1022, 972, 891, 851, 804, 684, 665, 644, 630, 546 cm^{-1} . HPLC purity, 98.1% (t_R = 10.27 min).

4-Phenethyl-1-(prop-2-yn-1-yl)piperidine (93). Synthesized from **56** (1.040 g, 3.593 mmol, 1.0 equiv) via general procedures D and E. Column chromatography, EtOAc/n-hex = 1/2 (v/v). Yield: 56% (202 mg); yellow oil. 1H NMR (400 MHz, $CDCl_3$): δ 1.24–1.39 (m, 3H), 1.56–1.62 (m, 2H), 1.75–1.81 (m, 2H), 2.15–2.22 (m, 2H), 2.24 (t, J = 2.5 Hz, 1H), 2.62–2.66 (m, 2H), 2.87–2.92 (m,

2H), 3.30 (d, J = 2.5 Hz, 2H), 7.16–7.21 (m, 3H), 7.26–7.31 (m, 2H). ^{13}C NMR (100 MHz, $CDCl_3$): δ 32.05, 32.89, 34.58, 38.15, 47.03, 52.34, 72.74, 79.02, 125.44, 128.10 (4 \times C), 142.43. HRMS (ESI+): m/z calcd for $C_{16}H_{22}N$ $[M + H]^+$ 228.1752; found 228.1755. IR (ATR): 3297, 2935, 2908, 2801, 1496, 1337, 1313, 750, 700, 641 cm^{-1} . HPLC purity, 99.9% (t_R = 8.86 min).

4-(3-Fluorophenethyl)-1-(prop-2-yn-1-yl)piperidine (94). Synthesized from **57** (0.320 g, 1.04 mmol, 1.0 equiv) via general procedures D and E. Column chromatography, EtOAc/n-hex = 1/2 (v/v). Yield: 18% (46 mg); yellow oil. 1H NMR (400 MHz, $CDCl_3$): δ 1.21–1.37 (m, 3H), 1.52–1.58 (m, 2H), 1.73–1.78 (m, 2H), 2.14–2.20 (m, 2H), 2.23 (t, J = 2.4 Hz, 1H), 2.59–2.63 (m, 2H), 2.86–2.91 (m, 2H), 3.29 (d, J = 2.4 Hz, 2H), 6.83–6.89 (m, 2H), 6.92–6.95 (m, 1H), 7.18–7.24 (m, 1H). ^{13}C NMR (100 MHz, $CDCl_3$): δ 32.10, 32.76, 32.78, 34.64, 37.90, 47.14, 52.45, 72.93, 79.04, 112.46 (d, J_{CF} = 21.9 Hz), 115.04 (d, J_{CF} = 20.5 Hz), 123.90 (d, J_{CF} = 2.2 Hz), 129.60 (d, J_{CF} = 8.7 Hz), 145.18 (d, J_{CF} = 7.2 Hz), 162.83 (d, J_{CF} = 245.0 Hz). HRMS (ESI+): m/z calcd for $C_{16}H_{21}FN$ $[M + H]^+$ 246.1658; found 246.1659. IR (ATR): 3305, 2919, 2849, 2803, 2755, 1616, 1588, 1488, 1466, 1446, 1387, 1367, 1337, 1312, 1251, 1183, 1139, 1125, 1105, 1085, 1021, 995, 976, 959, 934, 888, 866, 782, 741, 719, 691, 629 cm^{-1} . HPLC purity, 97.6% (t_R = 9.26 min).

4-(2-Fluorophenethyl)-1-(prop-2-yn-1-yl)piperidine (95). Synthesized from **58** (0.220 g, 0.716 mmol, 1.0 equiv) via general procedures D and E. Column chromatography, EtOAc/n-hex = 1/2 (v/v). Yield: 8% (14 mg); yellow oil. 1H NMR (400 MHz, $CDCl_3$): δ 1.25–1.37 (m, 3H), 1.53–1.58 (m, 2H), 1.77–1.80 (m, 2H), 2.15–2.20 (m, 2H), 2.23 (t, J = 2.4 Hz, 1H), 2.63–2.67 (m, 2H), 2.87–2.90 (m, 2H), 3.30 (d, J = 2.4 Hz, 2H), 6.97–7.02 (m, 1H), 7.03–7.07 (m, 1H), 7.13–7.20 (m, 2H). ^{13}C NMR (100 MHz, $CDCl_3$): δ 26.17, 32.12, 34.85, 36.88, 47.20, 52.53, 72.89, 79.15, 115.15 (d, J_{CF} = 22.5 Hz), 123.88 (d, J_{CF} = 3.4 Hz), 127.32 (d, J_{CF} = 8.0 Hz), 129.41 (d, J_{CF} = 16.1 Hz), 130.41 (d, J_{CF} = 5.3 Hz), 161.08 (d, J_{CF} = 244.5 Hz). HRMS (ESI+): m/z calcd for $C_{16}H_{21}FN$ $[M + H]^+$ 246.1658; found 246.1657. IR (ATR): 3383, 2975, 2931, 1691, 1638, 1492, 1453, 1423, 1366, 1324, 1277, 1228, 1161, 1127, 1086, 1033, 966, 863, 804, 757 cm^{-1} . HPLC purity, 95.1% (t_R = 9.20 min).

4-(4-Methylphenethyl)-1-(prop-2-yn-1-yl)piperidine (96). Synthesized from **59** (0.28 g, 0.92 mmol, 1.0 equiv) via general procedures D and E. Column chromatography, EtOAc/n-hex = 1/3 (v/v). Yield: 36% (79 mg); yellow oil. 1H NMR (400 MHz, $CDCl_3$): δ 1.21–1.36 (m, 3H), 1.52–1.57 (m, 2H), 1.75–1.78 (m, 2H), 2.14–2.20 (m, 2H), 2.23 (t, J = 2.4 Hz, 1H), 2.31 (s, 3H), 2.56–2.60 (m, 2H), 2.86–2.89 (m, 2H), 3.29 (d, J = 2.4 Hz, 2H), 7.05–7.10 (m, 4H). ^{13}C NMR (100 MHz, $CDCl_3$): δ 20.97, 32.21, 32.57, 34.68, 38.43, 47.21, 52.55, 72.83, 79.05, 128.17, 128.97, 135.05, 139.58. HRMS (ESI+): m/z calcd for $C_{17}H_{24}N$ $[M + H]^+$ 242.1909; found 242.1904. IR (ATR): 3183, 2932, 2917, 2847, 2798, 2752, 1515, 1451, 1333, 1293, 1270, 1144, 1103, 1080, 974, 850, 800, 784, 739, 559, 506 cm^{-1} . HPLC purity, 97.4% (t_R = 9.75 min).

4-(4-Isopropylphenethyl)-1-(prop-2-yn-1-yl)piperidine (97). Synthesized from **60** (0.290 g, 0.875 mmol, 1.0 equiv) via general procedures D and E. Column chromatography, EtOAc/n-hex = 1/2 (v/v). Yield: 55% (112 mg); yellow oil. 1H NMR (400 MHz, $CDCl_3$): δ 1.28 (d, J = 7.0 Hz, 6H), 1.32–1.39 (m, 3H), 1.58–1.63 (m, 2H), 1.79–1.84 (m, 2H), 2.19–2.25 (m, 2H), 2.26 (t, J = 2.4 Hz, 1H), 2.62–2.66 (m, 2H), 2.88–2.95 (m, 3H), 3.33 (d, J = 2.5 Hz, 2H), 7.13–7.16 (m, 2H), 7.17–7.20 (m, 2H). ^{13}C NMR (100 MHz, $CDCl_3$): δ 24.02, 32.18, 32.56, 33.59, 34.76, 38.34, 47.16, 52.50, 72.78, 79.17, 126.24, 128.10, 139.90, 146.03. HRMS (ESI+): m/z calcd for $C_{19}H_{28}N$ $[M + H]^+$ 270.2222; found 270.2226. IR (ATR): 3282, 2958, 2933, 2908, 2801, 2753, 1512, 1128, 1105, 976, 817, 677, 654, 641 cm^{-1} . HPLC purity, 99.8% (t_R = 10.99 min).

4-(4-Chlorophenethyl)-1-(prop-2-yn-1-yl)piperidine (98). Synthesized from **61** (0.195 g, 0.602 mmol, 1.0 equiv) via general procedures D and E. Column chromatography, EtOAc/n-hex = 1/2 (v/v). Yield: 62% (85 mg); white crystals, mp 37–39 °C. 1H NMR (400 MHz, $CDCl_3$): δ 1.18–1.34 (m, 3H), 1.49–1.55 (m, 2H), 1.70–1.76 (m, 2H), 2.12–2.18 (m, 2H), 2.22 (t, J = 2.5 Hz, 1H), 2.55–2.59 (m, 2H), 2.84–2.89 (m, 2H), 3.27 (d, J = 2.5 Hz, 2H),

7.06–7.10 (m, 2H), 7.20–7.24 (m, 2H). ^{13}C NMR (100 MHz, CDCl_3): δ 32.11, 32.32, 34.60, 38.09, 47.13, 52.42, 72.82, 79.10, 128.28, 129.55, 131.21, 140.97. HRMS (ESI $^{+}$): m/z calcd for $\text{C}_{16}\text{H}_{21}\text{ClN}$ [$\text{M} + \text{H}$] $^{+}$ 262.1363; found 262.1362. IR (ATR): 3219, 2931, 2919, 2863, 2801, 2758, 1492, 1451, 1407, 1335, 1282, 1261, 1138, 1121, 1109, 1084, 1015, 992, 974, 826, 797, 729, 688, 631, 539 cm^{-1} . HPLC purity, 100% (t_R = 9.90 min).

4-(4-Methoxyphenethyl)-1-(prop-2-yn-1-yl)piperidine (99). Synthesized from **62** (0.230 g, 0.720 mmol, 1.0 equiv) via general procedures D and E. Column chromatography, EtOAc/n-hex = 1/1 (v/v). Yield: 57% (103 mg); white crystals, mp 31–32 °C. ^1H NMR (400 MHz, CDCl_3): δ 1.22–1.36 (m, 3H), 1.50–1.56 (m, 2H), 1.73–1.77 (m, 2H), 2.13–2.19 (m, 2H), 2.23 (t, J = 2.5 Hz, 1H), 2.54–2.58 (m, 2H), 2.85–2.90 (m, 2H), 3.28 (d, J = 2.5 Hz, 2H), 3.77 (s, 3H), 6.80–6.84 (m, 2H), 7.07–7.10 (m, 2H). ^{13}C NMR (100 MHz, CDCl_3): δ 32.01, 32.14, 34.57, 38.46, 47.13, 52.46, 55.10, 72.77, 79.15, 113.60, 129.04, 134.60, 157.51. HRMS (ESI $^{+}$): m/z calcd for $\text{C}_{17}\text{H}_{24}\text{NO}$ [$\text{M} + \text{H}$] $^{+}$ 258.1858; found 258.1857. IR (ATR): 3273, 2926, 2908, 2850, 2806, 1609, 1510, 1314, 1250, 1238, 1175, 1101, 1031, 975, 898, 832, 812, 702, 640, 577, 523 cm^{-1} . HPLC purity, 100% (t_R = 8.95 min).

1-(Prop-2-yn-1-yl)-4-(4-(trifluoromethyl)phenethyl)piperidine (100). Synthesized from **63** (0.23 g, 0.64 mmol, 1.0 equiv) via general procedures D and E. Column chromatography, EtOAc/n-hex = 1/2 (v/v). Yield: 7% (14 mg); brown crystals, mp 31–33 °C. ^1H NMR (400 MHz, CDCl_3): δ 1.23–1.37 (m, 3H), 1.54–1.60 (m, 2H), 1.74–1.78 (m, 2H), 2.14–2.20 (m, 2H), 2.23 (t, J = 2.4 Hz, 1H), 2.65–2.70 (m, 2H), 2.86–2.90 (m, 2H), 3.29 (d, J = 2.4 Hz, 2H), 7.26–7.28 (m, 2H), 7.51–7.53 (m, 2H). ^{13}C NMR (100 MHz, CDCl_3): δ 32.14, 32.91, 34.71, 37.97, 47.17, 52.45, 72.89, 79.11, 124.34 (q, $J_{\text{C,F}}$ = 270.0 Hz), 125.20 (q, $J_{\text{C,F}}$ = 7.9 Hz), 128.02 (q, $J_{\text{C,F}}$ = 32.3 Hz), 128.57, 146.77. HRMS (ESI $^{+}$): m/z calcd for $\text{C}_{17}\text{H}_{21}\text{F}_3\text{N}$ [$\text{M} + \text{H}$] $^{+}$ 296.1626; found 296.1625. IR (ATR): 3153, 2932, 2852, 2798, 1615, 1429, 1318, 1157, 1116, 1093, 1065, 1017, 978, 910, 854, 831, 735, 682, 637, 598, 552, 511 cm^{-1} . HPLC purity, 100% (t_R = 10.29 min).

1-(Prop-2-yn-1-yl)-4-(3-(trifluoromethyl)phenethyl)piperidine (101). Synthesized from **64** (0.27 g, 0.76 mmol, 1.0 equiv) via general procedures D and E. Column chromatography, EtOAc/n-hex = 1/3 (v/v). Yield: 29% (65 mg); yellow-orange oil. ^1H NMR (400 MHz, CDCl_3): δ 1.22–1.37 (m, 3H), 1.54–1.59 (m, 2H), 1.72–1.78 (m, 2H), 2.14–2.19 (m, 2H), 2.22 (t, J = 2.4 Hz, 1H), 2.64–2.69 (m, 2H), 2.86–2.90 (m, 2H), 3.28 (d, J = 2.46 Hz, 2H), 7.32–7.43 (m, 4H). ^{13}C NMR (100 MHz, CDCl_3): δ 32.10, 32.88, 34.82, 38.03, 47.13, 52.43, 72.86, 79.07, 122.51 (q, $J_{\text{C,F}}$ = 3.8 Hz), 124.21 (q, $J_{\text{C,F}}$ = 272.2 Hz), 124.88 (q, $J_{\text{C,F}}$ = 3.7 Hz), 128.63, 130.51 (q, $J_{\text{C,F}}$ = 31.8 Hz), 131.64, 143.48. HRMS (ESI $^{+}$): m/z calcd for $\text{C}_{17}\text{H}_{21}\text{NF}_3$ [$\text{M} + \text{H}$] $^{+}$ 296.1626; found 296.1629. IR (ATR): 3308, 2923, 2849, 2804, 2757, 1449, 1329, 1199, 1161, 1121, 1072, 976, 900, 879, 800, 735, 702, 660, 631 cm^{-1} . HPLC purity, 98.7% (t_R = 10.25 min).

4-(2-(1-(Prop-2-yn-1-yl)piperidin-4-yl)ethyl)benzonitrile (102). Synthesized from **65** (0.075 g, 0.239 mmol, 1.0 equiv) via general procedures D and E. Column chromatography, EtOAc/n-hex = 1/1 (v/v). Yield: 59% (106 mg); white crystals, mp 40–42 °C. ^1H NMR (400 MHz, CDCl_3): δ 1.20–1.36 (m, 3H), 1.53–1.58 (m, 2H), 1.72–1.77 (m, 2H), 2.13–2.19 (m, 2H), 2.22 (t, J = 2.4 Hz, 1H), 2.65–2.69 (m, 2H), 2.85–2.90 (m, 2H), 3.28 (d, J = 2.5 Hz, 2H), 7.25–7.28 (m, 2H), 7.54–7.57 (m, 2H). ^{13}C NMR (100 MHz, CDCl_3): δ 31.99, 33.13, 34.62, 37.60, 47.03, 52.28, 72.82, 78.97, 109.39, 118.96, 128.96, 132.01, 148.23. HRMS (ESI $^{+}$): m/z calcd for $\text{C}_{17}\text{H}_{21}\text{N}_2$ [$\text{M} + \text{H}$] $^{+}$ 253.1705; found 253.1706. IR (ATR): 3270, 2925, 2795, 2224, 1606, 1424, 1326, 1310, 1180, 1137, 1105, 977, 901, 852, 836, 821, 766, 682, 573, 545 cm^{-1} . HPLC purity, 96.0% (t_R = 8.42 min).

1-(Prop-2-yn-1-yl)-4-(4-propylphenethyl)piperidine (103). Synthesized from **66** (0.185 g, 0.561 mmol, 1.0 equiv) via general procedures D and E. Column chromatography, EtOAc/n-hex = 1/2 (v/v). Yield: 45% (68 mg); pale yellow oil. ^1H NMR (400 MHz, CDCl_3): δ 0.95 (t, J = 7.4 Hz, 3H), 1.25–1.37 (m, 3H), 1.53–1.59

(m, 2H), 1.60–1.68 (m, 2H), 1.76–1.80 (m, 2H), 2.15–2.21 (m, 2H), 2.23 (t, J = 2.4 Hz, 1H), 2.53–2.62 (m, 4H), 2.87–2.91 (m, 2H), 3.30 (d, J = 2.4 Hz, 2H), 7.07–7.11 (m, 4H). ^{13}C NMR (100 MHz, CDCl_3): δ 13.86, 24.60, 32.20, 32.60, 34.75, 37.61, 38.37, 47.19, 52.53, 72.80, 79.20, 128.07, 128.32, 139.80, 139.88. HRMS (ESI $^{+}$): m/z calcd for $\text{C}_{19}\text{H}_{28}\text{N}$ [$\text{M} + \text{H}$] $^{+}$ 270.2216; found 270.2215. IR (ATR): 3008, 2925, 2852, 2801, 2753, 1513, 1454, 1337, 1312, 1117, 1106, 1021, 976, 897, 806, 787, 679, 645, 623, 503 cm^{-1} . HPLC purity, 97.1% (t_R = 11.12 min).

(Z)-4-(2-(1-(Prop-2-yn-1-yl)piperidin-4-yl)vinyl)benzamide (104). Synthesized from **87** (0.065 g, 0.260 mmol, 1.0 equiv) via general procedure F. Column chromatography, $\text{CH}_2\text{Cl}_2/\text{MeOH}$ = 20/1 (v/v). Yield: 46% (32 mg); white crystals, mp 127–130 °C. ^1H NMR (400 MHz, CDCl_3): δ 1.49–1.59 (m, 2H), 1.68–1.74 (m, 2H), 2.20 (td, J = 11.7, 2.6 Hz, 2H), 2.23 (t, J = 2.4 Hz, 1H), 2.46–2.57 (m, 1H), 2.87 (dt, J = 11.0, 2.4 Hz, 2H), 3.28 (d, J = 2.5 Hz, 2H), 5.57 (dd, J = 11.7, 10.1 Hz, 1H), 6.27 (bs, 2H), 6.39 (d, J = 11.7 Hz, 1H), 7.27–7.30 (m, 2H), 7.77–7.80 (m, 2H). ^{13}C NMR (100 MHz, CDCl_3): δ 32.12, 34.58, 47.19, 51.77, 73.07, 78.89, 127.17, 127.34, 128.61, 131.35, 139.00, 141.40, 169.32. HRMS (ESI $^{+}$): m/z calcd for $\text{C}_{17}\text{H}_{21}\text{N}_2\text{O}$ [$\text{M} + \text{H}$] $^{+}$ 269.1654; found 269.1652. IR (ATR): 3331, 3307, 3285, 3204, 2928, 2806, 1658, 1604, 1550, 1418, 1386, 1309, 1259, 1131, 1122, 1104, 969, 856, 794, 765, 736, 659, 636, 509 cm^{-1} . HPLC purity, 98.2% (t_R = 6.34 min).

(E)-4-(2-(1-(Prop-2-yn-1-yl)piperidin-4-yl)vinyl)benzamide (105). Synthesized from **88** (0.080 g, 0.320 mmol, 1.0 equiv) via general procedure F. Column chromatography, $\text{CH}_2\text{Cl}_2/\text{MeOH}$ = 20/1 (v/v). Yield: 63% (54 mg); white crystals, mp 181–184 °C. ^1H NMR (400 MHz, $\text{DMSO}-d_6$): δ 1.42 (dq, J = 12.7, 3.9 Hz, 2H), 1.72–1.75 (m, 2H), 2.06–2.12 (m, 1H), 2.17 (td, J = 11.5, 2 Hz, 2H), 2.79–2.83 (m, 2H), 3.14 (t, J = 2.4 Hz, 1H), 3.26 (d, J = 2.4 Hz, 2H), 6.36–6.46 (m, 2H), 7.30 (bs, 1H), 7.45–7.47 (m, 2H), 7.80–7.82 (m, 2H), 7.93 (bs, 1H). ^{13}C NMR (100 MHz, $\text{DMSO}-d_6$): δ 31.34, 38.32, 46.38, 51.42, 75.53, 79.53, 125.53, 126.96, 127.75, 132.40, 137.04, 139.99, 167.43. HRMS (ESI $^{+}$): m/z calcd for $\text{C}_{17}\text{H}_{21}\text{N}_2\text{O}$ [$\text{M} + \text{H}$] $^{+}$ 269.1654; found 269.1656. IR (ATR): 3401, 3281, 3147, 2937, 2913, 2805, 1645, 1614, 1564, 1442, 1415, 1393, 1313, 1289, 1221, 1136, 1101, 976, 870, 829, 800, 767, 682, 647, 635, 599, 544 cm^{-1} . HPLC purity, 99.4% (t_R = 6.20 min).

4-(2-(1-(Prop-2-yn-1-yl)piperidin-4-yl)ethyl)benzamide (106). Synthesized from **102** (0.075 g, 0.297 mmol, 1.0 equiv) via general procedure F. Column chromatography, $\text{CH}_2\text{Cl}_2/\text{MeOH}$ = 9/1 (v/v). Yield: 42% (34 mg); white crystals, mp 155–158 °C. ^1H NMR (400 MHz, MeOD): δ 1.28–1.36 (m, 3H), 1.58–1.63 (m, 2H), 1.80–1.83 (m, 2H), 2.21 (t, J = 11.3 Hz, 2H), 2.69 (t, J = 2.5 Hz, 1H), 2.70–2.74 (m, 2H), 2.94–2.99 (m, 2H), 3.29 (d, J = 2.5 Hz, 2H), 7.30–7.32 (m, 2H), 7.79–7.82 (m, 2H), resonances for NH_2 missing (exchange with MeOD). ^{13}C NMR (100 MHz, MeOD): δ 32.74, 33.88, 35.92, 39.11, 47.65, 53.55, 75.10, 79.19, 128.82, 129.50, 132.39, 148.40, 172.38. HRMS (ESI $^{+}$): m/z calcd for $\text{C}_{17}\text{H}_{23}\text{N}_2\text{O}$ [$\text{M} + \text{H}$] $^{+}$ 269.1810; found 269.1816. IR (ATR): 3178, 2932, 2919, 2847, 2798, 2752, 2543, 2373, 1610, 1563, 1421, 1404, 1333, 1270, 1186, 1144, 1103, 1019, 973, 915, 859, 767, 755, 709, 594 cm^{-1} . HPLC purity, 99.6% (t_R = 6.29 min).

4-(2-(1-(Prop-2-yn-1-yl)piperidin-4-yl)ethyl)phenol (107). The methoxy substituted compound **99** (50 mg, 0.194 mmol, 1.0 equiv) was dissolved in anhydrous toluene (6 mL) under argon and cooled to –20 °C. BBr_3 (1 M in CH_2Cl_2 , 582 μL , 0.582 mmol, 3.0 equiv) was added dropwise and the reaction mixture was stirred for another hour at –20 °C. The mixture was allowed to warm up to room temperature (1 h). Saturated aqueous NaHCO_3 (10 mL) was added, and the resulting emulsion was stirred vigorously for 15 min before EtOAc (30 mL) was added. The phases were separated, and the organic layer was washed with saturated brine (50 mL), dried over Na_2SO_4 , and evaporated. Column chromatography, $\text{CH}_2\text{Cl}_2/\text{MeOH}$ = 20/1 (v/v). Yield: 57% (27 mg); white crystals, mp 104–106 °C. ^1H NMR (400 MHz, CDCl_3): δ 1.23–1.39 (m, 3H), 1.48–1.54 (m, 2H), 1.73–1.79 (m, 2H), 2.21–2.27 (m, 2H), 2.25 (t, J = 2.4 Hz, 1H), 2.51–2.55 (m, 2H), 2.90–2.94 (m, 2H), 3.32 (d, J = 2.5 Hz, 2H), 6.71–6.73 (m, 2H), 6.99–7.02 (m, 2H), resonance for OH

missing (exchange with water in solvent). ^{13}C NMR (100 MHz, CDCl_3): δ 31.89, 32.09, 34.56, 38.41, 47.07, 52.42, 73.33, 78.68, 115.28, 129.27, 134.34, 153.91. HRMS (ESI⁺): m/z calcd for $\text{C}_{16}\text{H}_{22}\text{NO}$ $[\text{M} + \text{H}]^+$ 244.1701; found 244.1697. IR (ATR): 3278, 2909, 2853, 2815, 2598, 1614, 1593, 1515, 1464, 1392, 1337, 1269, 1249, 1170, 1116, 974, 819, 785, 692, 636, 563, 516, 501 cm^{-1} . HPLC purity, 96.1% (t_R = 7.17 min).

Preparation of Hydrochloride Salts. Compounds **1**, **6**, **67**, **69**, **84**, **97**, and **100** were transformed into corresponding hydrochloride salts following the described procedure. Compound in the form of a free base (0.2–2.5 g, 1.0 equiv) was dissolved in MeOH (5–20 mL). Then a 2 M solution of HCl in Et_2O (2.0 equiv) was added at room temperature under vigorous stirring with magnetic stirrer. The precipitate formed was filtered off, washed with Et_2O (50–100 mL), and dried at reduced pressure to obtain hydrochloride salts. These salts were used for the crystallization, permeability, *ex vivo* and *in vivo* experiments.

Biology. Protein Production, Enzymatic Assays, and X-ray Crystallography. All of the reagents were purchased from Sigma-Aldrich unless specified otherwise. The effects of the compounds on hMAO-A and hMAO-B were first investigated by determining the IC_{50} values using a previously described fluorimetric assay.⁴² The inhibitory activities of the compounds were determined according to their effects on the generation of hydrogen peroxide (H_2O_2) as a side-product of hMAO activity. For details on protein production, enzymatic assays, and X-ray crystallography, see [Supporting Information](#).

Cell Culture and Treatments. The human neuroblastoma SH-SY5Y cell line was purchased from American Type Culture Collection (CRL-2266; VA, USA). These cells were cultured in Advanced Dulbecco's modified Eagle's medium (Gibco, Thermo Fisher Scientific, MA, USA) supplemented with 10% fetal bovine serum (Gibco), 2 mM L-glutamine, 50 U/mL penicillin, and 50 $\mu\text{g}/\text{mL}$ streptomycin (Sigma, MO, USA) in a humidified atmosphere of 95% air and 5% CO_2 at 37 °C and grown to 80% confluence. Prior to cell treatments, the complete medium was replaced with serum-depleted medium. Compounds were prepared as stock solutions of 20 mM in DMSO and were used at concentrations of 5–50 μM . For the cytotoxic stimuli, the 10 mM 6-OHDA (Sigma, MO, USA) stock was prepared in phosphate buffered saline, pH 7.4, with 0.01% ascorbic acid. For the detailed experimental procedures see [Supporting Information](#).

Animals. Adult male Swiss mice (weight, 25–30 g) and adult male Wistar rats (weight, 200–300 g) were obtained from the Central Animal House of the School of Pharmacy and Biochemistry, University of Buenos Aires, Buenos Aires, Argentina. For behavioral assays, the mice were housed in groups of five in a controlled environment (20–23 °C), with free access to food and water, and maintained on a 12 h/12 h day/night cycle, with light on at 07:00 h. The housing, handling, and experimental procedures for both the mice and rats complied with the recommendations set out by the National Institutes of Health Guide for Care and Use of Laboratory Animals (NIH Publication No. 8023, revised 1996) and the Institutional Committees for the Care and Use of Laboratory Animals of the Faculty of Pharmacy and Biochemistry, University of Buenos Aires, Argentina (Code 31682/2014). All efforts were taken to minimize animal suffering. The number of animals used was the minimum number consistent with obtaining significant data. The mice were randomly assigned to the treatment groups and were used only once. The pharmacological tests were evaluated by experimenters who were not aware of the treatments administered and were performed between 10:00 h and 14:00 h.

Administrations and Procedures. The test compounds (used as their hydrochloride salts) were dissolved in 0.9% saline. Haloperidol, diazepam, and imipramine were diluted by sequential additions of DMSO, an aqueous solution of 0.25% Tween 80, and 0.9% saline to their final concentrations of 5%, 20%, and 75%, respectively. In each session, a control group of mice received only vehicle, in parallel with the mice that received the drug treatments. The volumes of the ip injections and oral gavage (po) administrations were 0.10–0.20 mL/

30 g body weight and 0.30 mL/30 g body weight, respectively. The protein concentrations in the mouse brain homogenates were determined using the method of Bradford, with bovine serum albumin as the standard.

For the acute behavioral assays, all of the compounds were tested 30 min after ip administrations. For the chronic treatments, the mice were injected ip with 0.3 mg/kg **69**, **100** or 0.9% saline (control group) once a day between 09:00 and 10:00 h over 10 consecutive days. On days 1, 3, 5, 7, and 9, these mice were weighted. On day 8, at 30 min after the relevant ip treatment, the mice were submitted to the plus maze (for **69**) or the hole-board tests (for **100**), and their locomotor activity was recorded immediately afterward. On day 10, at 30 min after the relevant ip treatment, the mice were submitted to the tail suspension test (for **69**) or the haloperidol-induced catalepsy assay (for **100**) ([Figures S10 and S11](#)). For all of these behavioral assays, the arena/apparatus was cleaned with 60% ethanol between each trial with each mouse. Behavioral assays are described in detail in [Supporting Information](#).

Mouse Brain Homogenate Preparation. The mice were killed humanely by decapitation at 30 min after drug or 0.9% saline treatment (for acute ip injections), at 60 min after drug or 0.9% saline treatment (for acute oral gavage), or on day 10 at 90 min after the last drug or 0.9% saline ip treatment after the tail suspension test (for the mice chronically treated with **69**) or after haloperidol-induced catalepsy test (for the mice chronically treated with **100**). Also, three mice that were chronically treated with **100** or 0.9% saline ip but without the haloperidol injection were also tested to determine any haloperidol effects in the *ex vivo* MAO-B activity assay ([Figures S10 and S11](#)). After removal of the olfactory bulb, the whole mouse brains were washed several times in ice-cold 50 mM potassium phosphate buffer (pH 7.4, 0.05% [v/v] Triton X-114). Then, each brain was independently homogenized using a blender homogenizer (PRO Scientific Inc., CT, USA) at 30 000 rpm for 1 min, in 1.5 mL of 100 mM potassium phosphate buffer (pH 7.4, 0.1% [v/v] Triton X-114) at 4 °C (in ice). The homogenate was then centrifuged at 3000g for 20 min at 4 °C. The supernatant was stored at –20 °C until the following day for the MAO inhibition assays.

Ex Vivo MAO Inhibition Assay. The *ex vivo* effects of **69** on MAO-A and **100** on MAO-B enzymatic activities (ip or oral administration, 30 min before decapitation) in the mouse brain homogenates were investigated using a previously described fluorimetric assay, with minor modifications.⁴² For details see [Supporting Information](#).

■ ASSOCIATED CONTENT

Supporting Information

The Supporting Information is available free of charge at <https://pubs.acs.org/doi/10.1021/acs.jmedchem.9b01886>.

Supplementary figures, supplementary tables, supplementary results and discussion, supplementary methods, HPLC traces for representative final compounds, and ^1H and ^{13}C NMR spectra for final compounds ([PDF](#))

Movie for undocking experiment, MAO-A ([MP4](#))

Movie for undocking experiment, MAO-B ([MP4](#))

Molecular formula strings and activity data ([CSV](#))

Model of undocking in [Figure 3](#) ([PDB](#))

Model of undocking in [Figure 3](#) ([PDB](#))

Model of undocking in [Figure 3](#) ([PDB](#))

Model of undocking in [Figure 3](#) ([PDB](#))

Accession Codes

The coordinates and structure factors have been deposited in the PDB under accession codes 6RKB (compound **1**), 6RKP (compound **84**), and 6RLE (compound **97**). Authors will release the atomic coordinates and experimental data upon article publication.

■ AUTHOR INFORMATION

Corresponding Authors

Claudia Binda – Department of Biology and Biotechnology, University of Pavia, Pavia 27100, Italy; orcid.org/0000-0003-2038-9845; Email: claudia.binda@unipv.it

Mariel Marder – Universidad de Buenos Aires, Consejo Nacional de Investigaciones Científicas y Técnicas, and Instituto de Química y Físicoquímica Biológicas, Facultad de Farmacia y Bioquímica, Universidad de Buenos Aires, Buenos Aires C1113AAD, Argentina; Email: mmarder@qb.ffyb.uba.ar

Stanislav Gobec – Faculty of Pharmacy, University of Ljubljana, Ljubljana 1000, Slovenia; orcid.org/0000-0002-9678-3083; Email: stanislav.gobec@ffa.uni-lj.si

Authors

Damijan Knez – Faculty of Pharmacy, University of Ljubljana, Ljubljana 1000, Slovenia

Natalia Colettis – Universidad de Buenos Aires, Consejo Nacional de Investigaciones Científicas y Técnicas, and Instituto de Química y Físicoquímica Biológicas, Facultad de Farmacia y Bioquímica, Universidad de Buenos Aires, Buenos Aires C1113AAD, Argentina

Luca G. Iacovino – Department of Biology and Biotechnology, University of Pavia, Pavia 27100, Italy

Matej Sova – Faculty of Pharmacy, University of Ljubljana, Ljubljana 1000, Slovenia

Anja Pišlar – Faculty of Pharmacy, University of Ljubljana, Ljubljana 1000, Slovenia

Janez Konc – National Institute of Chemistry, Ljubljana 1000, Slovenia

Samo Lešnik – National Institute of Chemistry, Ljubljana 1000, Slovenia

Josefina Higgs – Universidad de Buenos Aires, Consejo Nacional de Investigaciones Científicas y Técnicas, and Instituto de Química y Físicoquímica Biológicas, Facultad de Farmacia y Bioquímica, Universidad de Buenos Aires, Buenos Aires C1113AAD, Argentina

Fabiola Kamecki – Universidad de Buenos Aires, Consejo Nacional de Investigaciones Científicas y Técnicas, and Instituto de Química y Físicoquímica Biológicas, Facultad de Farmacia y Bioquímica, Universidad de Buenos Aires, Buenos Aires C1113AAD, Argentina

Irene Mangialavori – Universidad de Buenos Aires, Consejo Nacional de Investigaciones Científicas y Técnicas, and Instituto de Química y Físicoquímica Biológicas, Facultad de Farmacia y Bioquímica, Universidad de Buenos Aires, Buenos Aires C1113AAD, Argentina

Ana Dolšak – Faculty of Pharmacy, University of Ljubljana, Ljubljana 1000, Slovenia

Simon Žakelj – Faculty of Pharmacy, University of Ljubljana, Ljubljana 1000, Slovenia

Jurij Trontelj – Faculty of Pharmacy, University of Ljubljana, Ljubljana 1000, Slovenia

Janko Kos – Faculty of Pharmacy, University of Ljubljana, Ljubljana 1000, Slovenia

Complete contact information is available at:

<https://pubs.acs.org/10.1021/acs.jmedchem.9b01886>

Author Contributions

#D.K., N.C., and L.G.I. contributed equally to this work. D.K. designed the inhibitors, performed the chemistry and *in vitro* MAO inhibition, participated in the inhibition kinetic studies, crystallographic studies, and *ex vivo* and *in vivo* evaluations, and

oversaw the full study. N.C. performed the *ex vivo* and *in vivo* assays and contributed to the statistical analysis of the data. L.G.I. performed the inhibition kinetic studies and UV–vis measurements and refined and analyzed the crystallographic data. M.S. performed the chemistry. A.P. performed the cytotoxicity and neuroprotection assays with the SH-SY5Y cells. J.K. and S.L. performed the molecular modeling. J.H. performed the *in vitro* binding experiments and participated in the *in vivo* assays. F.K. performed the *ex vivo* assays and participated in the *in vitro* binding experiments. I.M. participated in the *ex vivo* assays and contributed to the statistical analysis of the data. A.D. performed the chemistry. S.Ž. performed the *in vitro* permeability assays and contributed to the LC–MS analysis. J.T. performed the LC–MS analysis. J.K. oversaw the cytotoxicity and neuroprotection assays with the SH-SY5Y cells. C.B. supervised the inhibition kinetic studies, UV–vis measurements, and crystallography analysis. M.M. designed and performed the *in vivo* experiments. S.G. designed and oversaw the project and contributed to the editing of the manuscript. All of the authors contributed to the design, analysis, and discussion of the research and the writing of the manuscript.

Notes

The authors declare no competing financial interest.

■ ACKNOWLEDGMENTS

This work was supported by ARRS (Grants P1-0208, L1-8157, BI-AR/15-17-003, P4-0127, L7-8269), Fondazione Cariplo (Grant 2014-0672), MIUR “Dipartimenti di Eccellenza” Programme (2018–2022), and European Community Seventh Framework Programme (FP7/2007–2013) under BioStruct-X (Grants 7551 and 10205) and CALIPSOplus (Horizon 2020 EC access program). Financial support is acknowledged from CONICET (PIP No. 112 201501 00410), UBA (UBACyT No. 20020100100415 and 20020150100012BA), ANPCyT (PICT No. 2011-0328), and MINCYT. We thank ESRF (Grenoble) and SLS (Villigen) for use of synchrotrons. We also thank Chris Berrie for critical reading of the manuscript.

■ ABBREVIATIONS USED

DMSO, dimethylsulfoxide; FAD, flavin adenine dinucleotide; hMAO-A/B, human monoamine oxidases A and B; KHMDs, potassium bis(trimethylsilyl)amide; NaHMDs, sodium bis(trimethylsilyl)amide; n-hex, n-hexane; LDH, lactate dehydrogenase; MAO, monoamine oxidase; PI, propidium iodide; SAR, structure–activity relationship; TBTU, 2-(1H-benzotriazole-1-yl)-1,1,3,3-tetramethylammonium tetrafluoroborate; THF, tetrahydrofuran

■ REFERENCES

- (1) Persch, E.; Dumele, O.; Diederich, F. Molecular Recognition in Chemical and Biological Systems. *Angew. Chem., Int. Ed.* **2015**, *54* (11), 3290–3327.
- (2) Kasprzyk-Hordern, B. Pharmacologically Active Compounds in the Environment and Their Chirality. *Chem. Soc. Rev.* **2010**, *39* (11), 4466–4503.
- (3) Brooks, W. H.; Guida, W. C.; Daniel, K. G. The Significance of Chirality in Drug Design and Development. *Curr. Top. Med. Chem.* **2011**, *11* (7), 760–770.
- (4) Nafisi, S.; Norouzi, Z. A Comparative Study on the Interaction of Cis- and Trans-Platin with DNA and RNA. *DNA Cell Biol.* **2009**, *28* (9), 469–477.

- (5) Robertson, D. W.; Katzenellenbogen, J. A.; Long, D. J.; Rorke, E. A.; Katzenellenbogen, B. S. Tamoxifen Antiestrogens. A Comparison of the Activity, Pharmacokinetics, and Metabolic Activation of the *Cis* and *Trans* Isomers of Tamoxifen. *J. Steroid Biochem.* **1982**, *16* (1), 1–13.
- (6) Gaspari, R.; Protá, A. E.; Bargsten, K.; Cavalli, A.; Steinmetz, M. O. Structural Basis of *Cis*- and *Trans*-Combretastatin Binding to Tubulin. *Chem-US* **2017**, *2* (1), 102–113.
- (7) Bach, A. W.; Lan, N. C.; Johnson, D. L.; Abell, C. W.; Bembenek, M. E.; Kwan, S. W.; Seeburg, P. H.; Shih, J. C. Cdn Cloning of Human Liver Monoamine Oxidase A and B: Molecular Basis of Differences in Enzymatic Properties. *Proc. Natl. Acad. Sci. U. S. A.* **1988**, *85* (13), 4934–4938.
- (8) De Colibus, L.; Li, M.; Binda, C.; Lustig, A.; Edmondson, D. E.; Mattevi, A. Three-Dimensional Structure of Human Monoamine Oxidase A (Mao A): Relation to the Structures of Rat MAO A and Human MAO B. *Proc. Natl. Acad. Sci. U. S. A.* **2005**, *102* (36), 12684–12689.
- (9) Milczek, E. M.; Binda, C.; Rovida, S.; Mattevi, A.; Edmondson, D. E. The 'Gating' Residues Ile199 and Tyr326 in Human Monoamine Oxidase B Function in Substrate and Inhibitor Recognition. *FEBS J.* **2011**, *278* (24), 4860–4869.
- (10) Ramsay, R. R. Molecular Aspects of Monoamine Oxidase B. *Prog. Neuro-Psychopharmacol. Biol. Psychiatry* **2016**, *69*, 81–89.
- (11) Ramsay, R. R.; Albrecht, A. Kinetics, Mechanism, and Inhibition of Monoamine Oxidase. *J. Neural Transm. (Vienna)* **2018**, *125* (11), 1659–1683.
- (12) Kim, D.; Baik, S. H.; Kang, S.; Cho, S. W.; Bae, J.; Cha, M. Y.; Sailor, M. J.; Mook-Jung, I.; Ahn, K. H. Close Correlation of Monoamine Oxidase Activity with Progress of Alzheimer's Disease in Mice, Observed by in Vivo Two-Photon Imaging. *ACS Cent. Sci.* **2016**, *2* (12), 967–975.
- (13) Schedin-Weiss, S.; Inoue, M.; Hromadkova, L.; Teranishi, Y.; Yamamoto, N. G.; Wiehager, B.; Bogdanovic, N.; Winblad, B.; Sandebring-Matton, A.; Frykman, S.; Tjernberg, L. O. Monoamine Oxidase B is Elevated in Alzheimer Disease Neurons, is Associated with γ -Secretase and Regulates Neuronal Amyloid β -Peptide Levels. *Alzheimer's Res. Ther.* **2017**, *9* (1), 57.
- (14) Chiuccariello, L.; Houle, S.; Miller, L.; Cooke, R. G.; Rusjan, P. M.; Rajkowska, G.; Levitan, R. D.; Kish, S. J.; Kolla, N. J.; Ou, X.; Wilson, A. A.; Meyer, J. H. Elevated Monoamine Oxidase A Binding During Major Depressive Episodes is Associated with Greater Severity and Reversed Neurovegetative Symptoms. *Neuropsychopharmacology* **2014**, *39* (4), 973–980.
- (15) Deshwal, S.; Di Sante, M.; Di Lisa, F.; Kaludercic, N. Emerging Role of Monoamine Oxidase as a Therapeutic Target for Cardiovascular Disease. *Curr. Opin. Pharmacol.* **2017**, *33*, 64–69.
- (16) Shih, J. C. Monoamine Oxidase Isoenzymes: Genes, Functions and Targets for Behavior and Cancer Therapy. *J. Neural Transm. (Vienna)* **2018**, *125* (11), 1553–1566.
- (17) Thase, M. E. The Role of Monoamine Oxidase Inhibitors in Depression Treatment Guidelines. *J. Clin. Psychiatry* **2012**, *73* (Suppl. 1), 10–16.
- (18) Dezsí, L.; Vecsei, L. Monoamine Oxidase B Inhibitors in Parkinson's Disease. *CNS Neurol. Disord.: Drug Targets* **2017**, *16* (4), 425–439.
- (19) Youdim, M. B. H. Monoamine Oxidase Inhibitors, and Iron Chelators in Depressive Illness and Neurodegenerative Diseases. *J. Neural Transm. (Vienna)* **2018**, *125* (11), 1719–1733.
- (20) Youdim, M. B.; Edmondson, D.; Tipton, K. F. The Therapeutic Potential of Monoamine Oxidase Inhibitors. *Nat. Rev. Neurosci.* **2006**, *7* (4), 295–309.
- (21) Petrek, M.; Otyepka, M.; Banas, P.; Kosinova, P.; Koca, J.; Damborsky, J. Caver: A New Tool to Explore Routes from Protein Clefts, Pockets and Cavities. *BMC Bioinf.* **2006**, *7*, 316.
- (22) Filipovič, J.; Vávra, O.; Plhák, J.; Bednář, D.; Marques, S. M.; Brezovský, J.; Matyska, L.; Damborský, J. CaverDock: A Novel Method for the Fast Analysis of Ligand Transport. *arXiv* **2018**, 1809.03453.
- (23) Waldeck, D. H. Photoisomerization Dynamics of Stilbenes. *Chem. Rev.* **1991**, *91* (3), 415–436.
- (24) Albrecht, A.; Vovk, I.; Mavri, J.; Marco-Contelles, J.; Ramsay, R. R. Evidence for a Cyanine Link between Propargylamine Drugs and Monoamine Oxidase Clarifies the Inactivation Mechanism. *Front. Chem.* **2018**, *6*, 169.
- (25) Esteban, G.; Allan, J.; Samadi, A.; Mattevi, A.; Unzeta, M.; Marco-Contelles, J.; Binda, C.; Ramsay, R. R. Kinetic and Structural Analysis of the Irreversible Inhibition of Human Monoamine Oxidases by ASS234, a Multi-Target Compound Designed for Use in Alzheimer's Disease. *Biochim. Biophys. Acta, Proteins Proteomics* **2014**, *1844* (6), 1104–1110.
- (26) Binda, C.; Hubalek, F.; Li, M.; Herzig, Y.; Sterling, J.; Edmondson, D. E.; Mattevi, A. Crystal Structures of Monoamine Oxidase B in Complex with Four Inhibitors of the *N*-Propargylaminoindan Class. *J. Med. Chem.* **2004**, *47* (7), 1767–1774.
- (27) Reis, J.; Manzella, N.; Cagide, F.; Mialet-Perez, J.; Uriarte, E.; Parini, A.; Borges, F.; Binda, C. Tight-Binding Inhibition of Human Monoamine Oxidase B by Chromone Analogs: A Kinetic, Crystallographic, and Biological Analysis. *J. Med. Chem.* **2018**, *61* (9), 4203–4212.
- (28) Lopes, F. M.; Schroder, R.; da Frota Junior, M. L.; Zanotto-Filho, A.; Muller, C. B.; Pires, A. S.; Meurer, R. T.; Colpo, G. D.; Gelain, D. P.; Kapczinski, F.; Moreira, J. C. F.; da Cruz Fernandes, M.; Klamt, F. Comparison between Proliferative and Neuron-Like SS-SYSY Cells as an in Vitro Model for Parkinson Disease Studies. *Brain Res.* **2010**, *1337*, 85–94.
- (29) Finberg, J. P.; Rabey, J. M. Inhibitors of MAO-A and MAO-B in Psychiatry and Neurology. *Front. Pharmacol.* **2016**, *7*, 340.
- (30) Shulman, K. I.; Herrmann, N.; Walker, S. E. Current Place of Monoamine Oxidase Inhibitors in the Treatment of Depression. *CNS Drugs* **2013**, *27* (10), 789–797.
- (31) Kircanski, K.; LeMoult, J.; Ordaz, S.; Gotlib, I. H. Investigating the Nature of Co-Occurring Depression and Anxiety: Comparing Diagnostic and Dimensional Research Approaches. *J. Affective Disord.* **2017**, *216*, 123–135.
- (32) Akimova, E.; Lanzenberger, R.; Kasper, S. The Serotonin-1A Receptor in Anxiety Disorders. *Biol. Psychiatry* **2009**, *66* (7), 627–635.
- (33) Fernandez, S. P.; Wasowski, C.; Loscalzo, L. M.; Granger, R. E.; Johnston, G. A.; Paladini, A. C.; Marder, M. Central Nervous System Depressant Action of Flavonoid Glycosides. *Eur. J. Pharmacol.* **2006**, *539* (3), 168–176.
- (34) Bali, A.; Jaggi, A. S. Preclinical Experimental Stress Studies: Protocols, Assessment and Comparison. *Eur. J. Pharmacol.* **2015**, *746*, 282–292.
- (35) Tripathi, A. C.; Upadhyay, S.; Paliwal, S.; Saraf, S. K. Privileged Scaffolds as MAO Inhibitors: Retrospect and Prospects. *Eur. J. Med. Chem.* **2018**, *145*, 445–497.
- (36) Holt, A. On the Practical Aspects of Characterising Monoamine Oxidase Inhibition in Vitro. *J. Neural Transm. (Vienna)* **2018**, *125* (11), 1685–1705.
- (37) Pettersson, F.; Svensson, P.; Waters, S.; Waters, N.; Sonesson, C. Synthesis and Evaluation of a Set of Para-Substituted 4-Phenylpiperidines and 4-Phenylpiperazines as Monoamine Oxidase (MAO) Inhibitors. *J. Med. Chem.* **2012**, *55* (7), 3242–3249.
- (38) Heuson, E.; Storgaard, M.; Huynh, T. H.; Charmantray, F.; Gefflaut, T.; Bunch, L. Profiling Substrate Specificity of Two Series of Phenethylamine Analogs at Monoamine Oxidase A and B. *Org. Biomol. Chem.* **2014**, *12* (43), 8689–8695.
- (39) Kumar, S.; Ali, J.; Baboota, S. Design Expert(®) Supported Optimization and Predictive Analysis of Selegiline Nanoemulsion Via the Olfactory Region with Enhanced Behavioural Performance in Parkinson's Disease. *Nanotechnology* **2016**, *27* (43), 435101.
- (40) Daina, A.; Michielin, O.; Zoete, V. SwissADME: A Free Web Tool to Evaluate Pharmacokinetics, Drug-Likeness and Medicinal Chemistry Friendliness of Small Molecules. *Sci. Rep.* **2017**, *7*, 42717.
- (41) Baell, J. B.; Holloway, G. A. New Substructure Filters for Removal of Pan Assay Interference Compounds (PAINS) from

Screening Libraries and for Their Exclusion in Bioassays. *J. Med. Chem.* **2010**, 53 (7), 2719–2740.

(42) Zhou, M.; Panchuk-Voloshina, N. A One-Step Fluorometric Method for the Continuous Measurement of Monoamine Oxidase Activity. *Anal. Biochem.* **1997**, 253 (2), 169–174.